Interprétation de la radiographie standard du crâne en pédiatrie et âge osseux

Matina G. BOITSIOS, MD
Neuro-radiologue pédiatrique
Service d’imagerie pédiatrique

Hôpital Universitaire
des Enfants Reine Fabiola
Universitair **Kinderziekenhuis**
Koningin Fabiola

ULB

Introduction

1ère partie

Radiographie du crâne

- Anatomie
- Techniques
- Bonne indication

2ème partie

Rx âge osseux

- Historique
- Méthodes
- Âge osseux moderne

1ère partie

RADIOGRAPHIE DU CRÂNE

INTRODUCTION

Imagerie pédiatrique

- Radiosensibilité (principe ALARA)
- Limiter le nombre d'examen (anxiogène pour l'enfant et les parents, irradiant en fonction de la technique)
- Effet sur la prise en charge du patient ?
- Collaboration du patient et des parents
- Sédation (6 mois - 6 ans)
- Attention aux incidentalomes

Radiographie standard

- Projection en deux dimensions d'une structure tridimensionnelle
- Radio-transparence (tonalité)
- Indications de radiographie crâne limitées

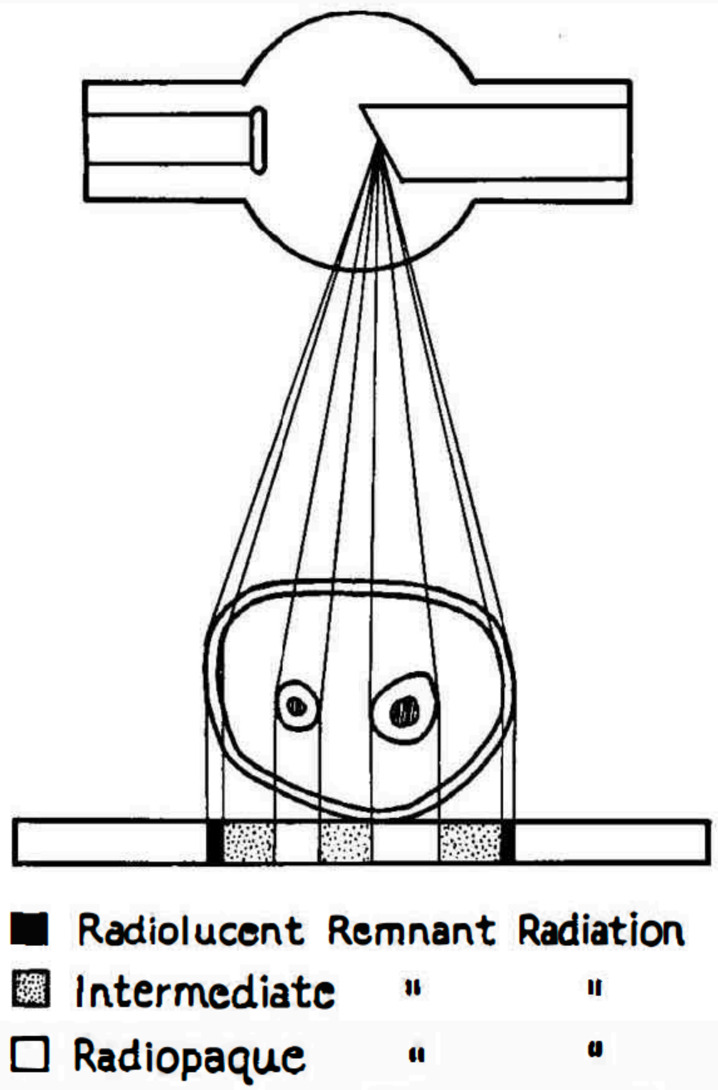

Figure 1–3. Diagrammatic illustration of how remnant radiation varies in intensity and radiopacity when x-rays pass through the tissues of the forearm; shown in cross section.

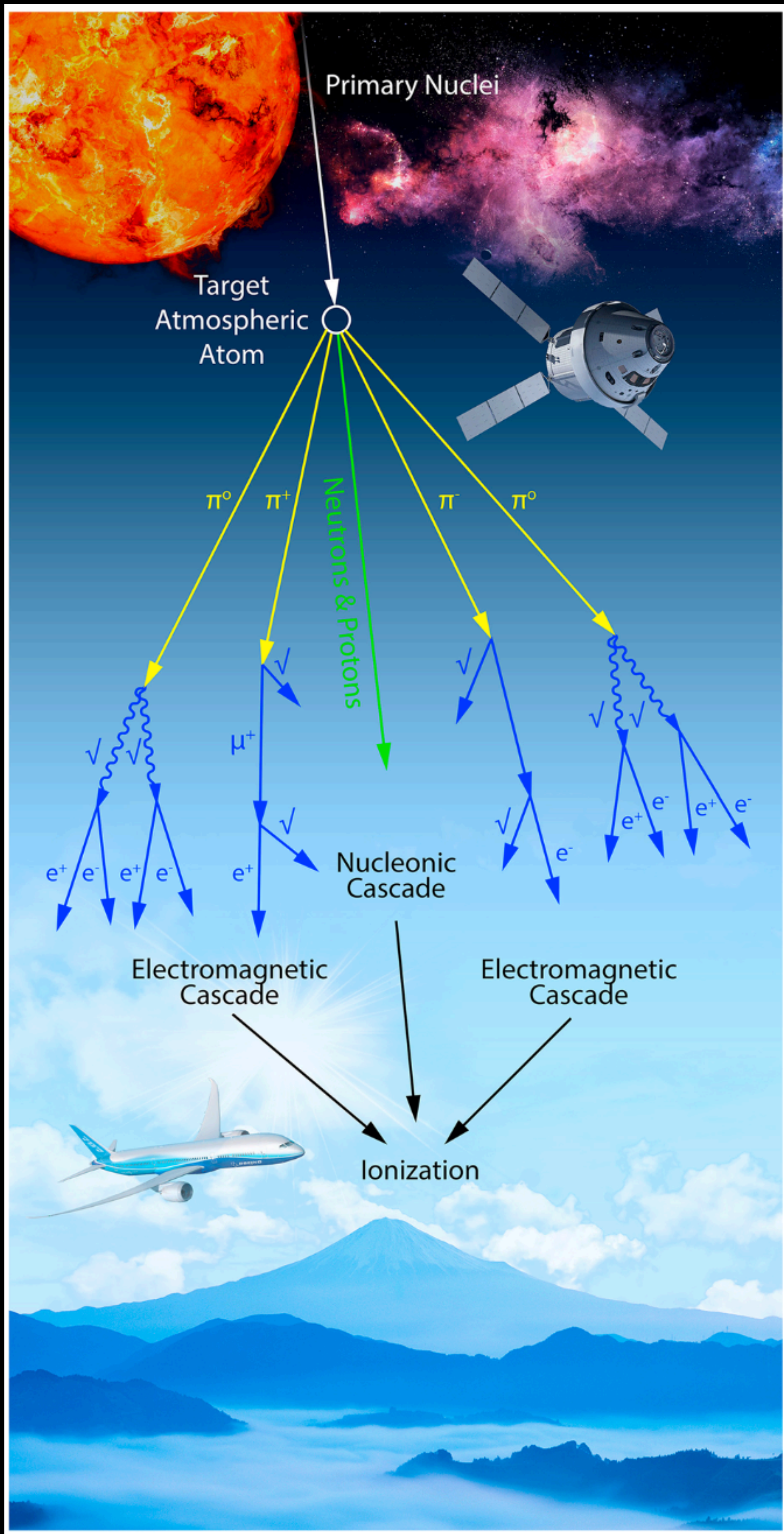

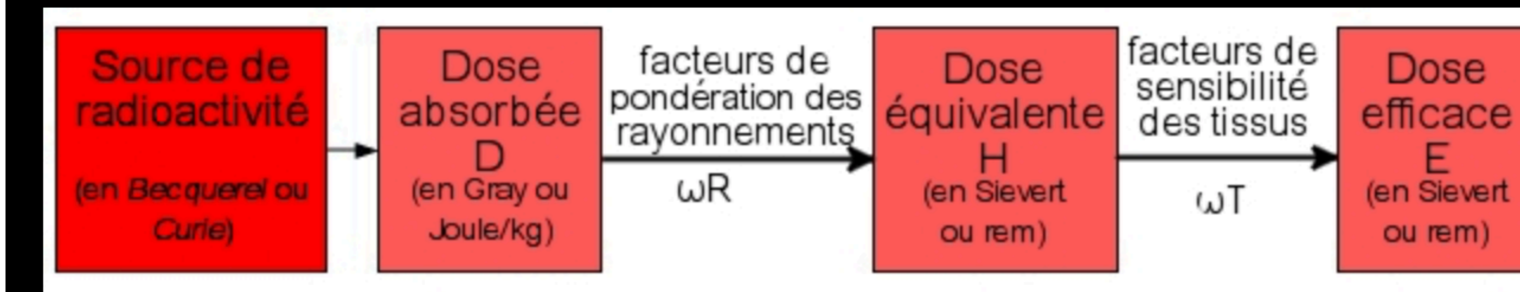

Dose effective (E):

$$E = \sum_T w_T H_T,$$

W_T : facteur de pondération tissulaire
H_T : dose équivalent

Table 7 The effect of a few trivial activities in all-day life on effective dose[a]

Action	Saving	Expense
Lowering radon (^{222}Rn) concentration at home with 1 Bq/m^3 [42] (e.g. by increasing ventilation; worldwide average conc. 40 Bq/m^3)	80 μSv/year	
Holidays on a cruise ship instead of on land [43]	2 μSv/day	
Large distance flying [44]		5 μSv/h
Visit of cave with relatively low radon concentration of 1 kBq/m^3 [45]		4 μSv/h
Person living in Cornwall (6.5 mSv/year due to radon only) going to London (1 mSv/year) [46]	15 μSv/day	
Living in The Netherlands (2 mSv/year)		5 μSv/day

[a] Approximate data, exact values depend on several details

Insights Imaging (2012) 3:23–32

Contents lists available at SciVerse ScienceDirect

European Journal of Radiology

journal homepage: www.elsevier.com/locate/ejrad

ELSEVIER

RADIOLOGY

CT in children – dose protection and general considerations when planning a CT in a child

E. Sorantin*, S. Weissensteiner, G. Hasenburger, M. Riccabona

Department of Radiology, Division of Pediatric Radiology, Medical University of Graz,Austria

Radiation exposure from CT scans in childhood and subsequent risk of leukaemia and brain tumours: a retrospective cohort study

Mark S Pearce, Jane A Salotti, Mark P Little, Kieran McHugh, Choonsik Lee, Kwang Pyo Kim, Nicola L Howe, Cecile M Ronckers, Preetha Rajaraman, Sir Alan W Craft, Louise Parker, Amy Berrington de González

Summary

Background Although CT scans are very useful clinically, potential cancer risks exist from associated ionising radiation, in particular for children who are more radiosensitive than adults. We aimed to assess the excess risk of leukaemia and brain tumours after CT scans in a cohort of children and young adults.

Methods In our retrospective cohort study, we included patients without previous cancer diagnoses who were first examined with CT in National Health Service (NHS) centres in England, Wales, or Scotland (Great Britain) between 1985 and 2002, when they were younger than 22 years of age. We obtained data for cancer incidence, mortality, and loss to follow-up from the NHS Central Registry from Jan 1, 1985, to Dec 31, 2008. We estimated absorbed brain and red bone marrow doses per CT scan in mGy and assessed excess incidence of leukaemia and brain tumours cancer with Poisson relative risk models. To avoid inclusion of CT scans related to cancer diagnosis, follow-up for leukaemia began 2 years after the first CT and for brain tumours 5 years after the first CT.

Findings During follow-up, 74 of 178 604 patients were diagnosed with leukaemia and 135 of 176 587 patients were diagnosed with brain tumours. We noted a positive association between radiation dose from CT scans and leukaemia (excess relative risk [ERR] per mGy 0·036, 95% CI 0·005–0·120; p=0·0097) and brain tumours (0·023, 0·010–0·049; p<0·0001). Compared with patients who received a dose of less than 5 mGy, the relative risk of leukaemia for patients who received a cumulative dose of at least 30 mGy (mean dose 51·13 mGy) was 3·18 (95% CI 1·46–6·94) and the relative risk of brain cancer for patients who received a cumulative dose of 50–74 mGy (mean dose 60·42 mGy) was 2·82 (1·33–6·03).

Interpretation Use of CT scans in children to deliver cumulative doses of about 50 mGy might almost triple the risk of leukaemia and doses of about 60 mGy might triple the risk of brain cancer. Because these cancers are relatively rare, the cumulative absolute risks are small: in the 10 years after the first scan for patients younger than 10 years, one excess case of leukaemia and one excess case of brain tumour per 10 000 head CT scans is estimated to occur. Nevertheless, although clinical benefits should outweigh the small absolute risks, radiation doses from CT scans ought to be kept as low as possible and alternative procedures, which do not involve ionising radiation, should be considered if appropriate.

Funding US National Cancer Institute and UK Department of Health.

Lancet 2012; 380: 499–505

Published Online
June 7, 2012
http://dx.doi.org/10.1016/S0140-6736(12)60815-0

See Comment page 455

See Perspectives page 465

Institute of Health and Society (M S Pearce PhD, J A Salotti PhD, N L Howe MSc) **and Northern Institute of Cancer Research** (Sir A W Craft MD), **Newcastle University, Sir James Spence Institute, Royal Victoria Infirmary, Newcastle upon Tyne, UK; Radiation Epidemiology Branch, Division of Cancer Epidemiology and Genetics, National Cancer Institute, Bethesda, MD, USA** (M P Little PhD, C Lee PhD, C M Ronckers PhD, P Rajaraman PhD, A B de González DPhil); **Great Ormond Street Hospital for Children NHS Trust, London, UK** (K McHugh FRCR); **Department of Nuclear Engineering, Kyung Hee University, Gyeongi-Do, South Korea** (K P Kim PhD); **Dutch Childhood Oncology Group—Longterm effects after childhood cancer**

Interpretation Use of CT scans in children to deliver cumulative doses of about 50 mGy might almost triple the risk of leukaemia and doses of about 60 mGy might triple the risk of brain cancer. Because these cancers are relatively rare, the cumulative absolute risks are small: in the 10 years after the first scan for patients younger than 10 years, one excess case of leukaemia and one excess case of brain tumour per 10 000 head CT scans is estimated to occur. Nevertheless, although clinical benefits should outweigh the small absolute risks, radiation doses from CT scans ought to be kept as low as possible and alternative procedures, which do not involve ionising radiation, should be considered if appropriate.

Dose reçue d'irradiation naturelle par an:

3 mSv/an

Examen radiologique	Dose effective (mSv)	Nombre de jours équivalents
Radiographie thoracique	0.02	2,4
Radiographie du crâne	0.07	8,5
Mammographie	0.7	80
Colonne lombaire	1.3	158
Urographie intraveineuse	2,5	304
transit	3	1 année
lavement baryté	7	2,3 années
scanner tête	2.0	243 jours
scanner thorax	8	2,7 années
scanner abdomen	10	3,3 années
coronarographie par scanner	21,4	6,9 années

https://www.info-radiologie.ch/dose_rayon_radiologie.php

ULB

Table A.3.1. Estimates of the thresholds for tissue effects in the adult human testes, ovaries, lens, and bone marrow (from ICRP 1984, *Publication 41*[1]).

Tissue and effect	Threshold		
	Total dose received in a single brief exposure (Gy)	Total dose received in highly fractionated or protracted exposures (Gy)	Annual dose rate if received yearly in highly fractionated or protracted exposures for many years (Gy y^{-1})
Testes			
Temporary sterility	0.15	NA[2]	0.4
Permanent sterility	3.5–6.0[3]	NA	2.0
Ovaries			
Sterility	2.5–6.0	6.0	>0.2
Lens			
Detectable opacities	0.5–2.0[4]	5	>0.1
Visual impairment (Cataract)[5]	5.0[5]	>8	>0.15
Bone marrow			
Depression of hematopoiesis	0.5	NA	>0.4

See Table A.3.4 and Section A.3.1.7 for revised judgements.

[1] For further details consult *Publication 41* (ICRP 1984).

[2] NA denotes Not Applicable, since the threshold is dependent on dose rate rather than on total dose.

[3] See UNSCEAR (1988).

[4] See also Otake and Schull (1990).

[5] Given as 2–10 Sv (NCRP 1989) for acute dose threshold.

Valentin J, International Commission on Radiological Protection, editors. The 2007 recommendations of the International Commission on Radiological Protection. Oxford: Elsevier; 2007. 332 p. (ICRP publication)

ANATOMIE

Rôles de la boîte crânienne

- protection du cerveau
- soutien de la face
- insertion musculaire
- mastication

22 pièces osseuses

- 14 os de la face (nasal (2), lacrymal (2), maxillaire (2), Zygomatic (2), palatine (2), inferior nasal conchae (2) vomer (1), mandibule (1))
- 8 os de la boîte crânienne (frontal, pariétal (2), temporal (2), occipital, sphénoïde, ethmoïde)

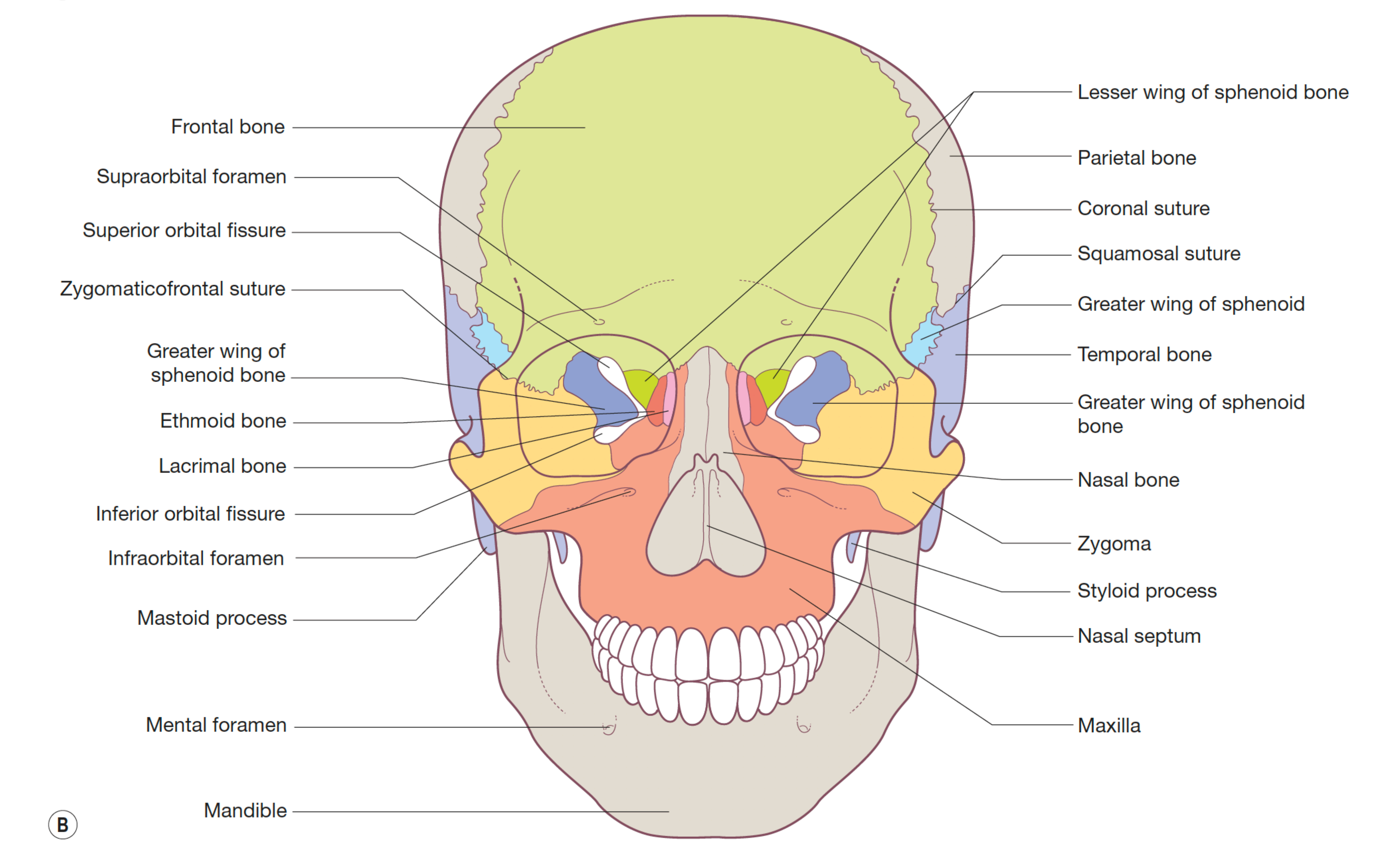

Figure 1.1 • (A) Lateral view of skull. (B) Frontal view of skull.

Ryan S, McNicholas M, Eustace SJ. Anatomy for diagnostic imaging. 3rd ed. Edinburgh; New York: Saunders/Elsevier; 2011. 337 p.

14 os de la face (nasal (2), lacrymal (2), maxillaire (2), Zygomatic (2), palatine (2), inferior nasal conchae (2) vomer (1), mandibule (1)

8 os de la boîte crânienne (frontal, pariétal (2), temporal (2), occipital, sphénoïde, ethmoïde)

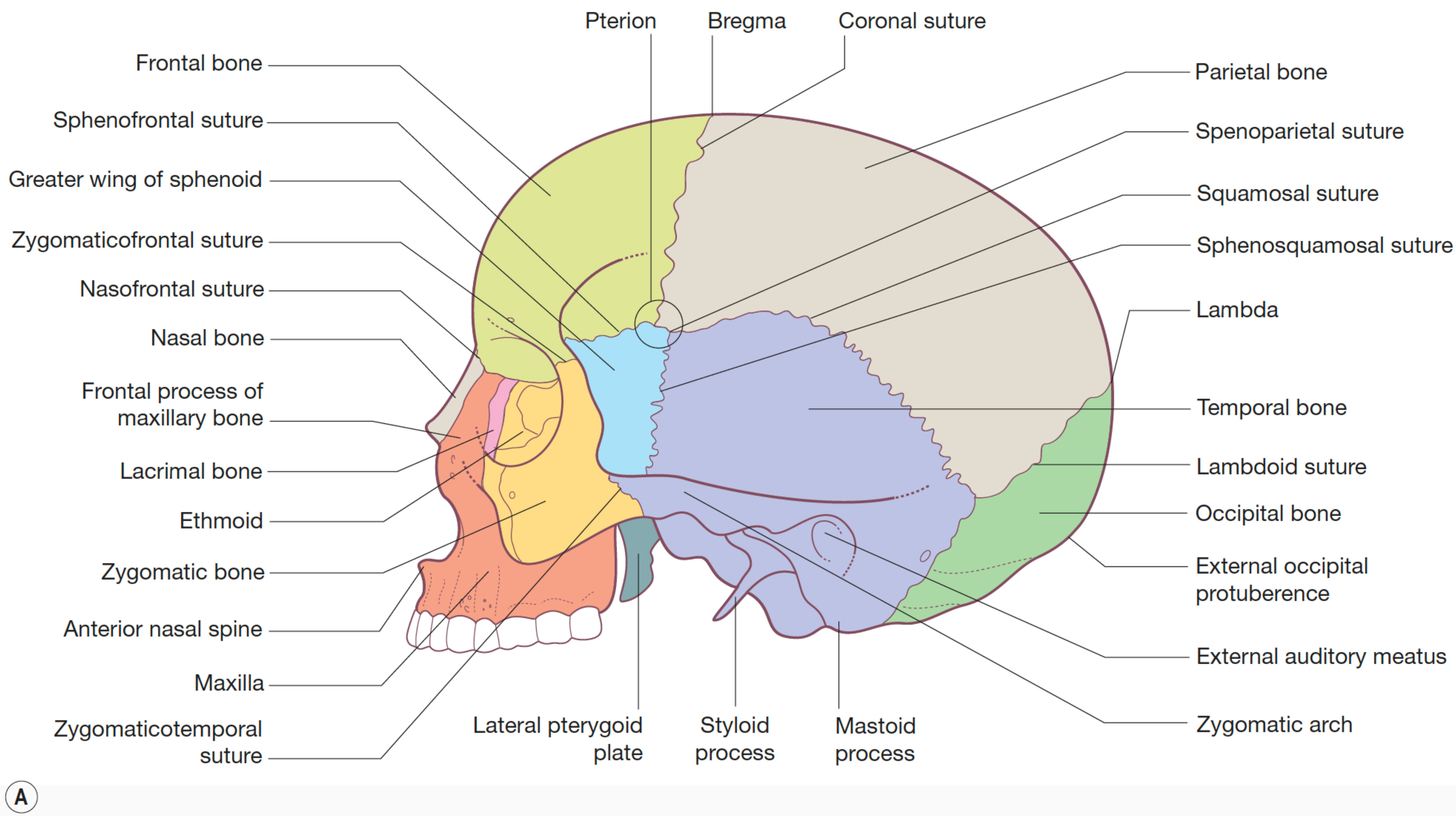

Ryan S, McNicholas M, Eustace SJ. Anatomy for diagnostic imaging. 3rd ed. Edinburgh; New York: Saunders/Elsevier; 2011. 337 p.

Table interne - Diploë - Table externe

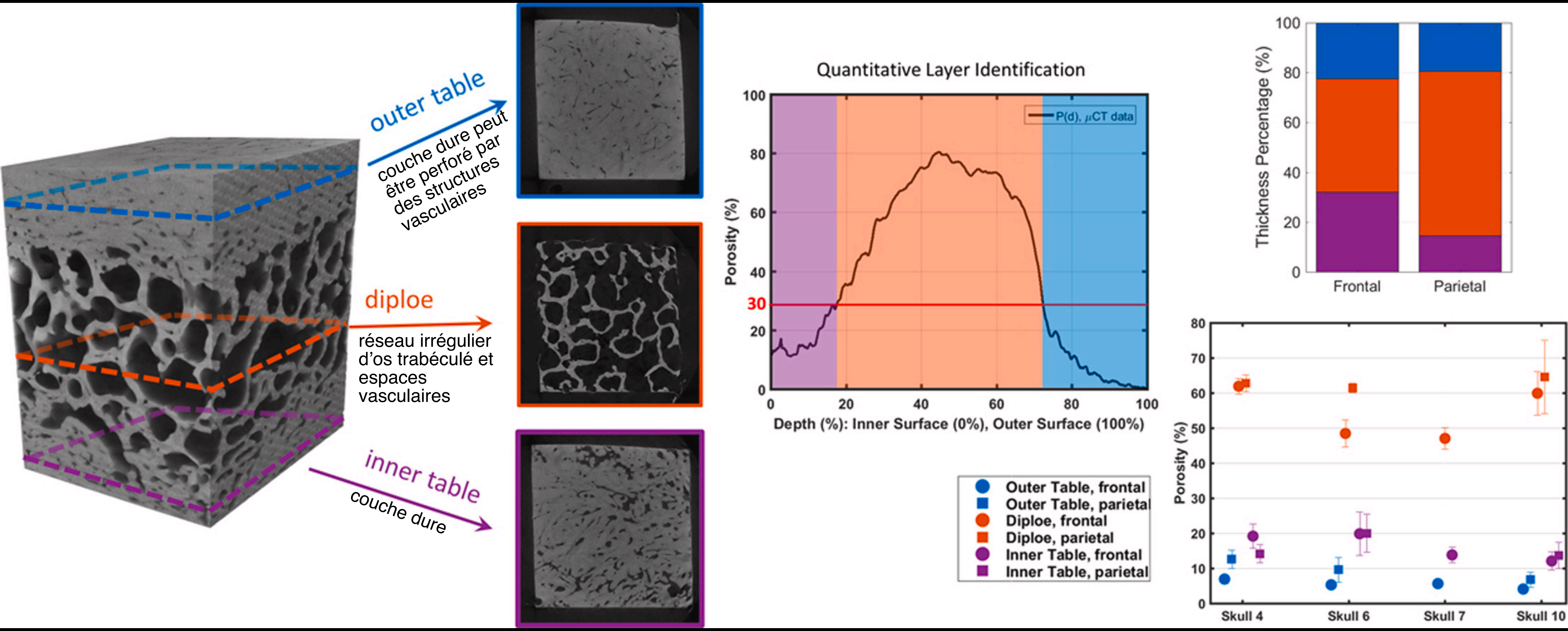

Alexander SL, Rafaels K, Gunnarsson CA, Weerasooriya T. Structural analysis of the frontal and parietal bones of the human skull. Journal of the Mechanical Behavior of Biomedical Materials. 2019 Feb;90:689–701

Fontanelles

Nouveau-né, 6 zones d'ossification incomplète

- fontanelle antérieure
- fontanelles mastoïdes (2) ou **Ptérion** (jonction entre l'os pariétal, la suture squameuse et la grande aile du sphénoïde)
- fontanelles sphénoïdes (2) ou **Astérion** (jonction entre l'os occipital, pariétal et mastoïde)
- fontanelle postérieure lambda

Age of closure of cranial fontanelles

Fontanelles	Age of closure
Anterior or bregmatic	24 months
Posterior or lambdoid	3 months
Anterolateral (Sphenoid)	6-24 months
Posterolateral (Mastoid)	6-24 months

Ghizoni E, Denadai R, Raposo-Amaral CA, Joaquim AF, Tedeschi H, Raposo-Amaral CE. Diagnosis of infant synostotic and nonsynostotic cranial deformities: a review for pediatricians. Revista Paulista de Pediatria (English Edition). 2016 Dec;34(4):495–502.

ULB

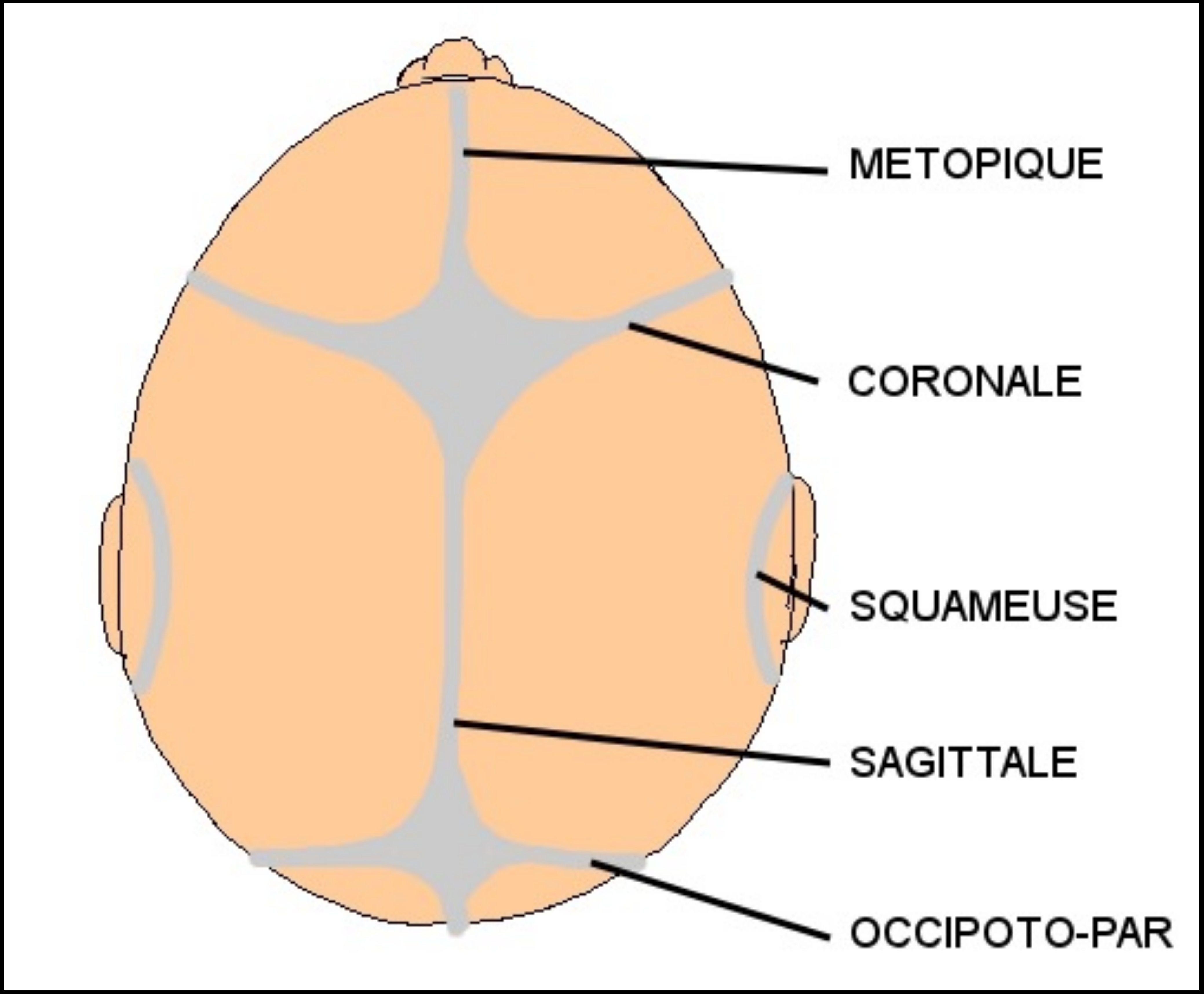

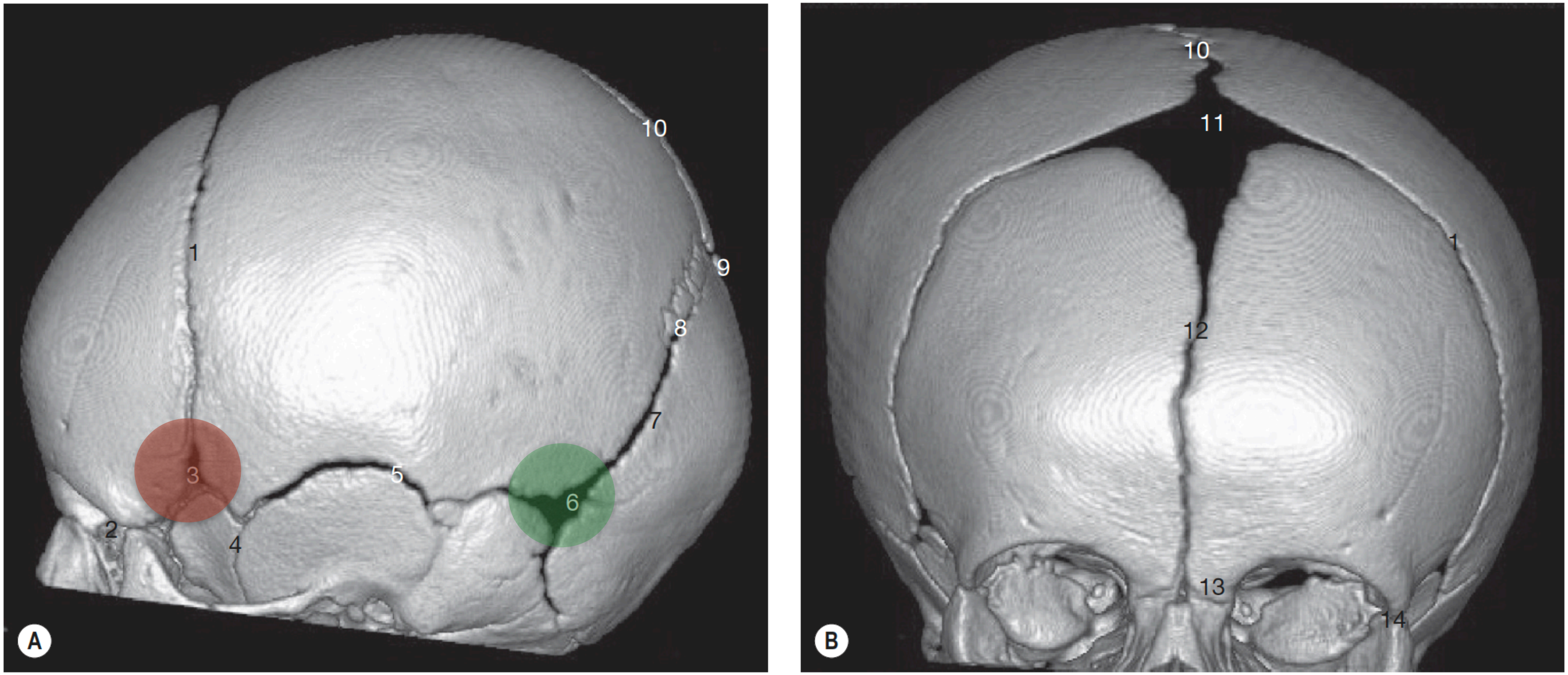

Figure 1.2 • Three-dimensional (3D) CT skull of a 2-month-old infant to show sutures, (A) lateral and (B) anterior.

1. Coronal suture
2. Zygomaticofrontal suture
3. Pterion
4. Sphenotemporal (sphenosquamosal) suture
5. Temporoparietal (squamosal) suture
6. Asterion
7. Lambdoid suture
8. Wormian bones
9. Lambda
10. Sagittal suture
11. Anterior fontanelle
12. Metopic suture
13. Nasofrontal suture
14. Zygomaticofrontal suture

Ryan S, McNicholas M, Eustace SJ. Anatomy for diagnostic imaging. 3rd ed. Edinburgh; New York: Saunders/Elsevier; 2011. 337 p.

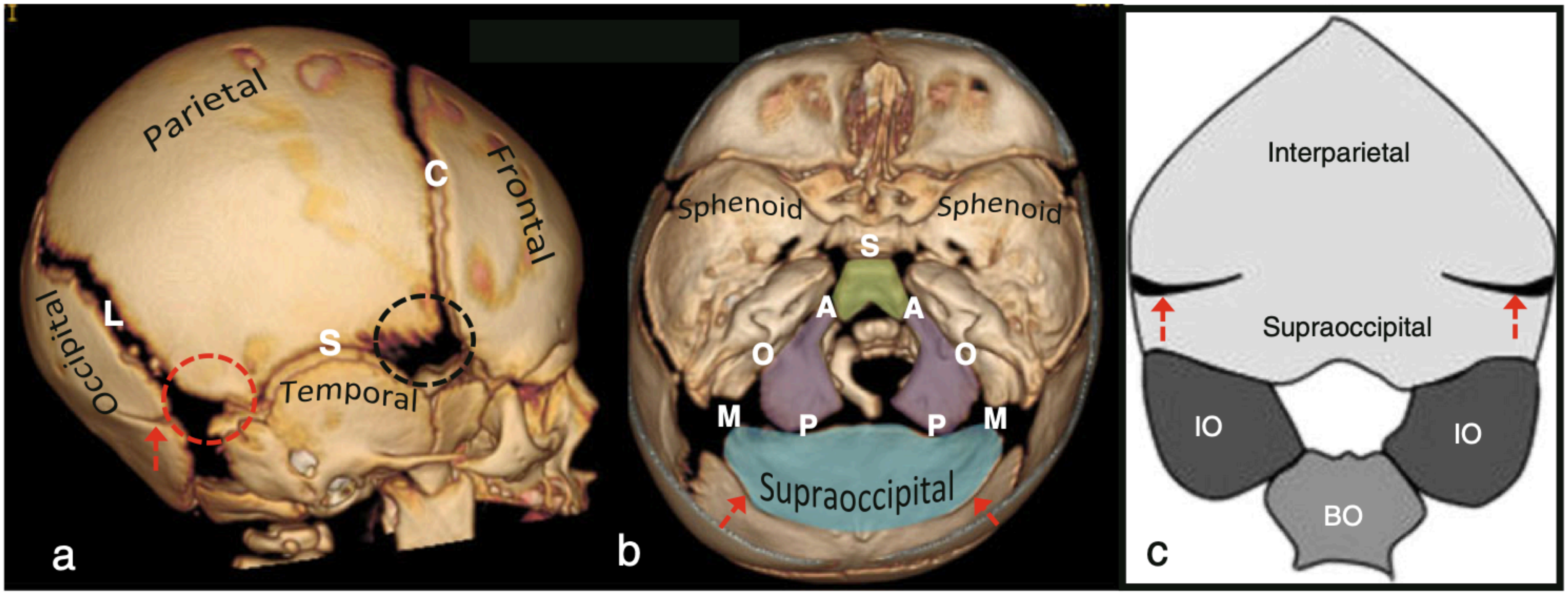

Fig. 1 Normal cranial anatomy at 1 month. **a** Three-dimensional CT, lateral view: sphenoidal fontanelle (*black circle*), mastoid fontanelle (*red circle*), mendosal suture (*red arrow*). *C* Coronal suture, *L* lambdoid suture, *S* squamosal suture. **b** Endocranial view and **c** posterior schematic of the occipital bone and its components. *BO* (*green*) Basioccipital bone, *IO* (*purple*) paired intraoccipital bones, (*blue*) supraoccipital bone. *S* Spheno-occipital suture, *A* anterior intraoccipital sutures, *P* posterior intraoccipital sutures, *O* petro-occipital sutures, *M* occipitomastoid suture. *Red arrows* Bilateral mendosal sutures

Badve CA, K. MM, Iyer RS, Ishak GE, Khanna PC. Craniosynostosis: imaging review and primer on computed tomography. Pediatr Radiol. 2013 Jun;43(6):728–42

Major and secondary skull sutures and age at the onset of fusion[3]

Sutures	Beginning of fusion
Metopic	2 months
Sagittal	22 months
Coronal	24 months
Lambdoid	26 months
Frontonasal	68 months
Frontosphenoidal	22 months
Temporal squamosal	35-39 months

Ghizoni E, Denadai R, Raposo-Amaral CA, Joaquim AF, Tedeschi H, Raposo-Amaral CE. Diagnosis of infant synostotic and nonsynostotic cranial deformities: a review for pediatricians. Revista Paulista de Pediatria (English Edition). 2016 Dec;34(4):495–502.

Classification of craniosynostoses.

1. *Primary*
Simple (involving a single suture): Sagittal, Coronal, Metopic, and Lambdoid
Complex (fusion of two or more sutures)
Nonsyndromic: Bicoronal
Syndromic: Crouzon, Apert, Pfeiffer, and Saethre-Chotzen
2. *Secondary*
Metabolic disorders: Hyperthyroidism, Inborn Errors of Metabolism
Various malformations: Microcephaly, Encephalocele
After ventricular shunt with excessive drainage of CSF (cerebrospinal fluid)
Fetal exposure to certain substances: Valproic acid, Phenytoin
Mucopolysaccharidosis

Ghizoni E, Denadai R, Raposo-Amaral CA, Joaquim AF, Tedeschi H, Raposo-Amaral CE. Diagnosis of infant synostotic and nonsynostotic cranial deformities: a review for pediatricians. Revista Paulista de Pediatria (English Edition). 2016 Dec;34(4):495–502.

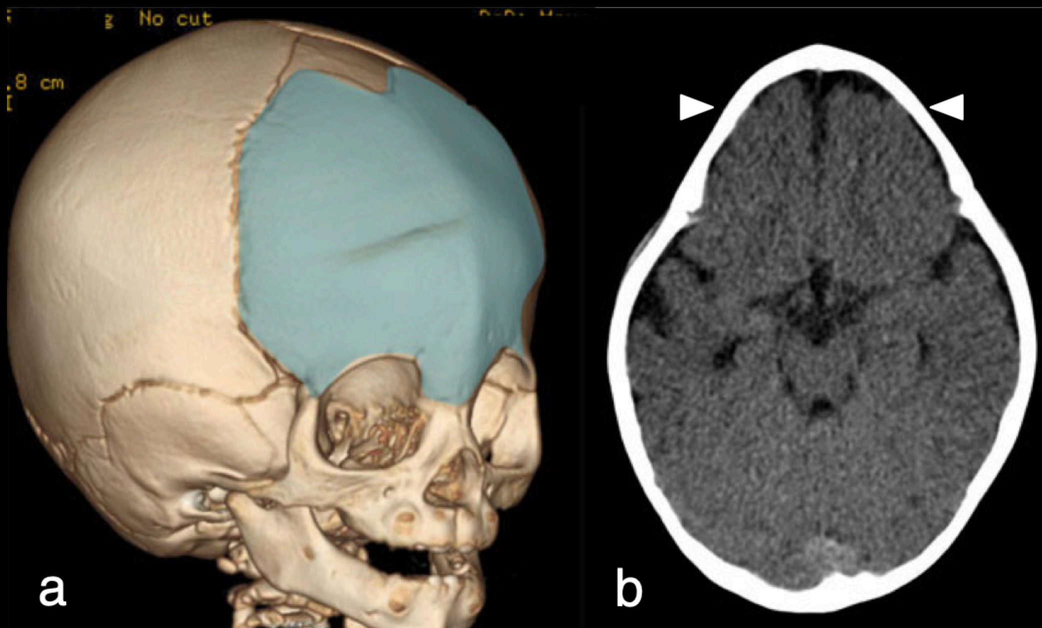

Trigonocephaly

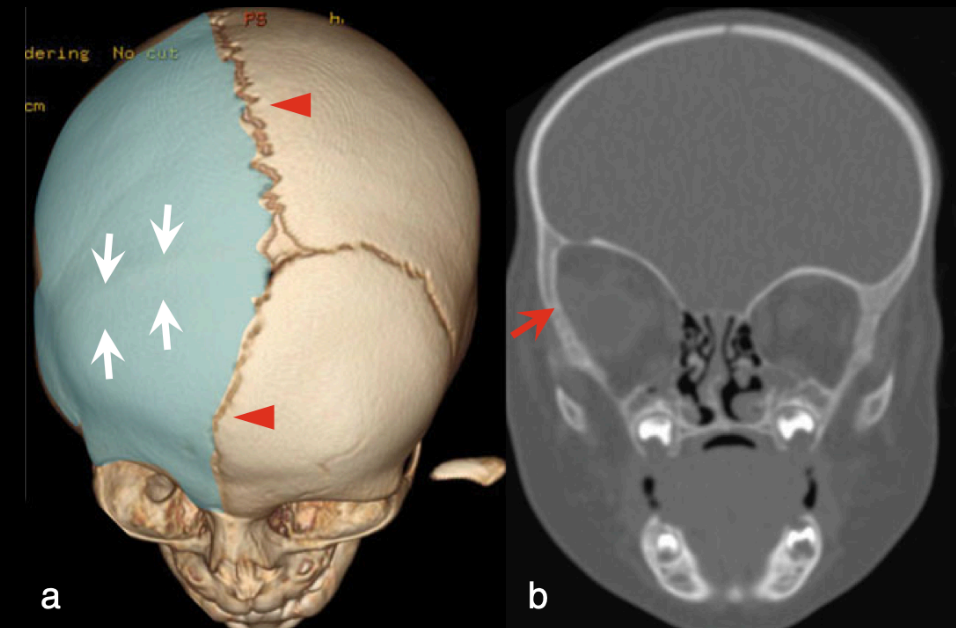

Anteriorplagiocephaly with unicoronal synostosis

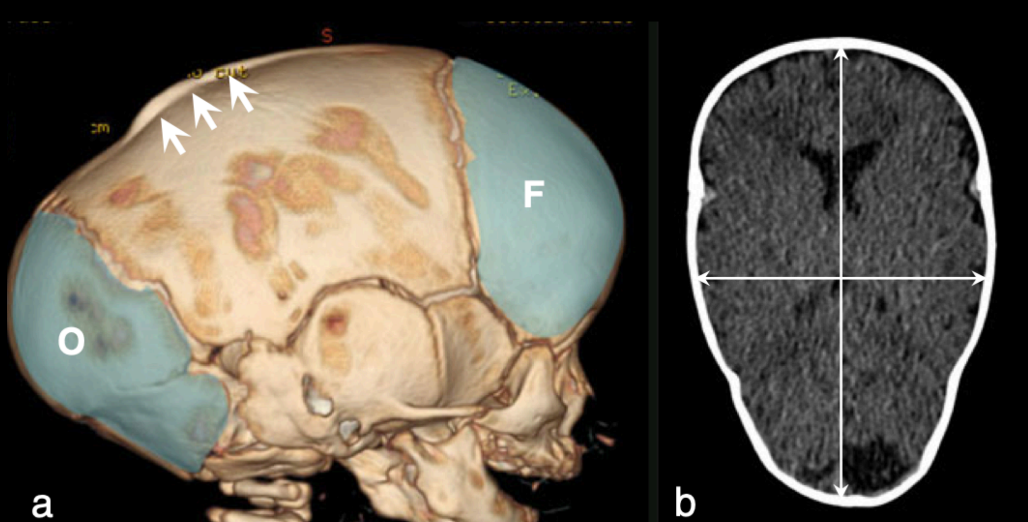

Scaphocephaly

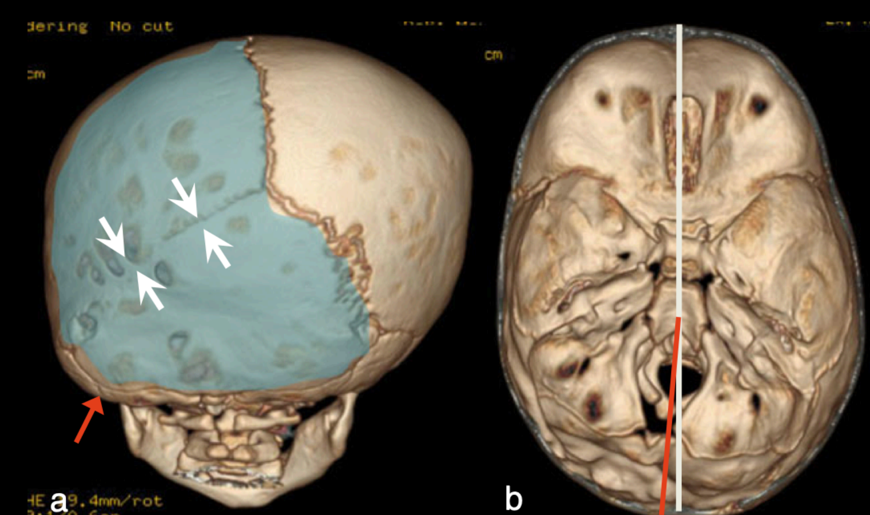

Posterior plagiocephaly with unilateral lambdoid synostosis

Badve CA, K. MM, Iyer RS, Ishak GE, Khanna PC. Craniosynostosis: imaging review and primer on computed tomography. Pediatr Radiol. 2013 Jun;43(6):728–42

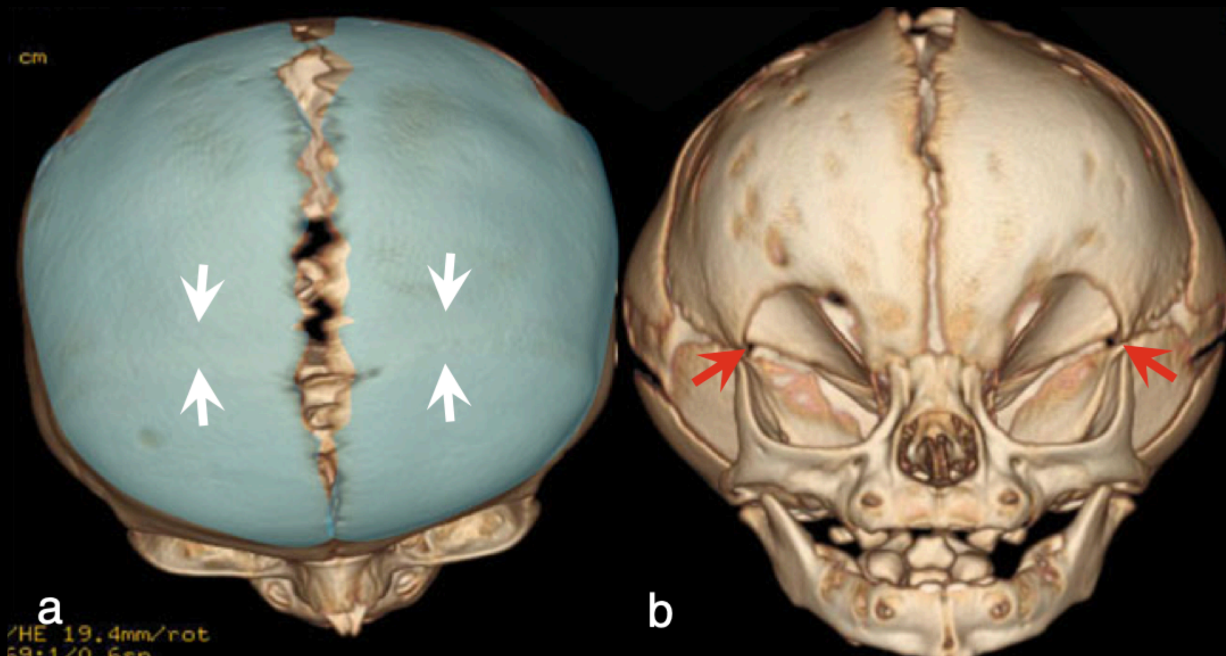

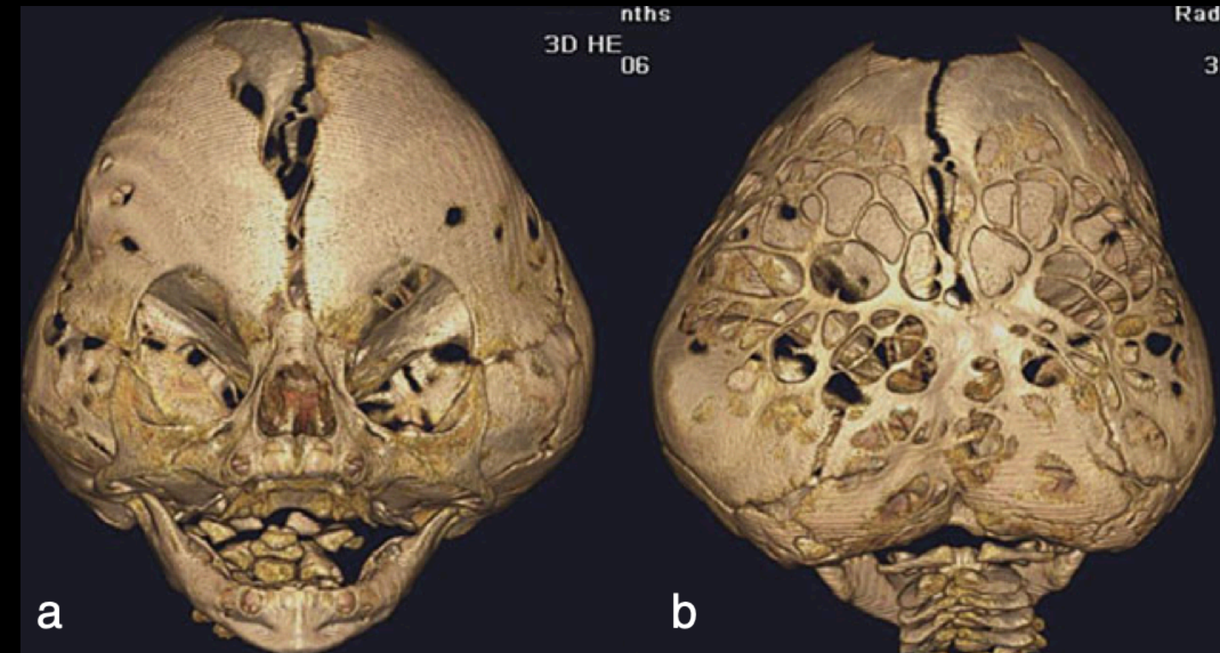

Crouzon syndrome with bicoronal synostosis

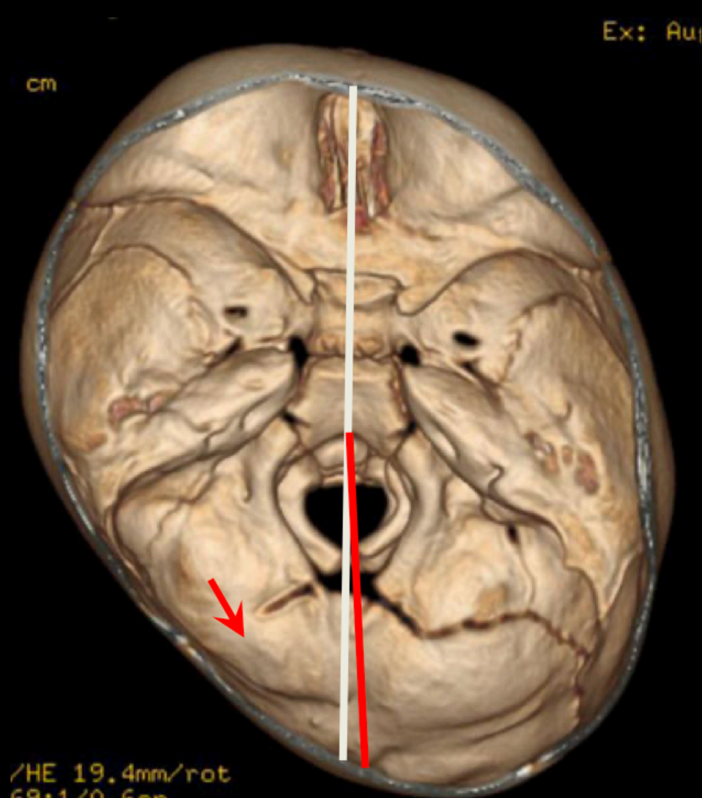

Isolated minor suture synostosis

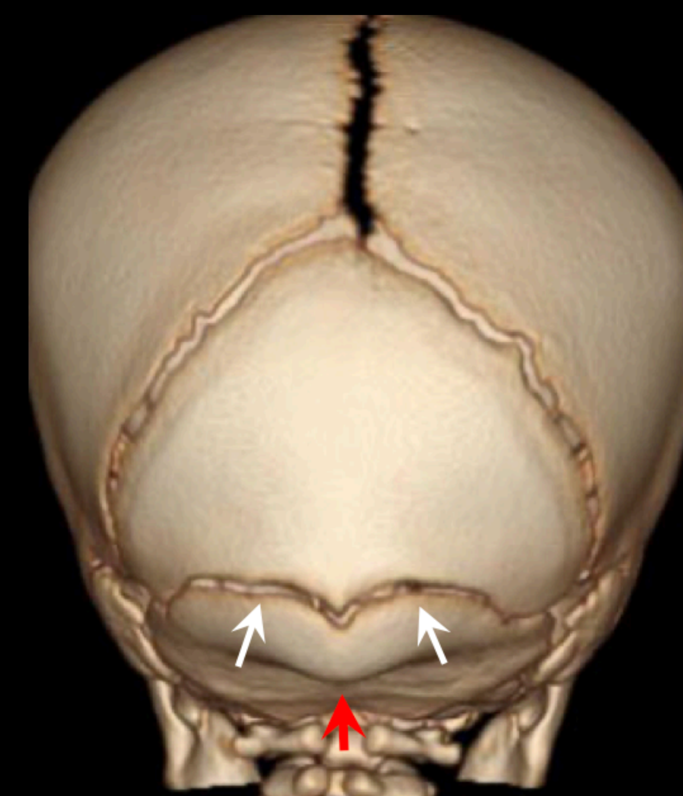

Bathrocephaly

Badve CA, K. MM, Iyer RS, Ishak GE, Khanna PC. Craniosynostosis: imaging review and primer on computed tomography. Pediatr Radiol. 2013 Jun;43(6):728–42

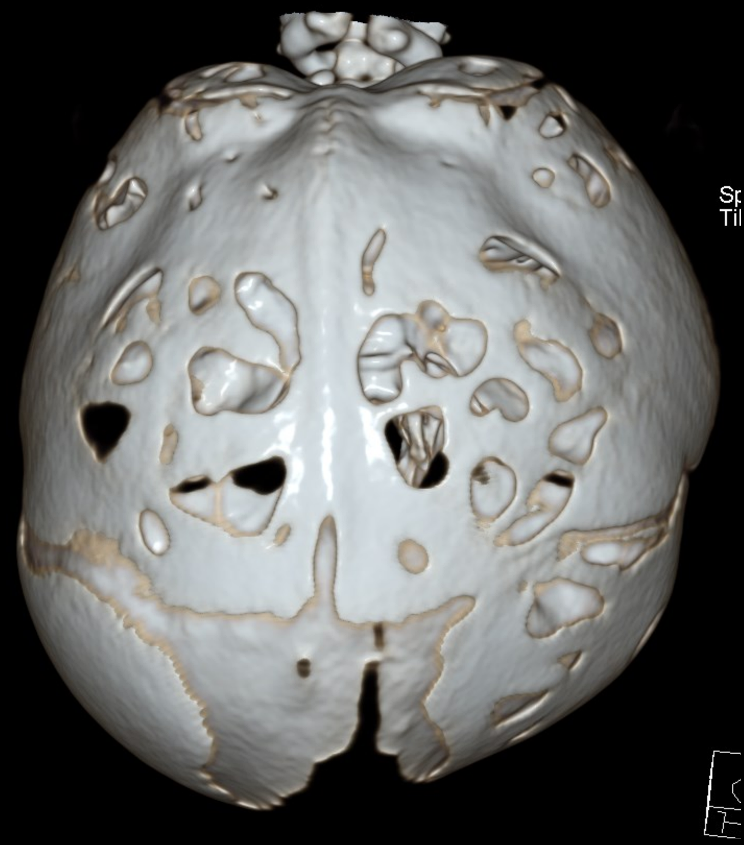

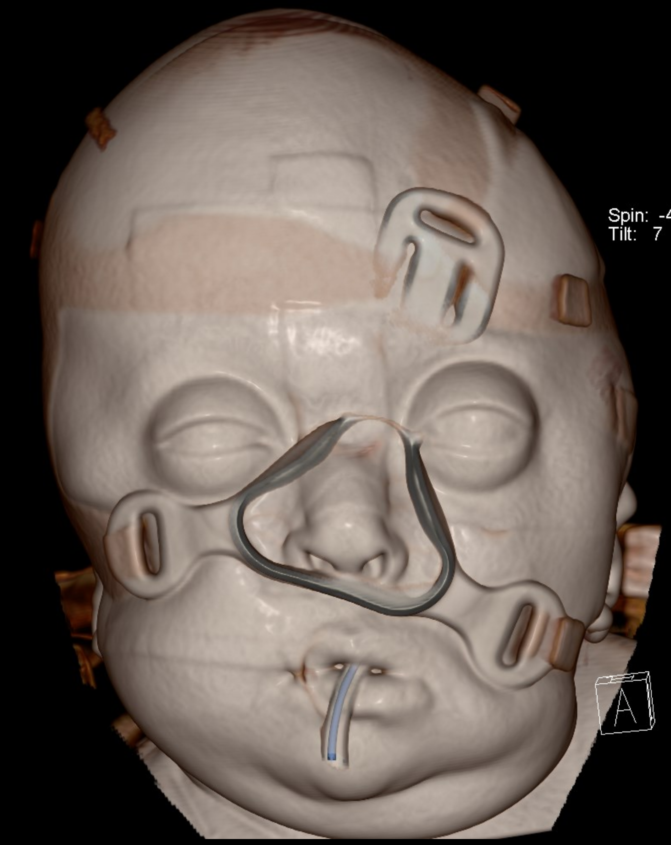

Pfeiffer Syndrome

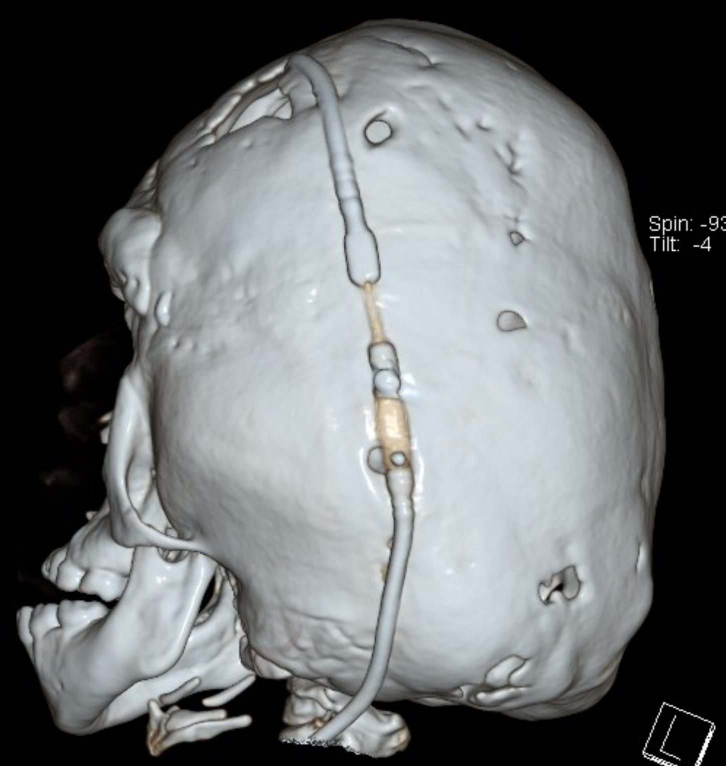

Fosses crâniennes

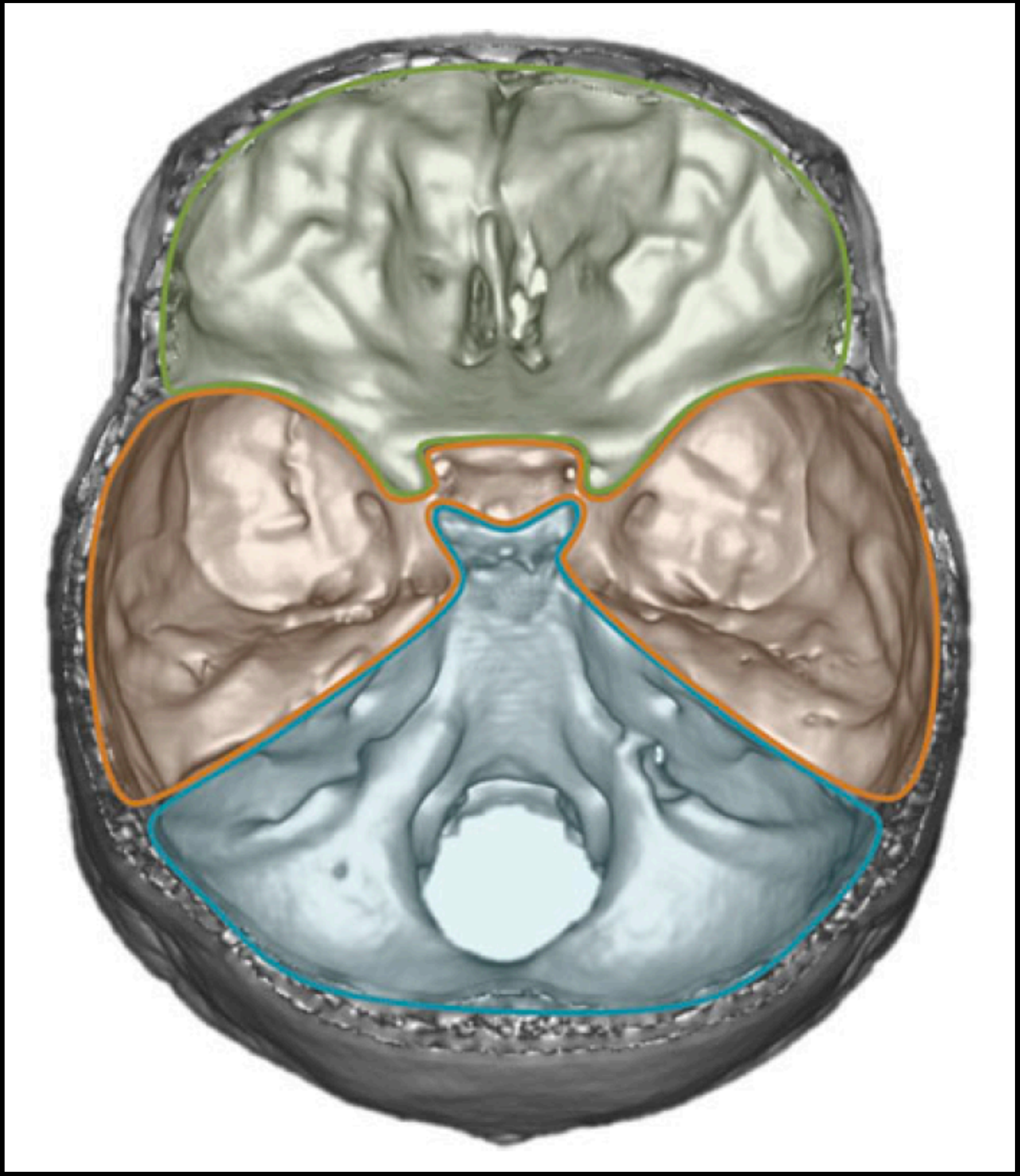

ANTERIEURE

MOYENNE

POSTERIEURE

Clinical Neuroradiology The ESNR Textbook [Internet]. 2019 [cited 2020 Nov 9]. Available from: https://doi.org/10.1007/978-3-319-68536-6

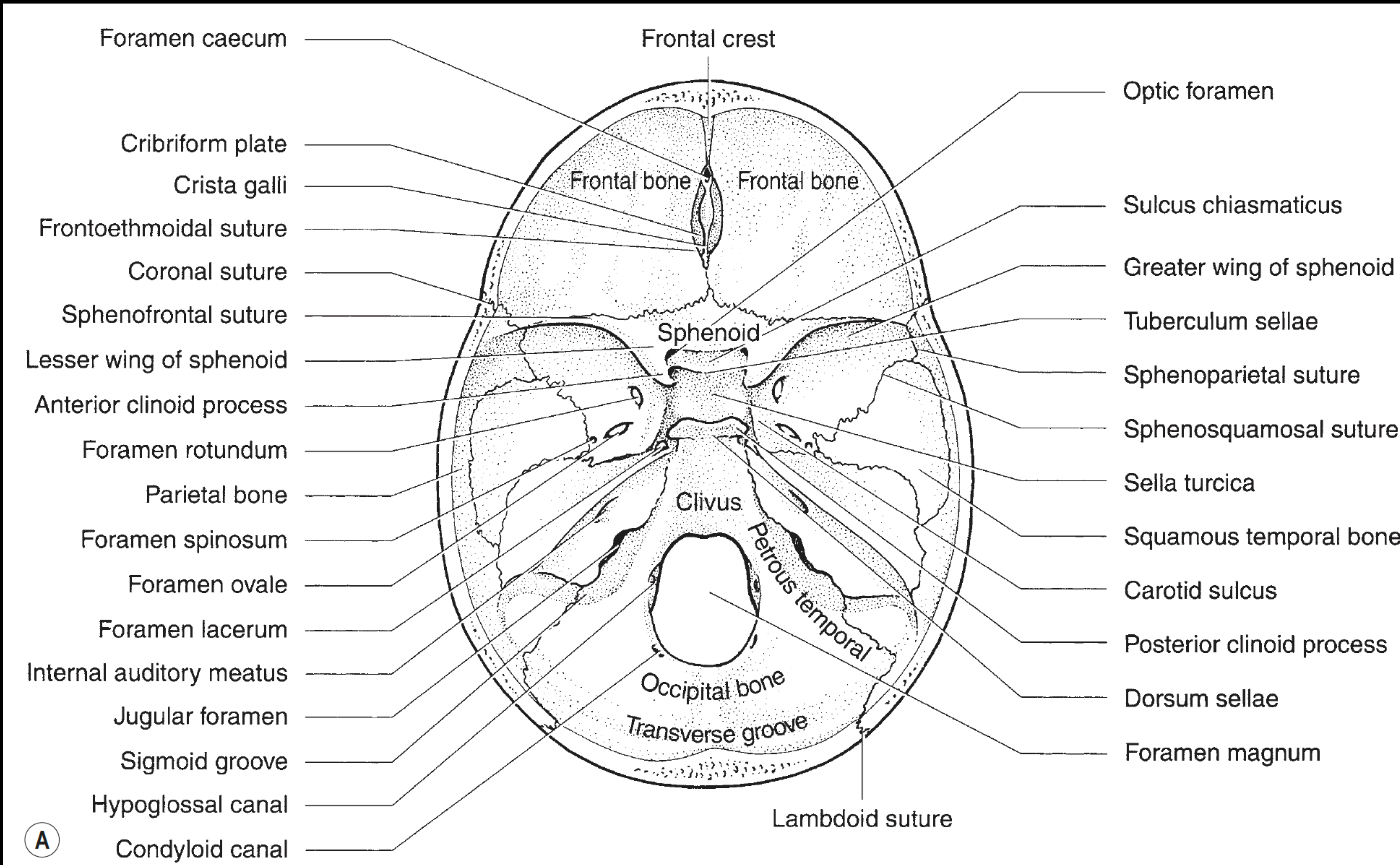

Ryan S, McNicholas M, Eustace SJ. Anatomy for diagnostic imaging. 3rd ed. Edinburgh; New York: Saunders/Elsevier; 2011. 337 p.

Table 1.1 Foramina of the skull base

		Comment	Transmits
Optic canals	Sphenoid bone	Middle cranial fossa to orbital apex	Optic nerves and ophthalmic arteries
Superior orbital fissure	Sphenoid bone	From the middle cranial fossa to the orbital apex	First (orbital) division of the fifth, and the third, fourth and sixth cranial nerves, superior orbital vein and a branch of the middle meningeal artery
Inferior orbital fissure	Between maxilla and sphenoid bones	At its posterior part it forms an opening between the orbit and the pterygopalatine fossa, and more anteriorly between the orbital cavity and the infratemporal fossa	Infraorbital nerve and infraorbital artery and the inferior ophthalmic veins
Foramen rotundum	Sphenoid bone	From the middle cranial fossa to the pterygopalatine fossa	Second (maxillary) division of the fifth cranial nerve
Foramen ovale	Sphenoid bone	From the middle cranial fossa to the infratemporal fossa	Third (mandibular) division of the fifth cranial nerve and the accessory meningeal artery
Foramen spinosum	Sphenoid bone	From the infratemporal to the middle cranial fossa	The middle meningeal artery
Foramen lacerum	Apex of temporal bone		Carotid artery passes through its posterior wall
IAM	Petrous temporal bone	From the posterior cranial fossa to inner ear	Seventh and eighth cranial nerves and the internal auditory artery
Jugular foramen	Junction of occipital and petrous temporal bones	Not visible on SMV	Internal jugular vein, ninth, tenth and eleventh cranial nerves. Inferior petrosal sinus (which drains into the internal jugular vein), and ascending occipital and pharyngeal arterial branches
Hypoglossal canal	Occipital bone		Twelfth (hypoglossal) cranial nerve
Foramen magnum	Occipital bone	From the posterior cranial fossa to the spinal canal	Medulla oblongata/spinal cord, along vertebral and spinal arteries and veins and the spinal root of the eleventh cranial nerve

Ryan S, McNicholas M, Eustace SJ. Anatomy for diagnostic imaging. 3rd ed. Edinburgh; New York: Saunders/Elsevier; 2011. 337 p.

Orbite

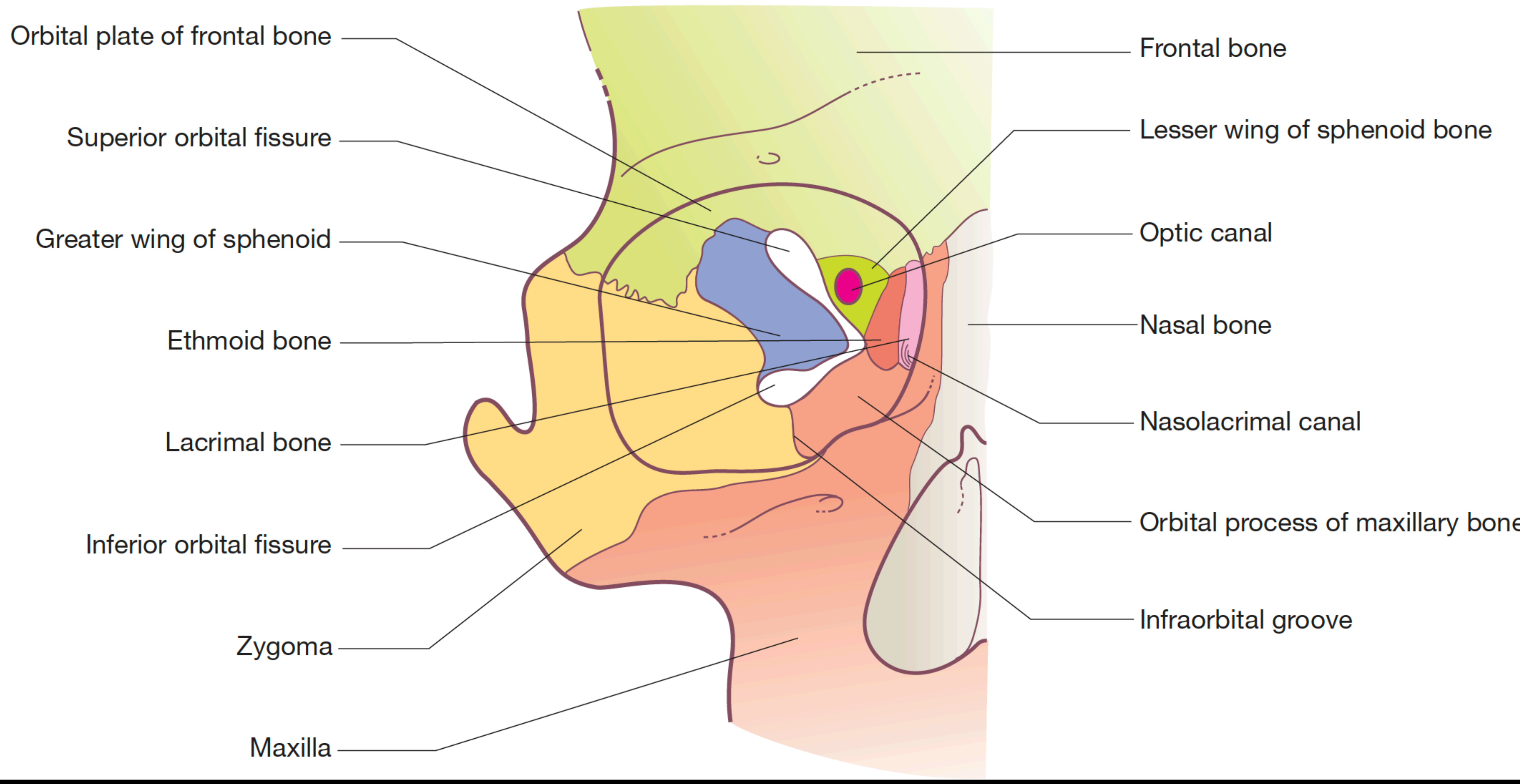

Ryan S, McNicholas M, Eustace SJ. Anatomy for diagnostic imaging. 3rd ed. Edinburgh; New York: Saunders/Elsevier; 2011. 337 p.

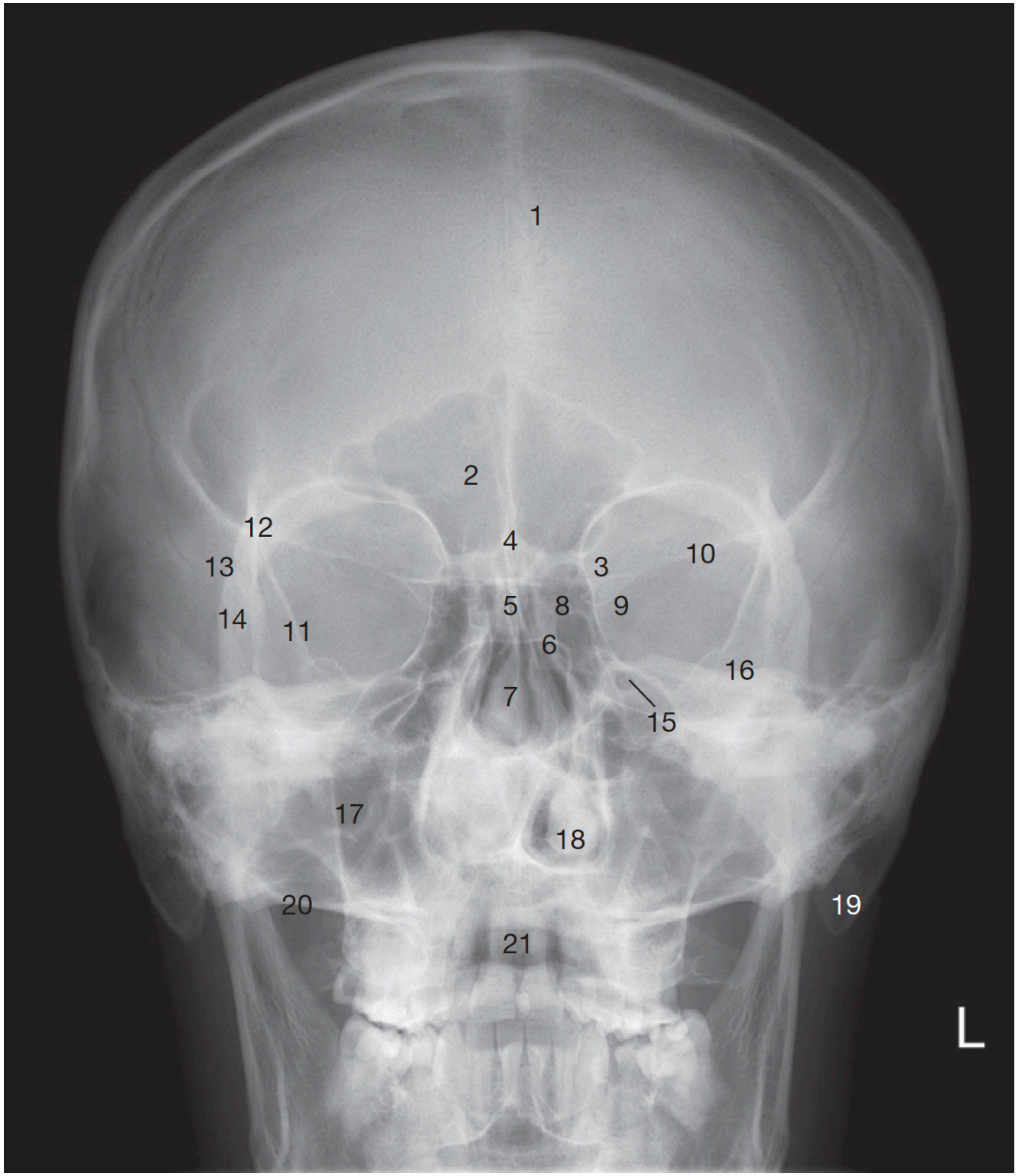

Figure 1.4 • OF20 skull radiograph.

1. Sagittal suture
2. Frontal sinus
3. Planum sphenoidale
4. Crista galli
5. Perpendicular plate of ethmoid
6. Floor of pituitary fossa
7. Nasal septum
8. Ethmoid air cells
9. Superior orbital fissure
10. Lesser wing of sphenoid
11. Innominate line
12. Zygomatic process of frontal bone
13. Zygomaticofrontal suture
14. Frontal process of zygomatic bone
15. Foramen rotundum
16. Petrous ridge
17. Maxillary sinus
18. Inferior nasal turbinate
19. Mastoid process
20. Occipital bone
21. Dens of atlas

Ryan S, McNicholas M, Eustace SJ. Anatomy for diagnostic imaging. 3rd ed. Edinburgh; New York: Saunders/Elsevier; 2011. 337 p.

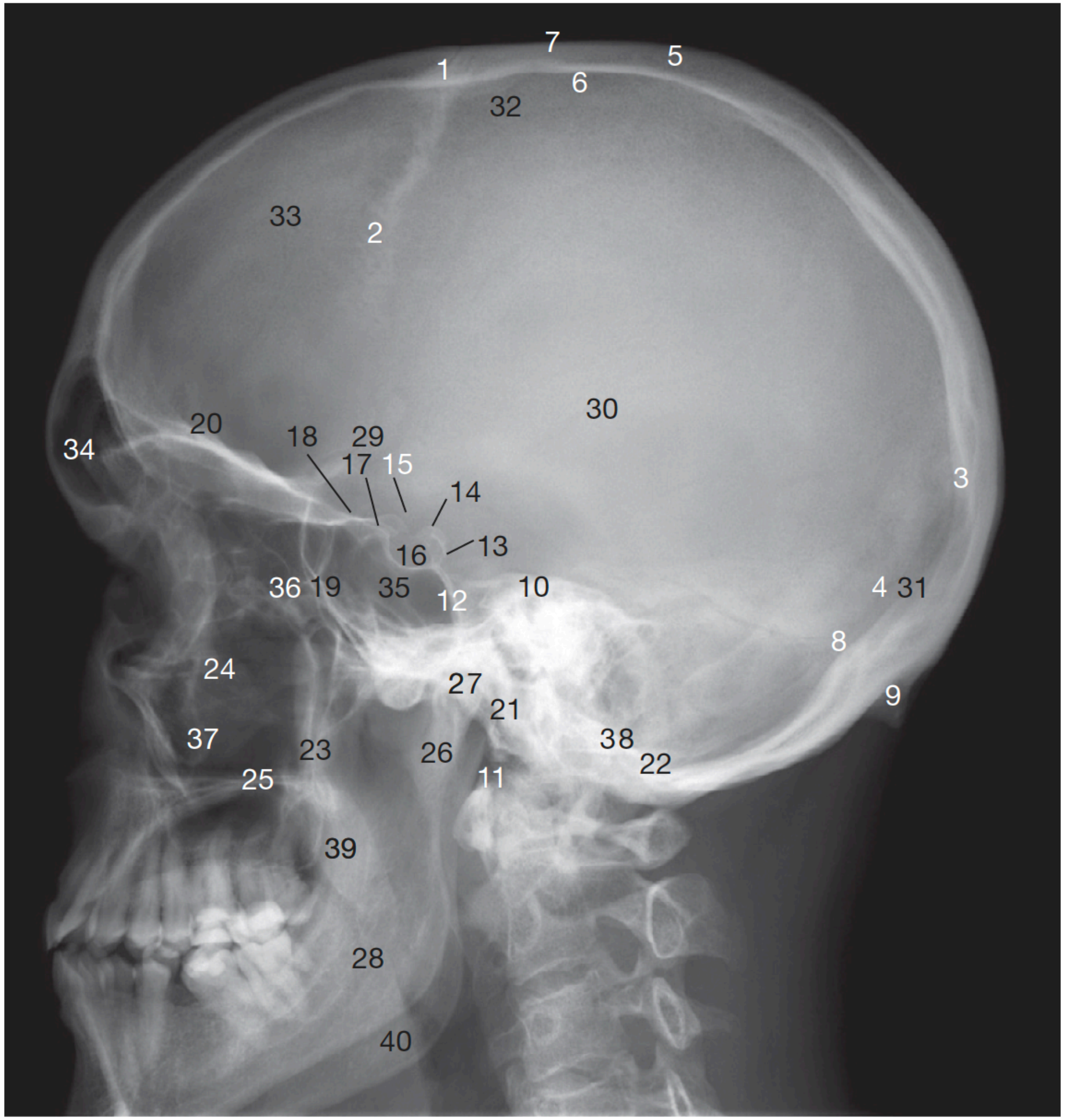

Figure 1.3 • Lateral skull radiograph.

Bony landmarks

1. Bregma
2. Coronal suture
3. Lambda
4. Lambdoid suture
5. Vertex
6. Inner skull table
7. Outer skull table
8. Internal occipital protuberance
9. External occipital protuberance
10. External auditory meatus
11. Styloid process
12. Clivus
13. Dorsum sellae
14. Posterior clinoid process
15. Anterior clinoid process
16. Pituitary fossa (sella turcica)
17. Tuberculum sellae
18. Planum sphenoidale
19. Greater wings of sphenoid
20. Undulating floor of anterior cranial fossa (roof of orbit)
21. Anterior limit of foramen magnum
22. Posterior limit of foramen magnum
23. Posterior wall of maxillary sinus
24. Floor of orbit
25. Hard palate
26. Neck of mandible
27. Temporomandibular joint
28. Condylar (mandibular) canal

Ryan S, McNicholas M, Eustace SJ. Anatomy for diagnostic imaging. 3rd ed. Edinburgh; New York: Saunders/Elsevier; 2011. 337 p.

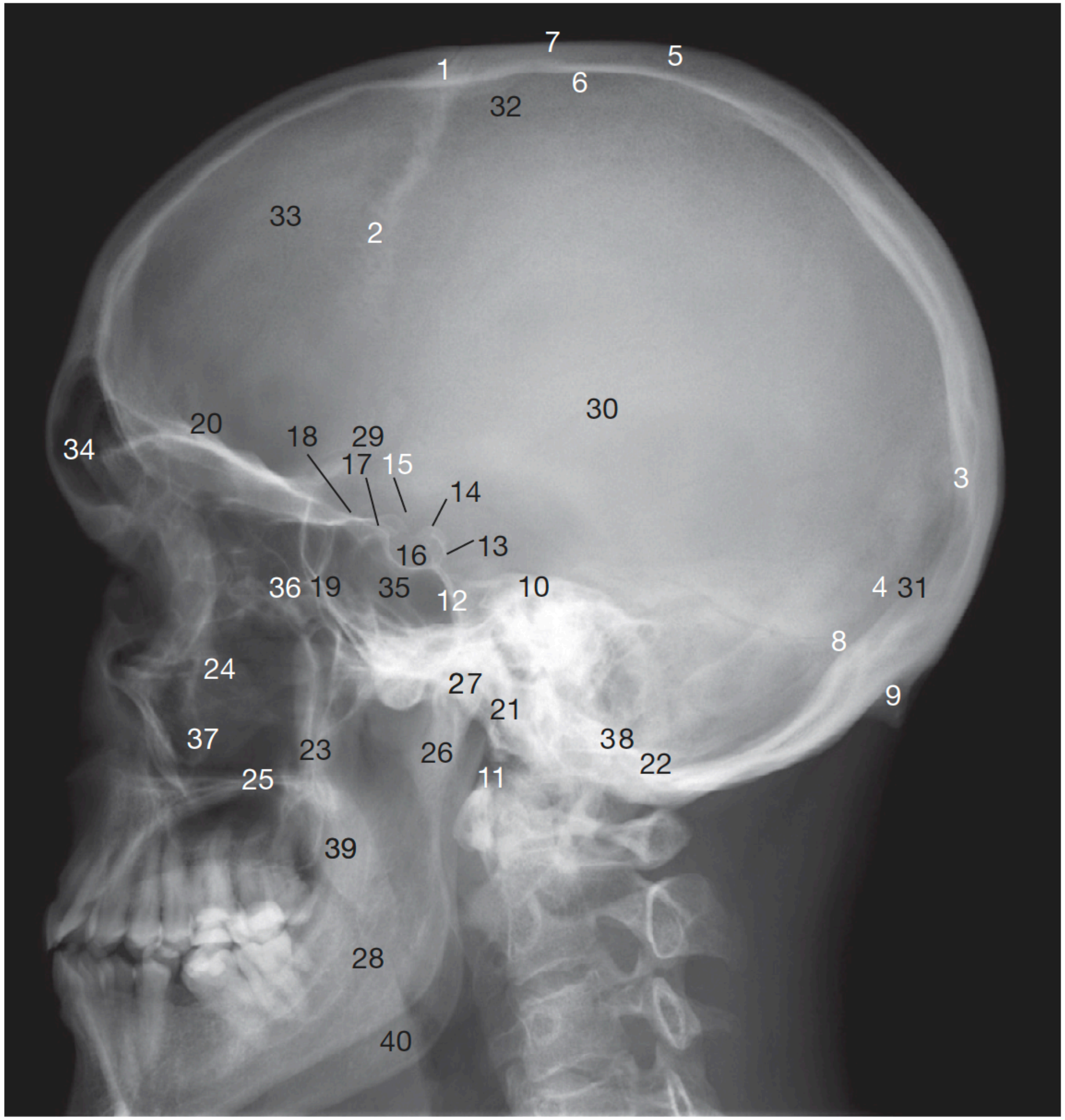

Vascular markings

29. Middle meningeal vessels: anterior branches
30. Middle meningeal vessels: posterior branches
31. Transverse sinus
32. Diploic vein
33. Diploic venous confluence: parietal star

Sinuses/air cells

34. Frontal sinus
35. Sphenoid sinus
36. Posterior ethmoidal cells
37. Maxillary sinus
38. Mastoid air cells

Soft tissues

39. Soft palate
40. Base of tongue

Ryan S, McNicholas M, Eustace SJ. Anatomy for diagnostic imaging. 3rd ed. Edinburgh; New York: Saunders/Elsevier; 2011. 337 p.

Incidences

Face

Profil

Incidences

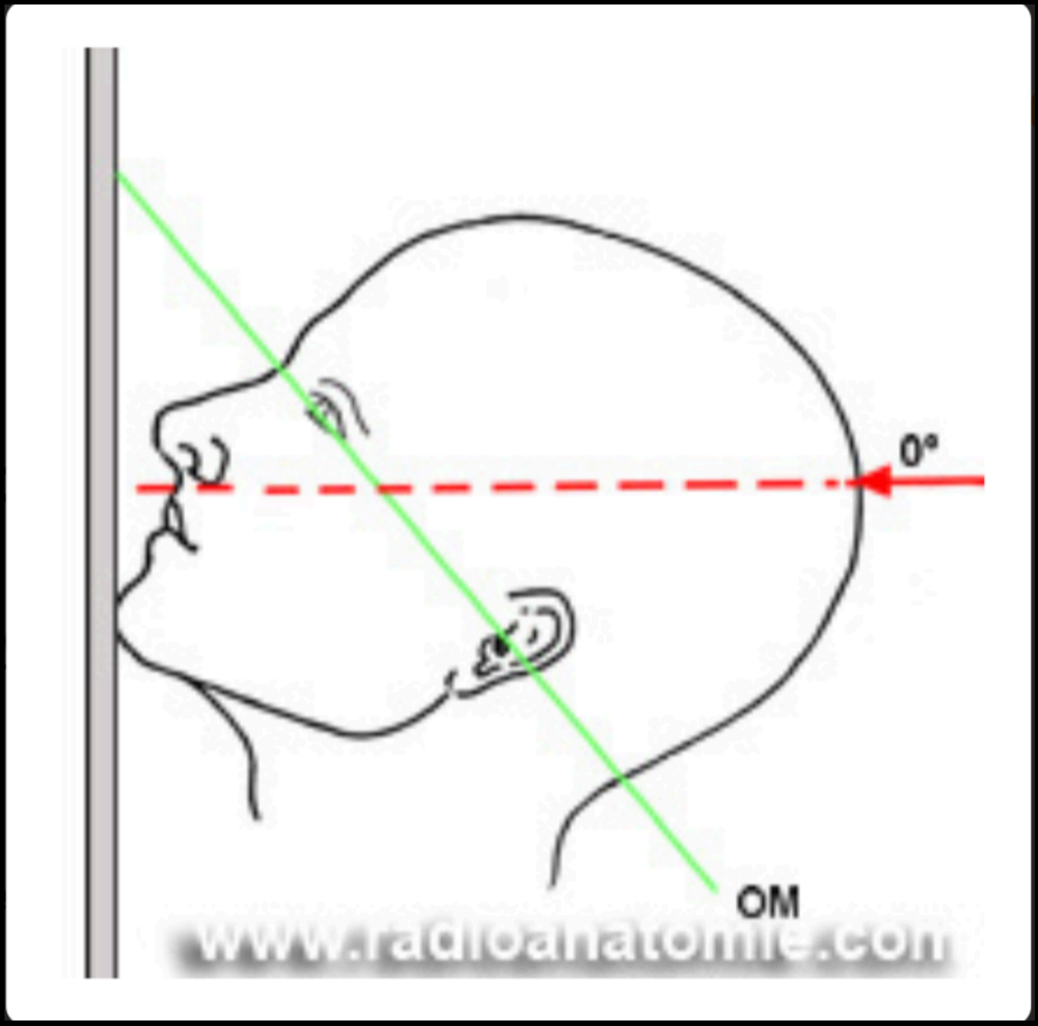

Incidence de Blondeau

INDICATIONS

Radiographie du crâne

- Cadre médico-légal (assurance école)
- Critères disponibles sur le net
  - ACR (American College of Radiology) appropriateness criteria

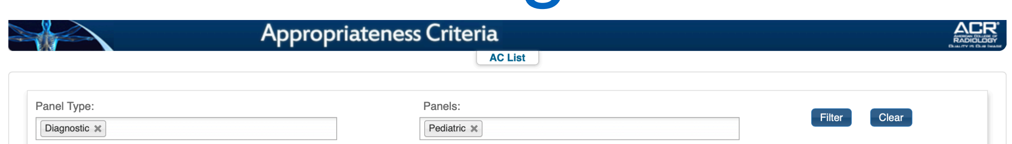

  - iGuide ESR

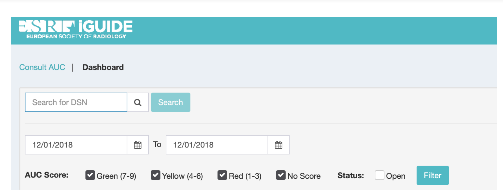

  - SFR guide en ligne

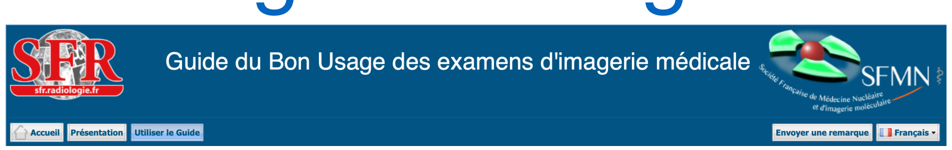

Traumatisme


D

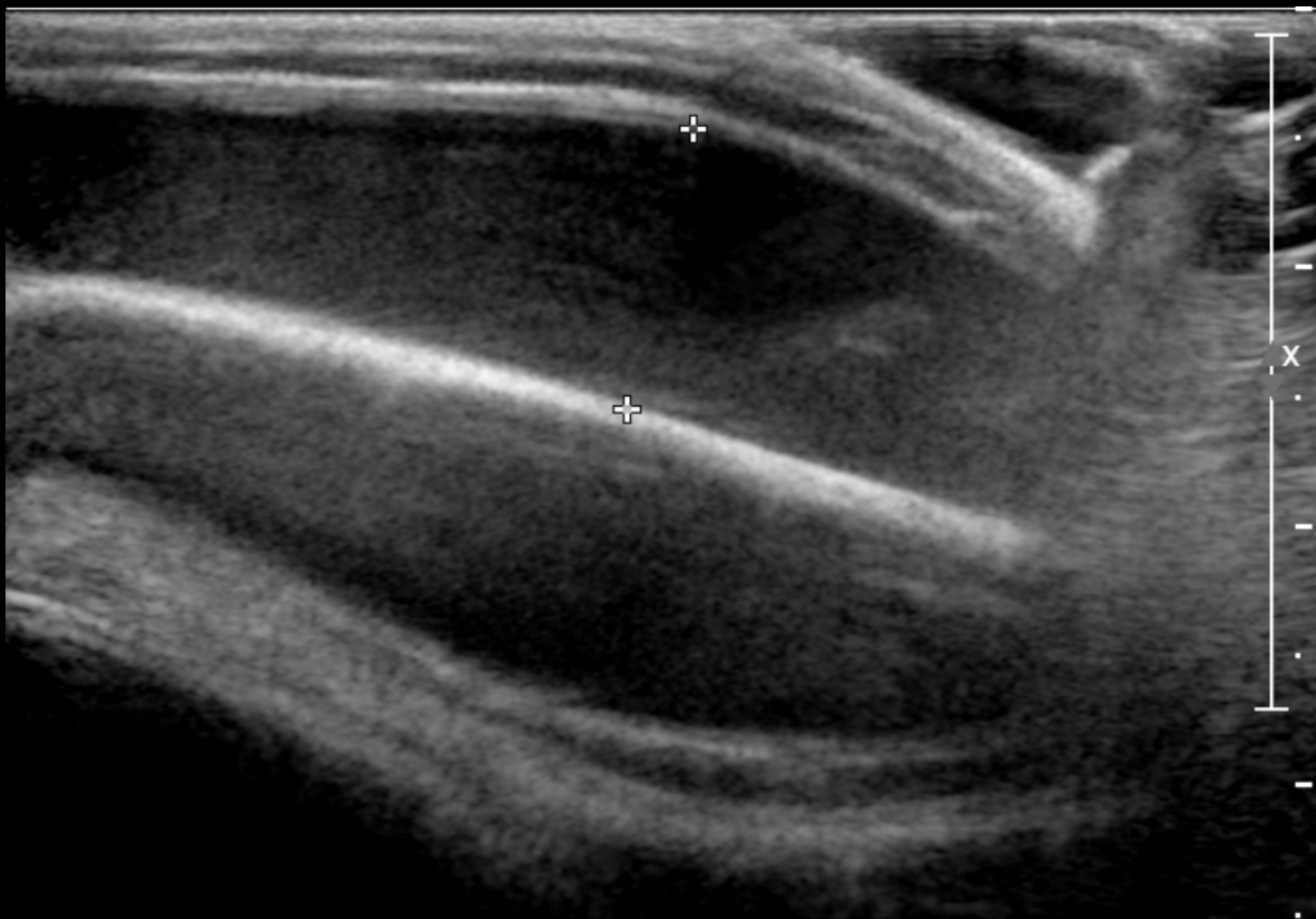
X

artéfact en miroir

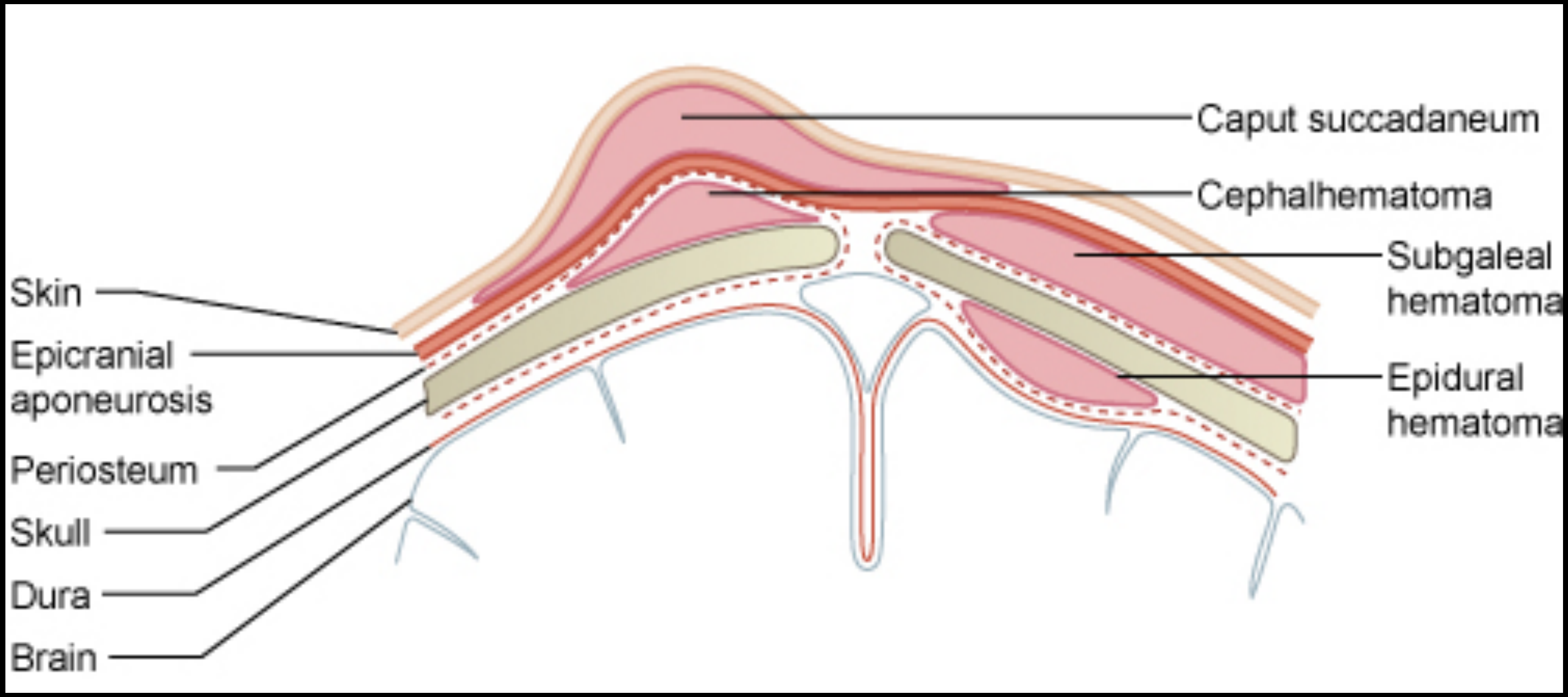

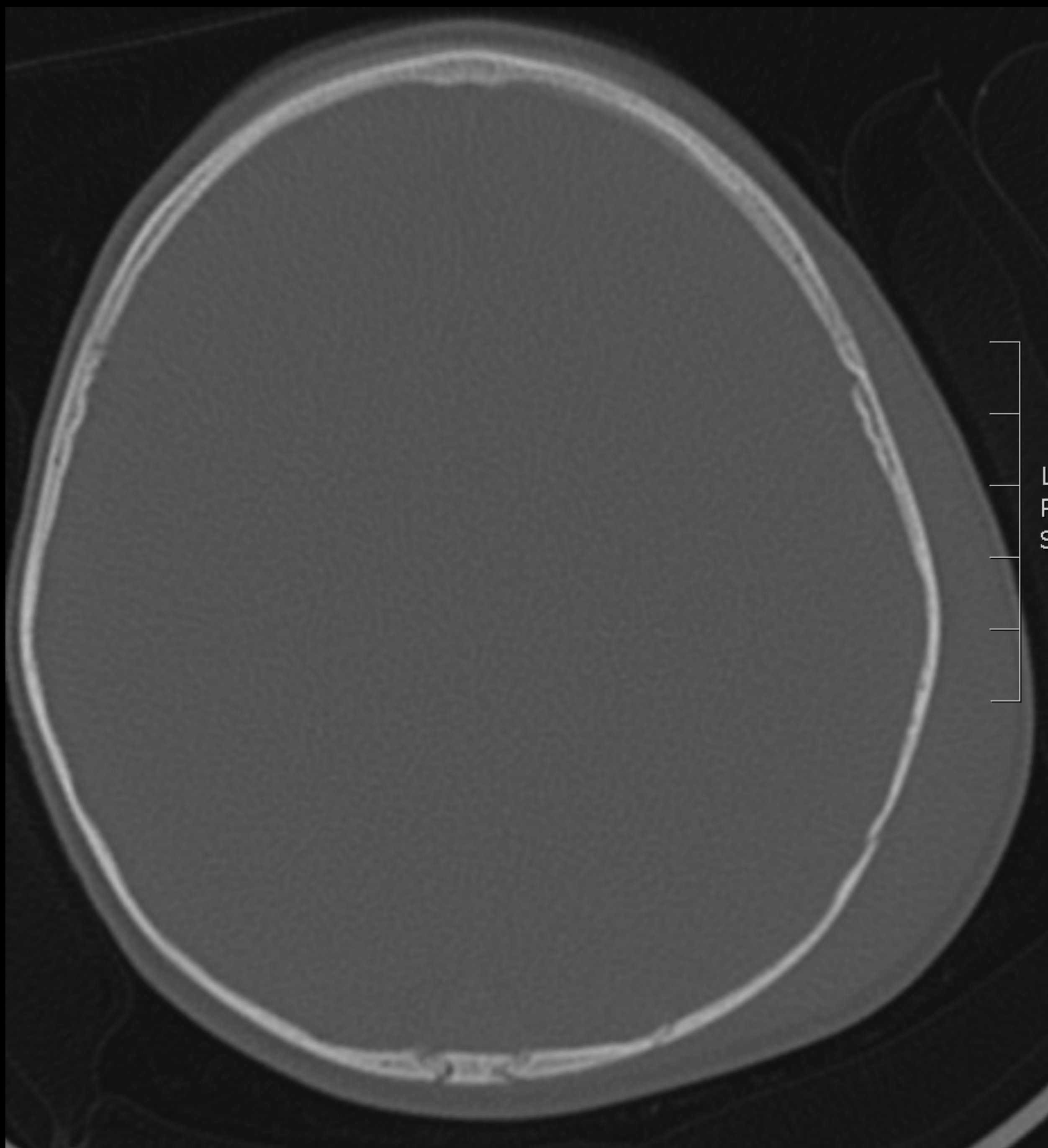
L
P
S

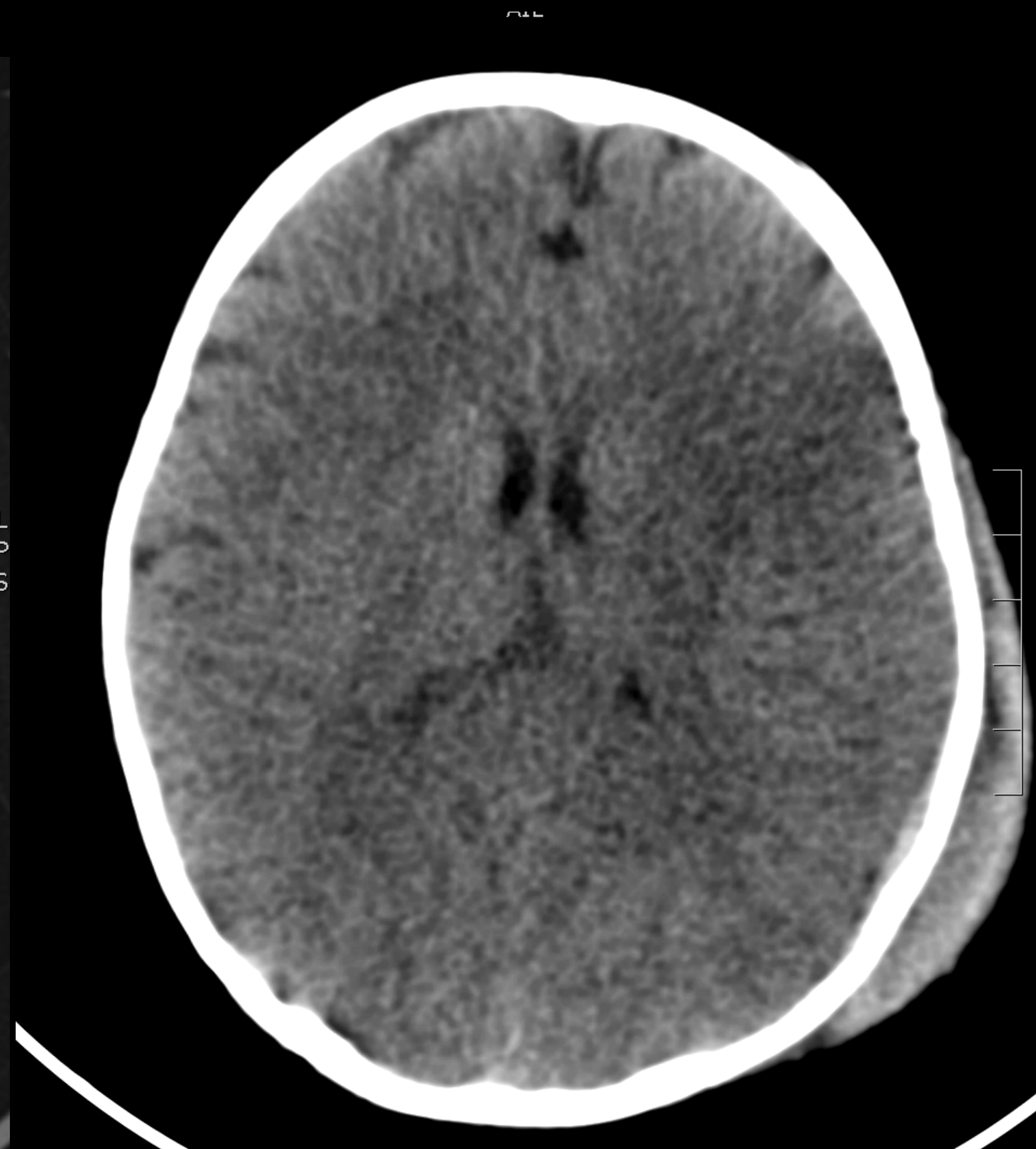

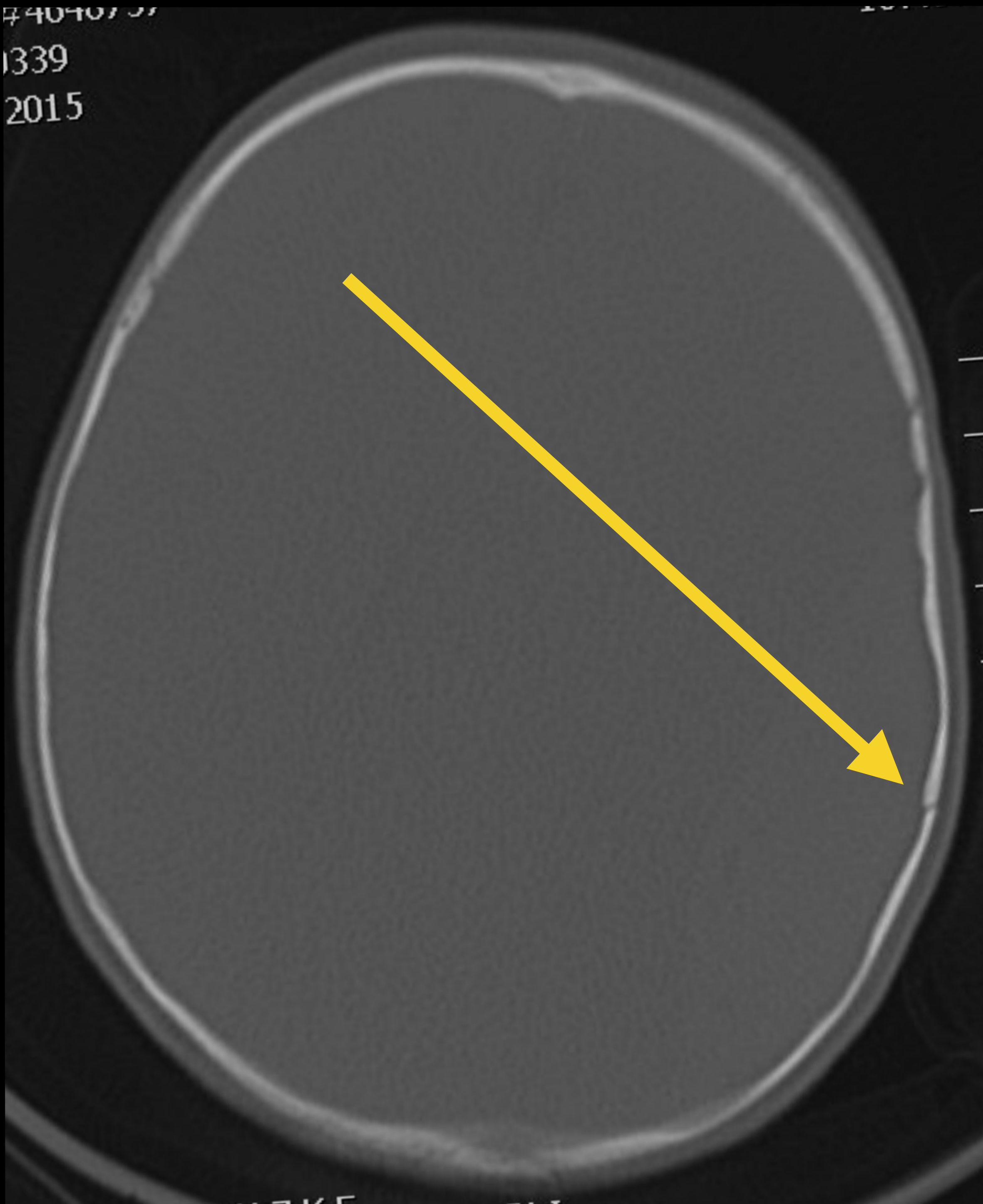
339
2015
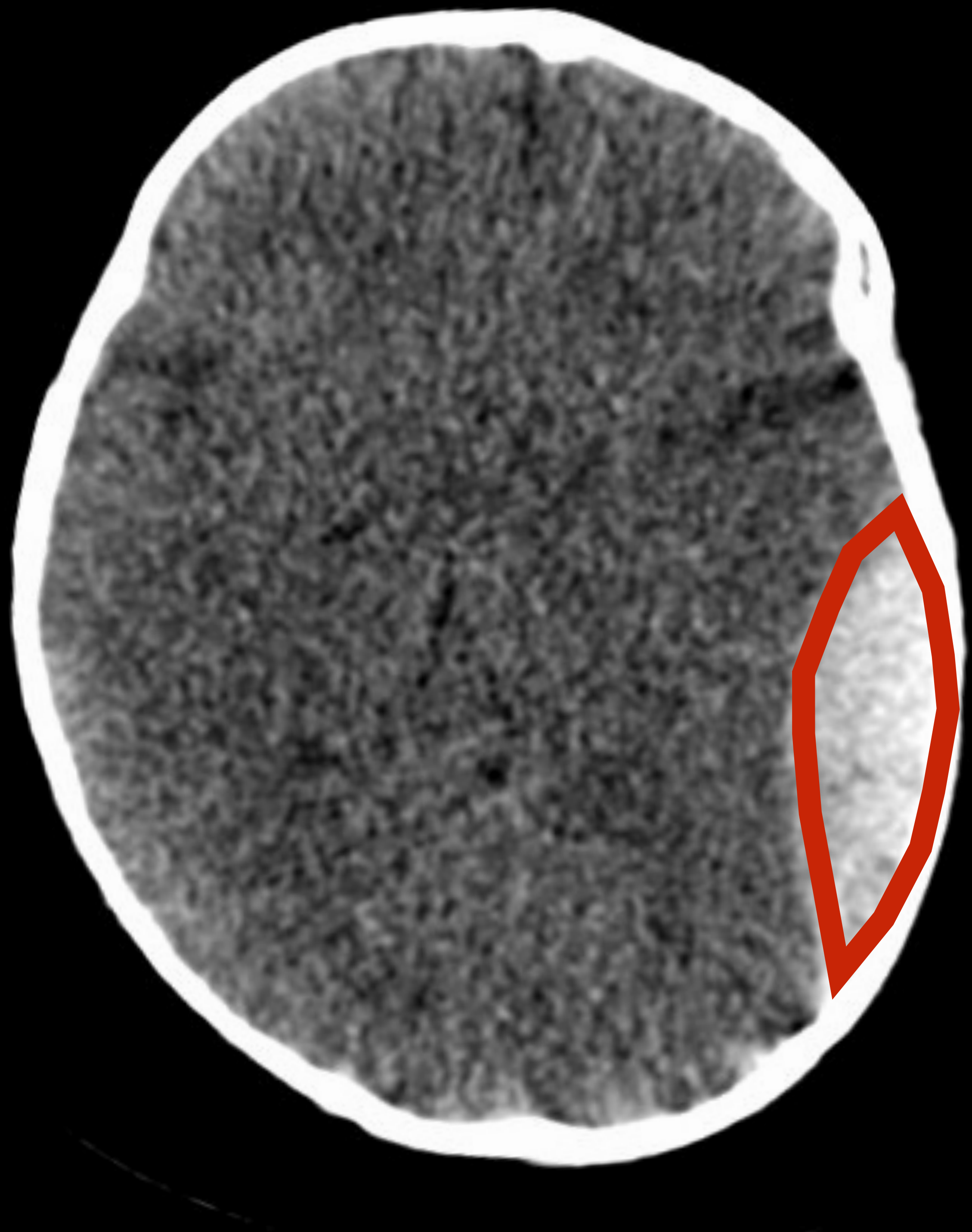

TDM axiale

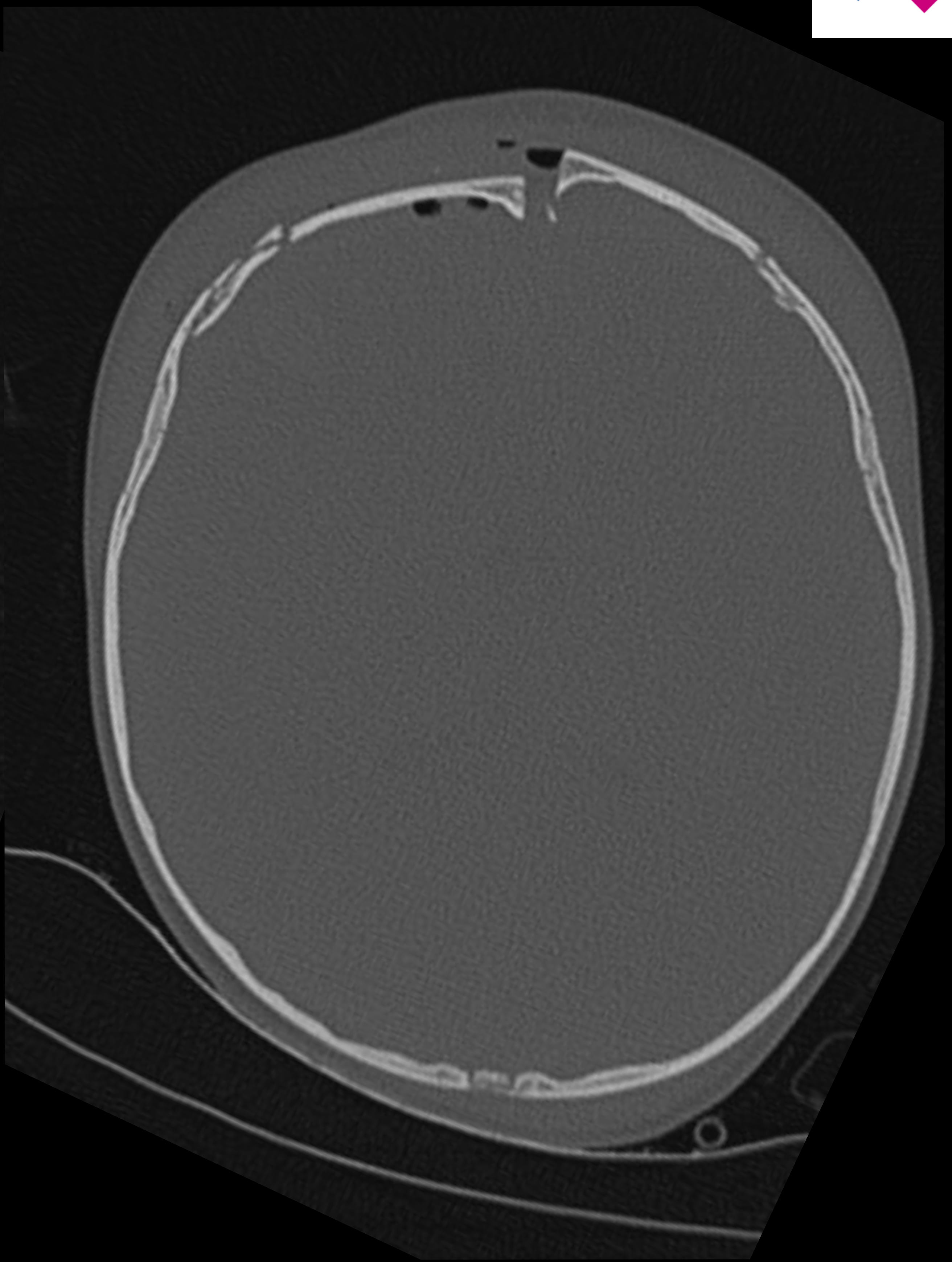

TDM axiale

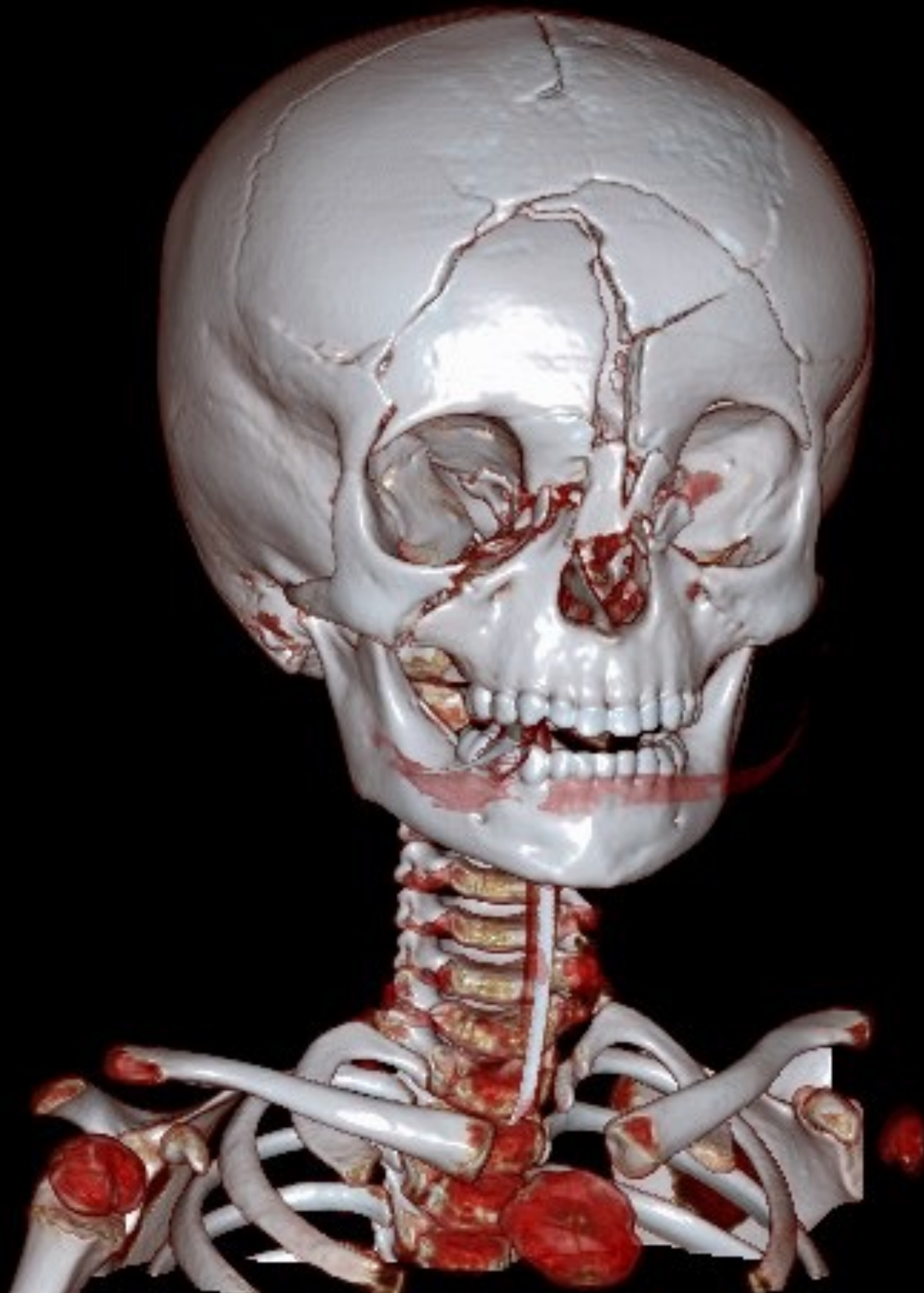

TDM reconstructions volumiques

TDM axiale

TDM axiale

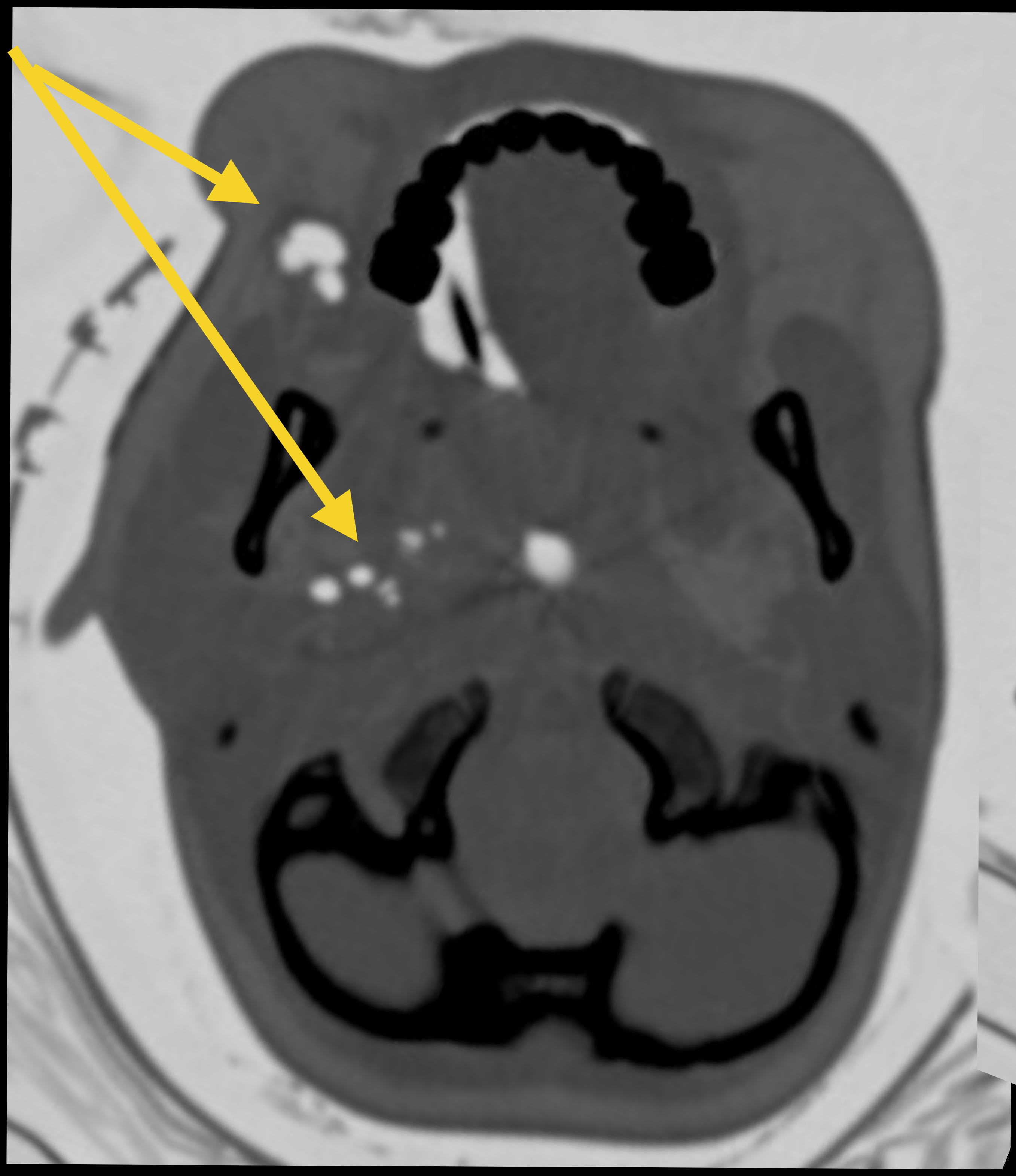

TDM axiale

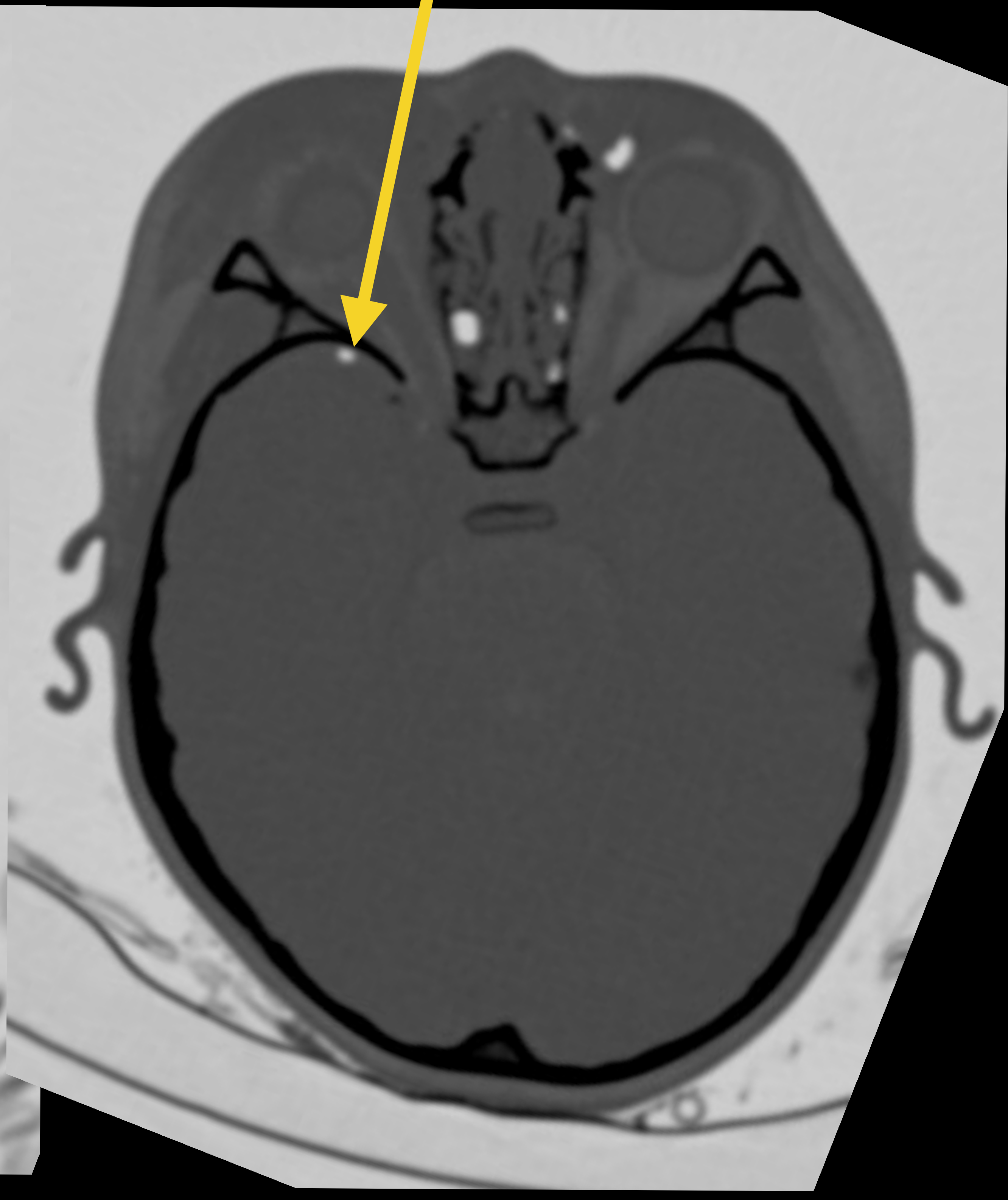

TDM axiale

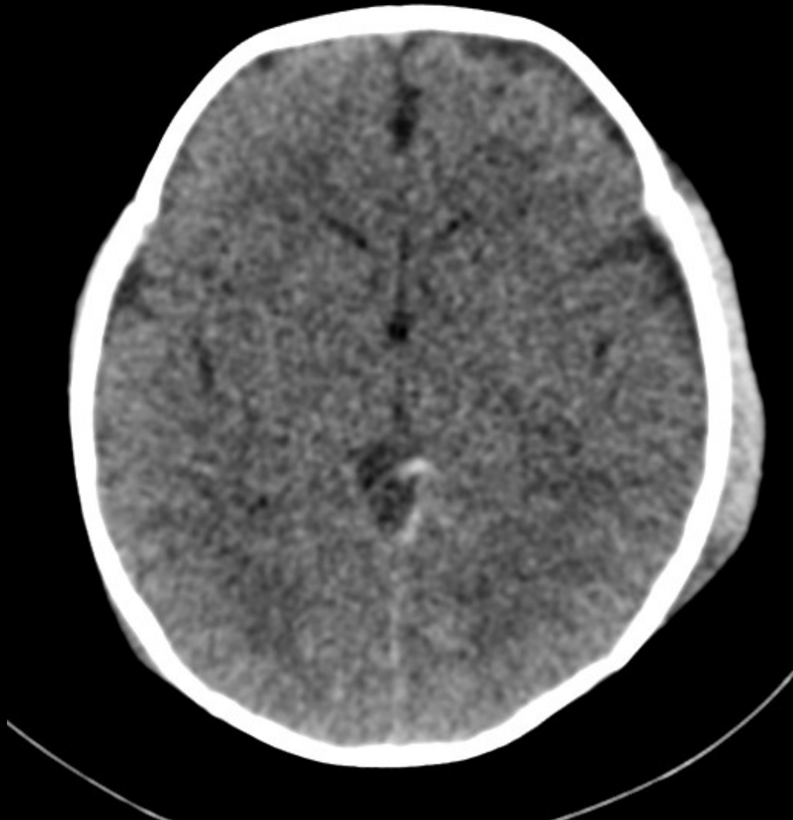

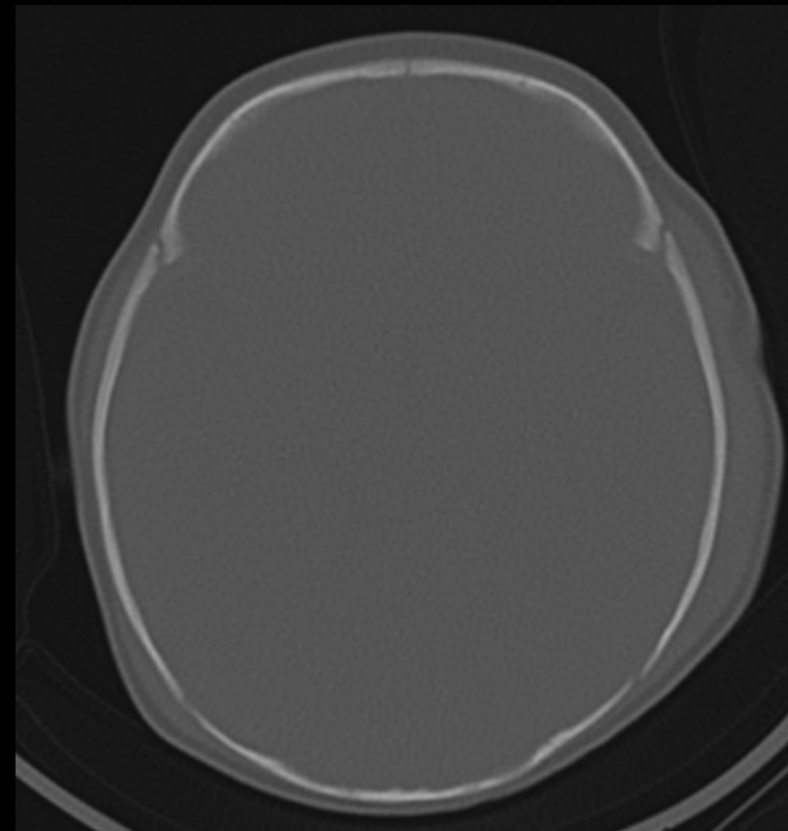

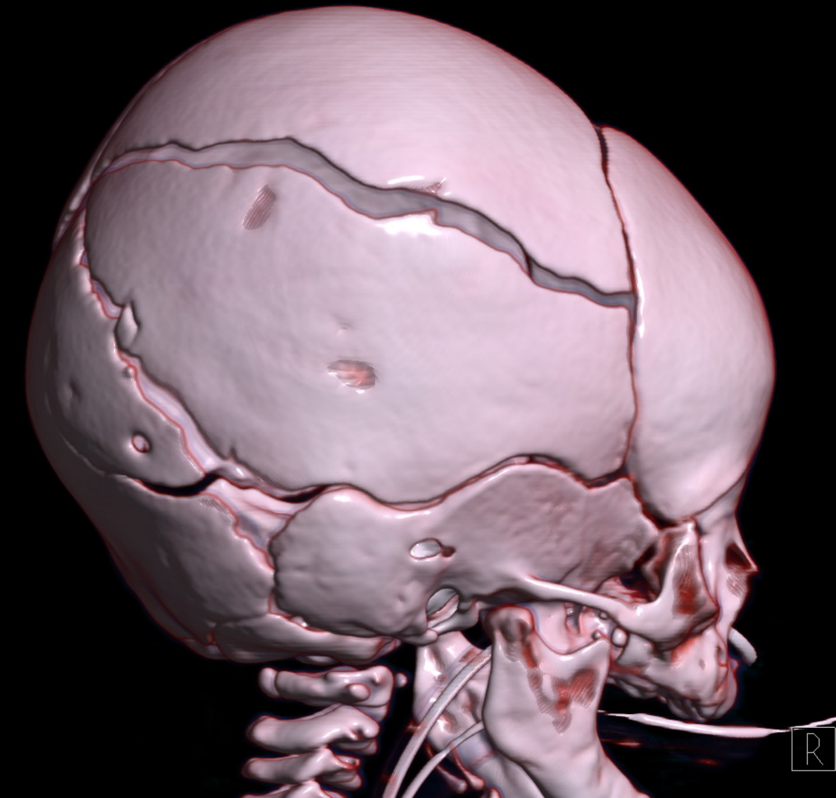

Traumatisme non accidentel

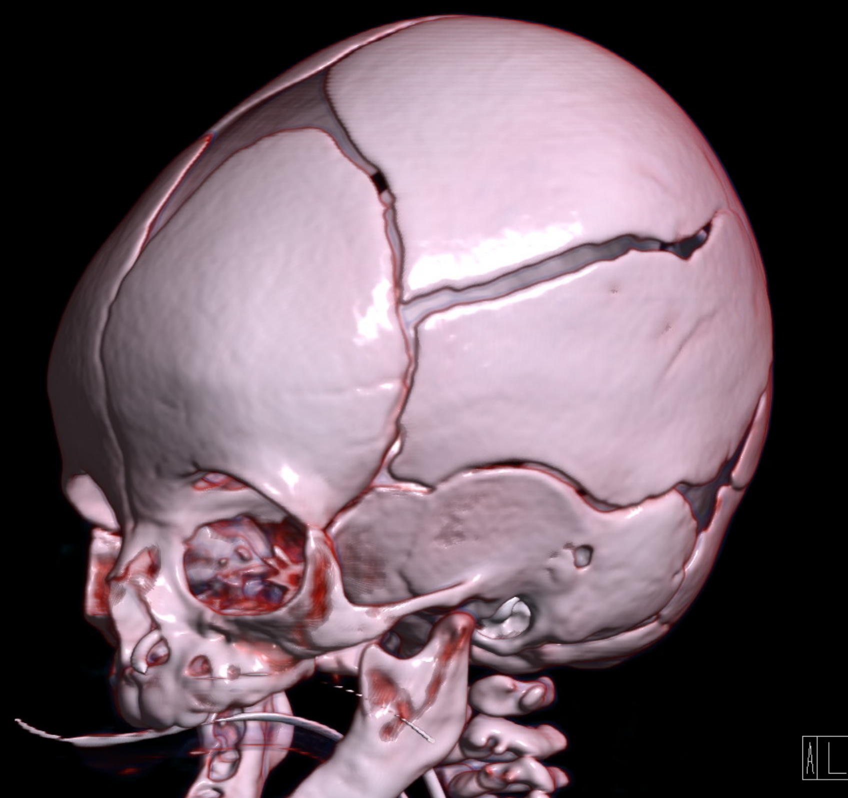

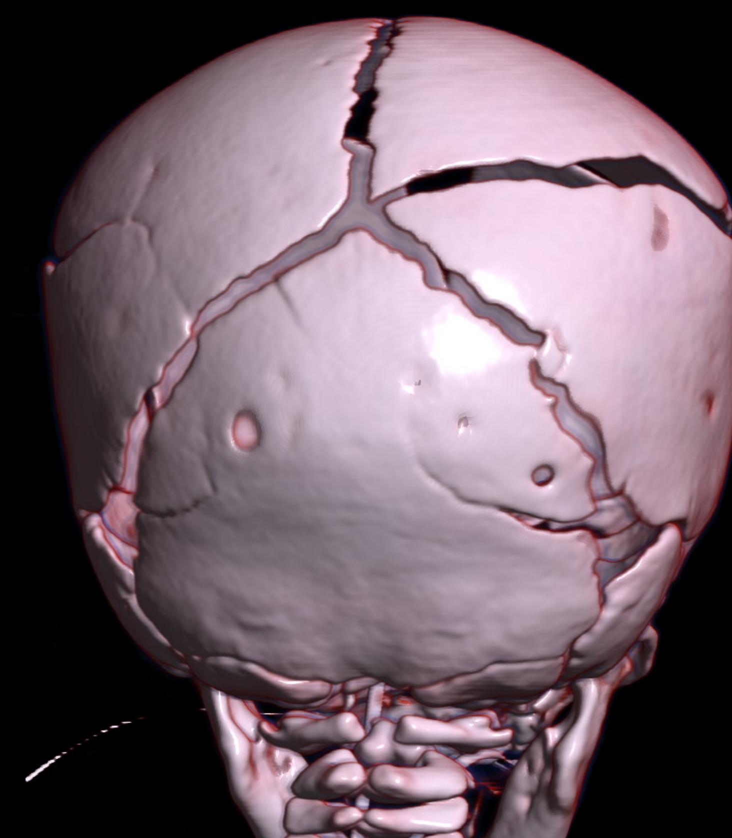

Corps étranger

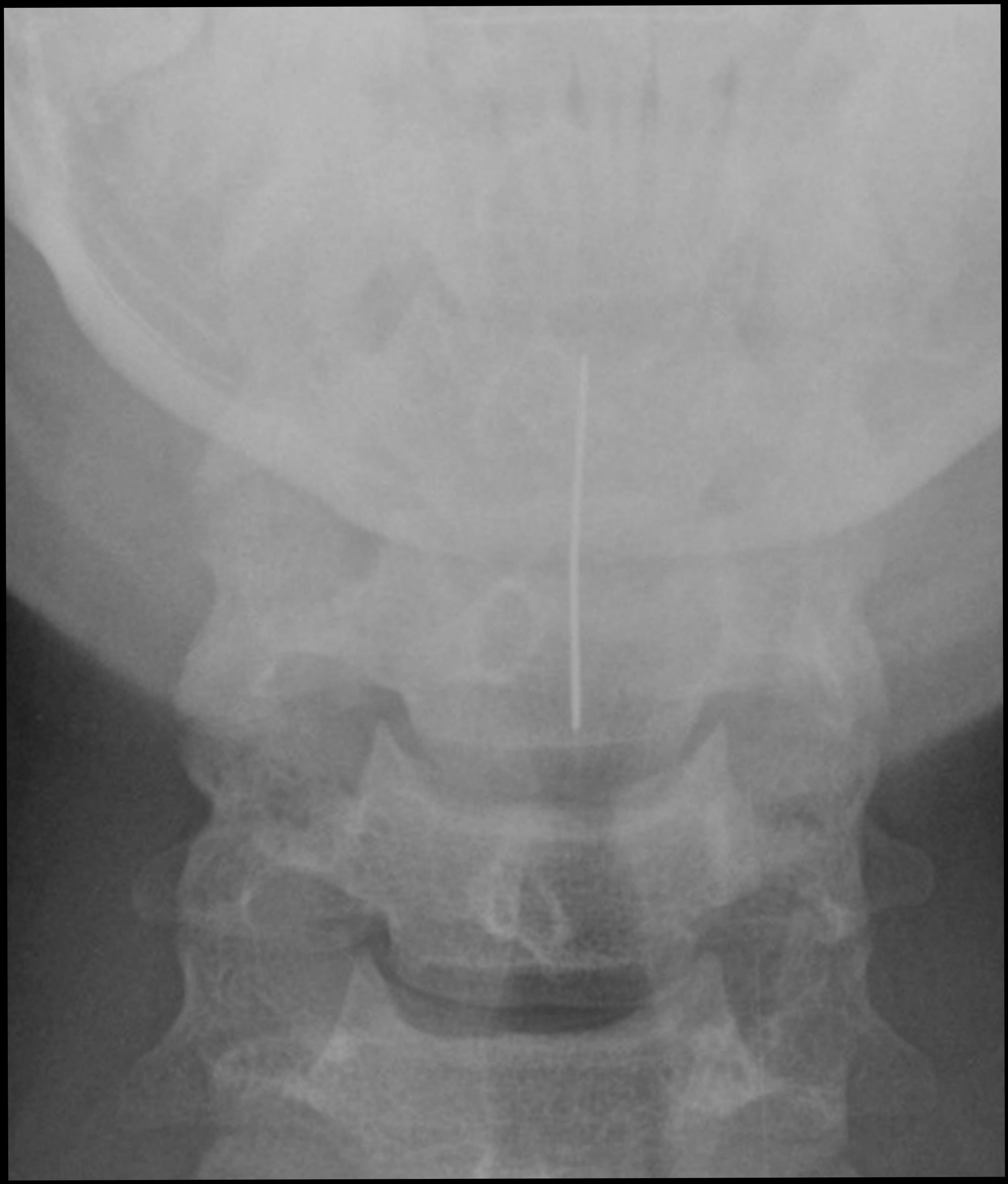

Corps étranger (aiguille) ingéré

Drain ventriculo-péritonéal

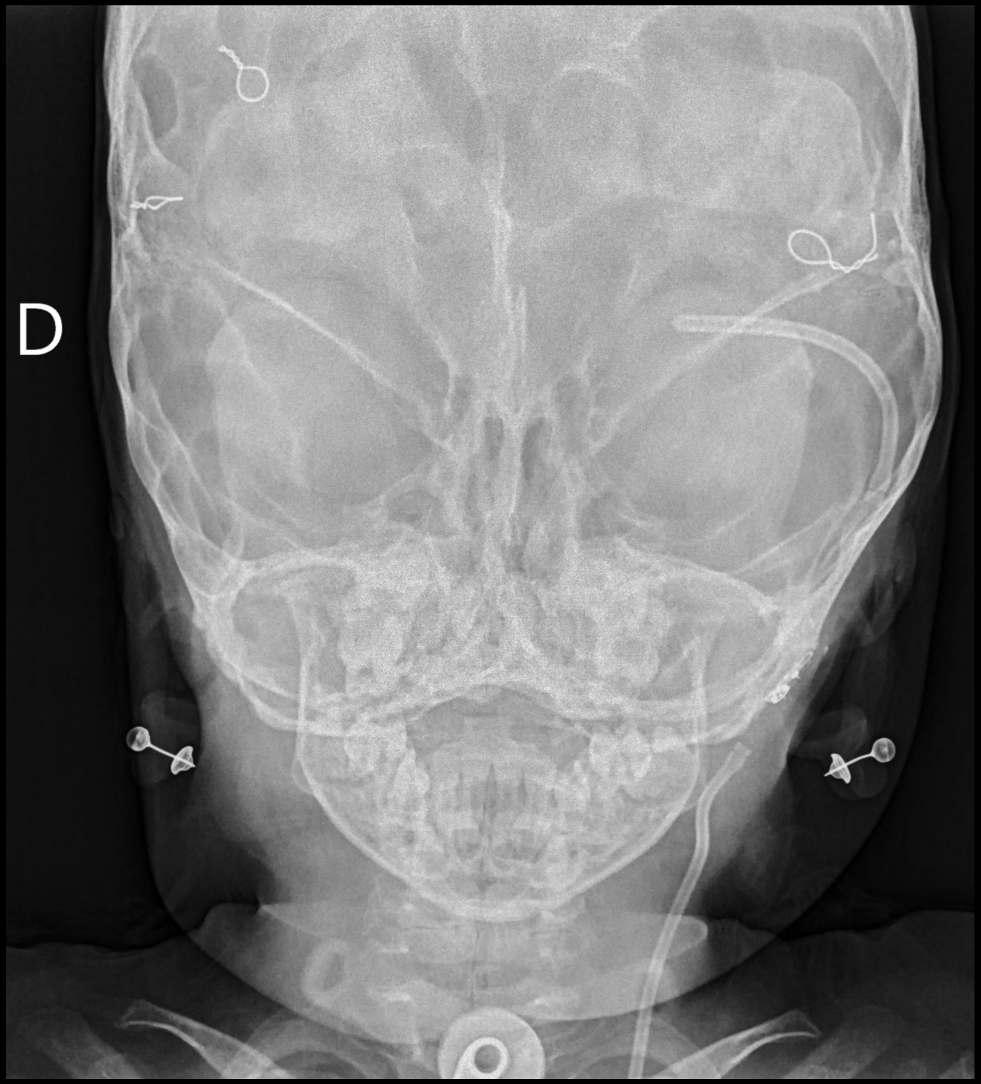

Implants cochléaires

Position du matériel (implant cochléaire)

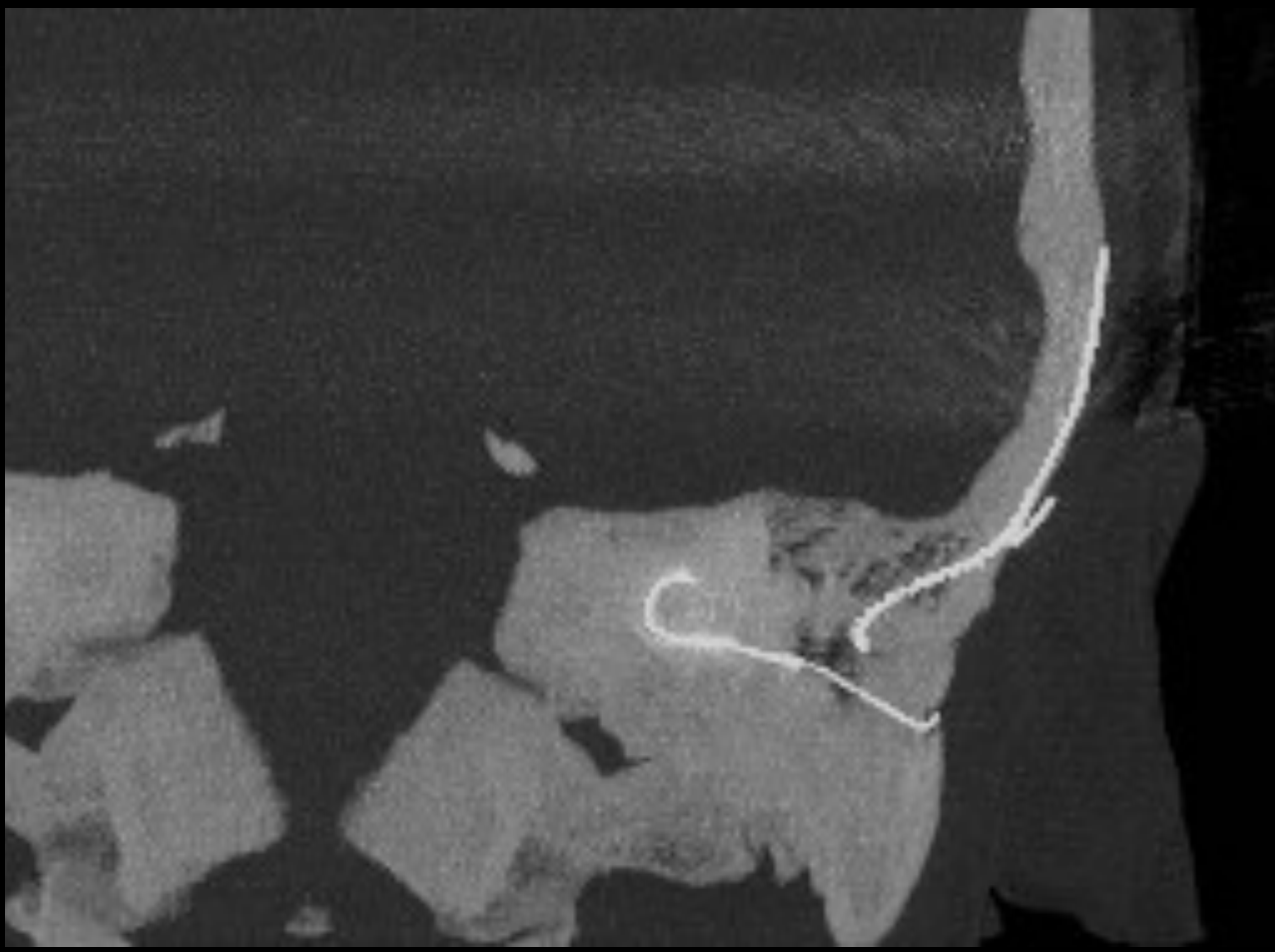

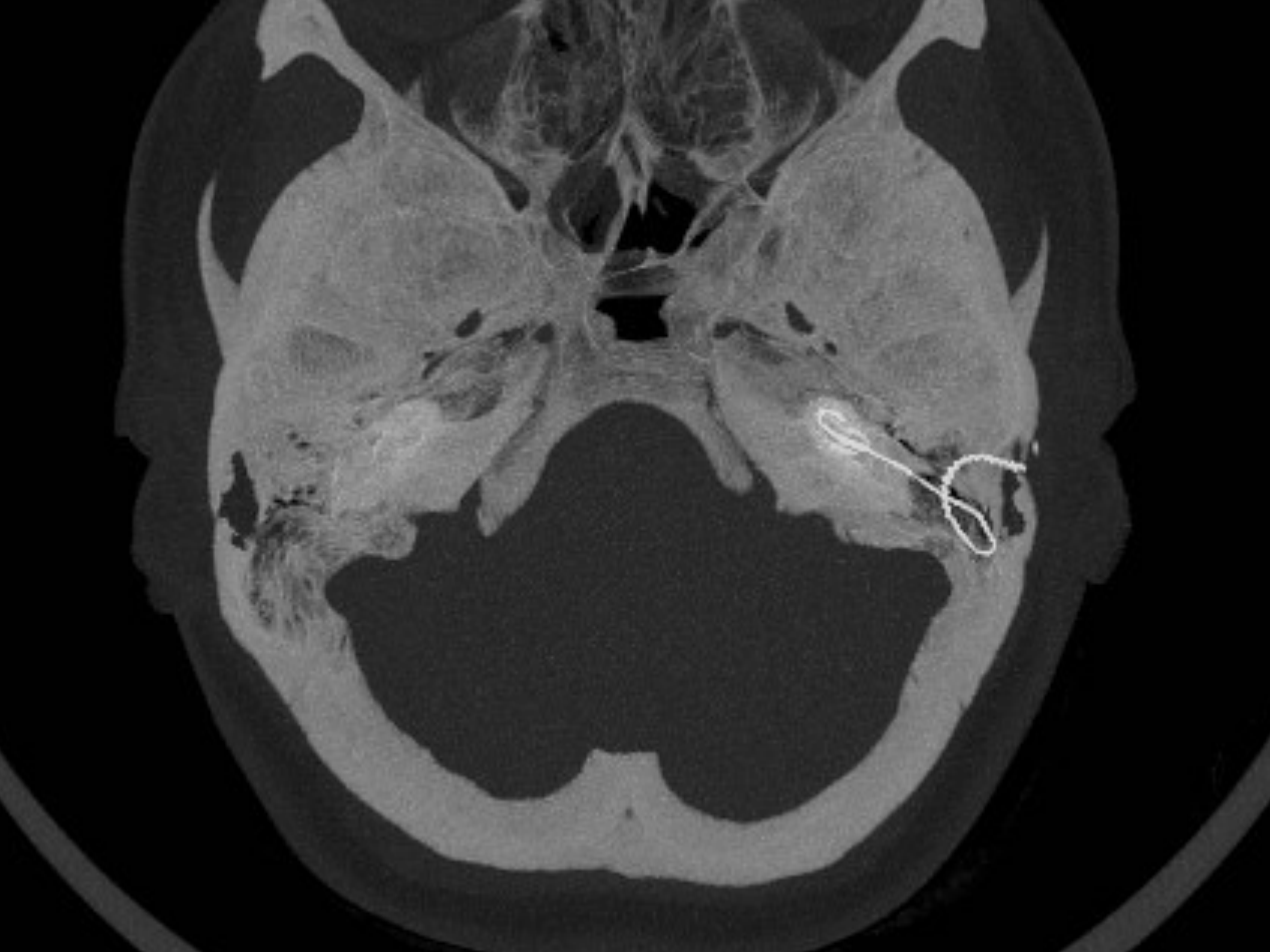

Hypertrophie des végétations adénoïdes

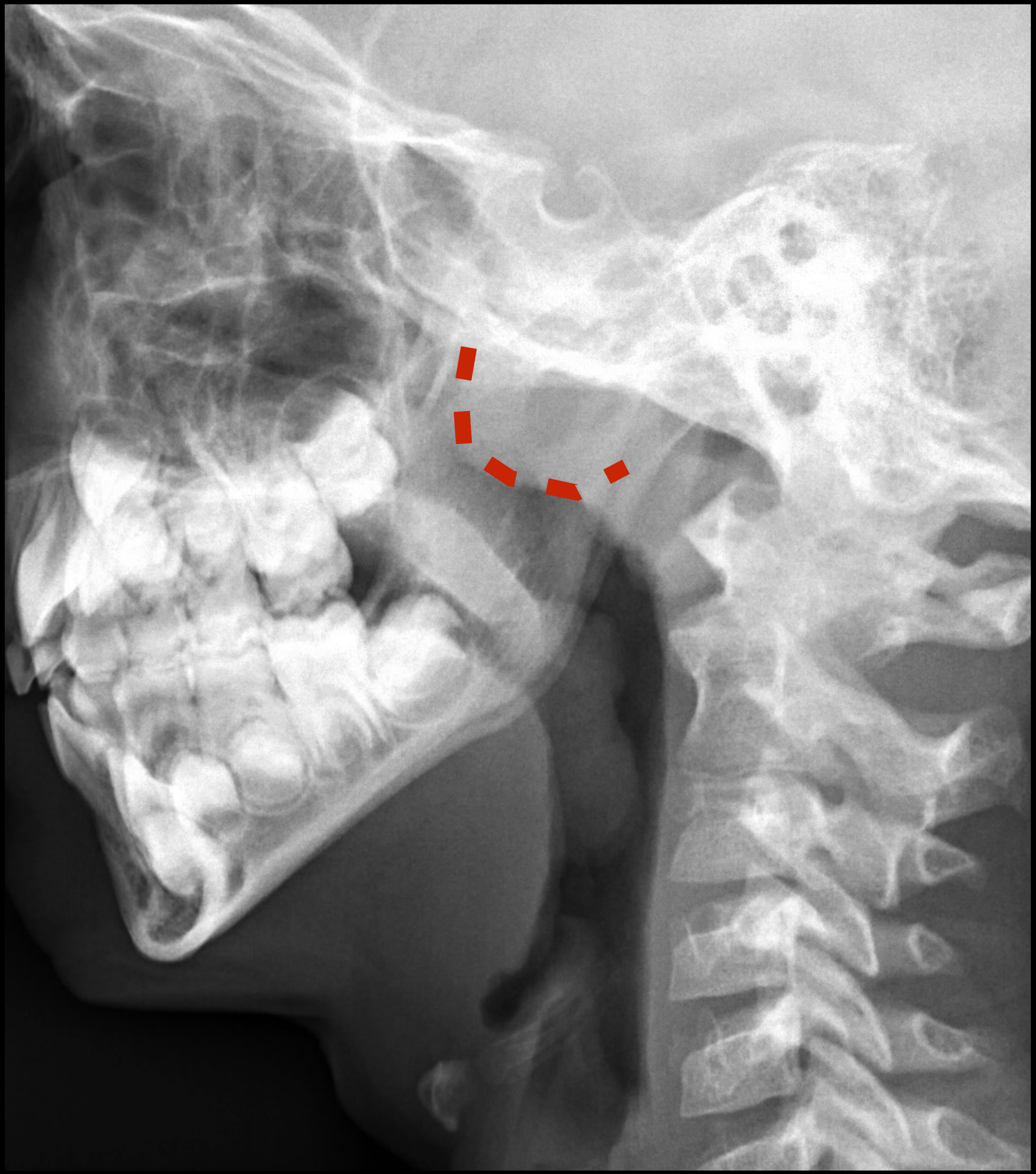

Normal

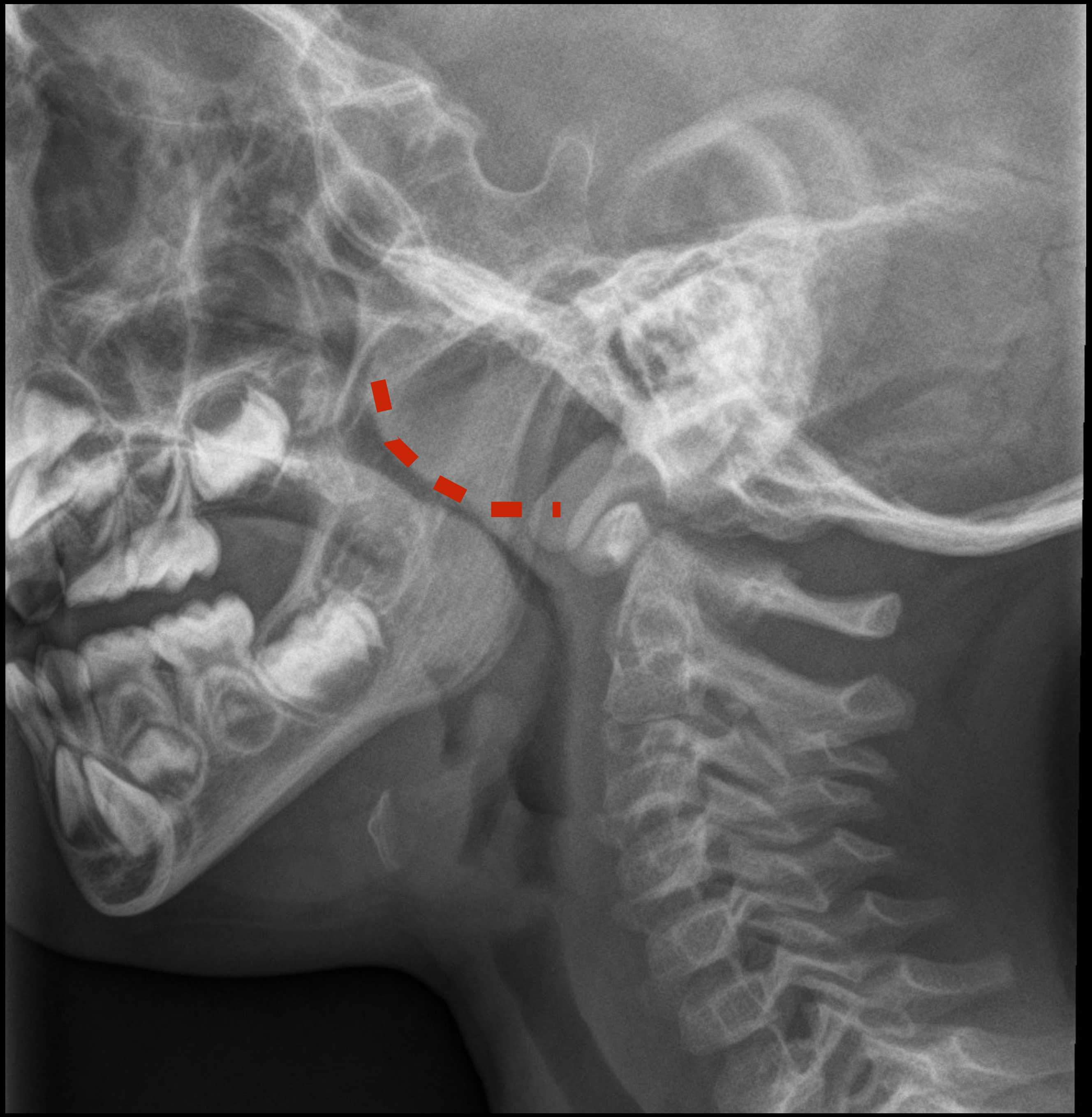

Hypertrophie des végétations

Panorex - Télécrâne

Histiocytose de Langerhans

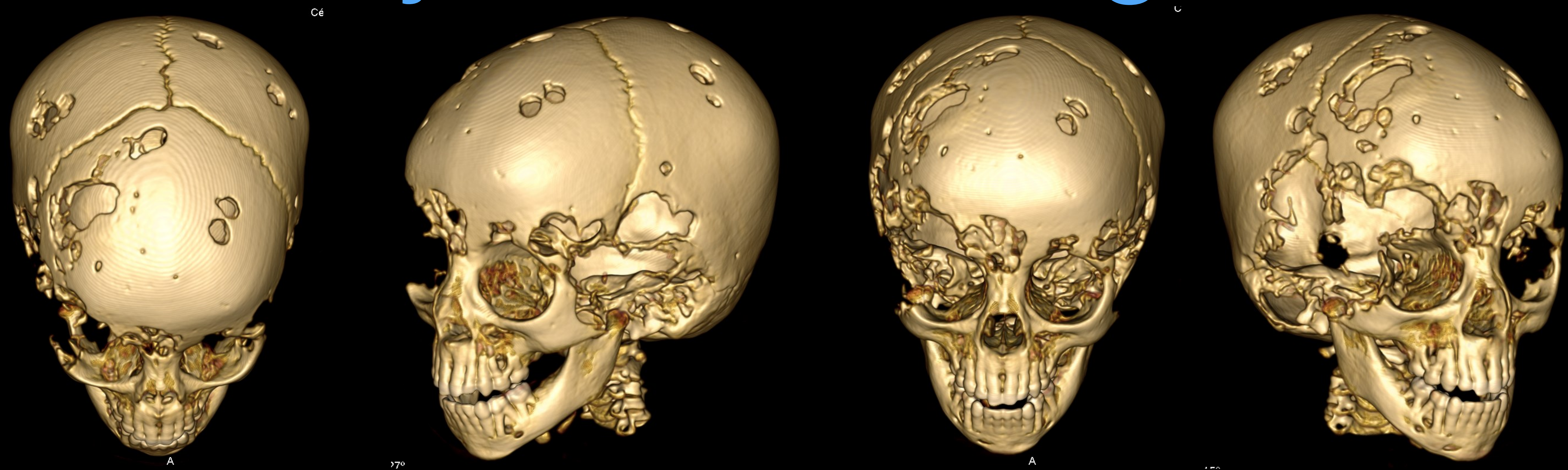

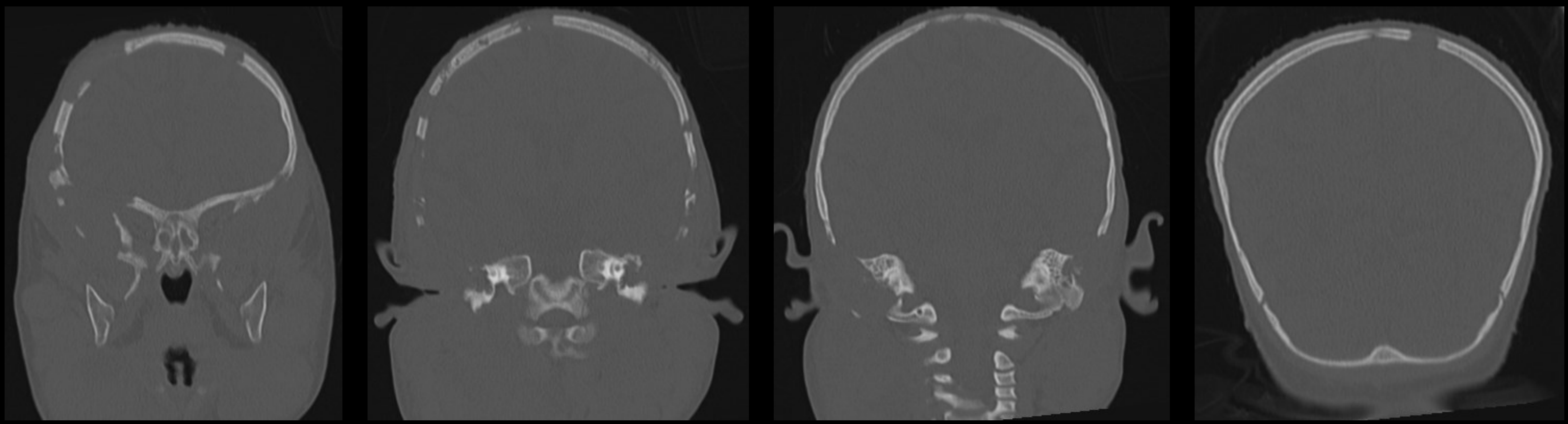

CONCLUSION

RX crâne: conclusion

- Indications limitées pour une radiographie du crâne/massif facial chez l'enfant
  - devices, DVP, implants cochléaires, panorex, traitement orthodontique
- Attention aux régions anatomiques radio-sensibles (cristallin)
- Importance de réaliser l'examen si effet sur la prise en charge

2ème partie

AGE OSSEUX

INTRODUCTION

Bone age

- Skeletal maturity in children
- Often used
  - For medical reasons:
    - bone maturation dysfunction assessment
    - advanced or delayed puberty assessment
    - treatment effects detection and follow-up
    - adult height prediction
  - For legal purposes

BONE AGE

ATLAS APPROACH

SINGLE BONE APPROACH

Skeletal maturation

- Second sex characteristics appear earlier than some decades before
- Skeletal growth most rapid in infants (< 1 year old) and toddlers
  - Accurate bone age assessment challenging
  - Linear maturation
- Average bone growth: 4% per year

Bone types

- Three types of bones:
  - longs (limbs)
  - shorts (ankle, wrist)
  - plate (skull, scapula, sternum)

Bone ossification

- **Endochondral ossification** (cartilage replaced by bone)
  - long
  - short
  - irregular bones

- **Intramembranous ossification** (bone develops within sheets of connective tissue
  - flat bones

Endochondral bone formation

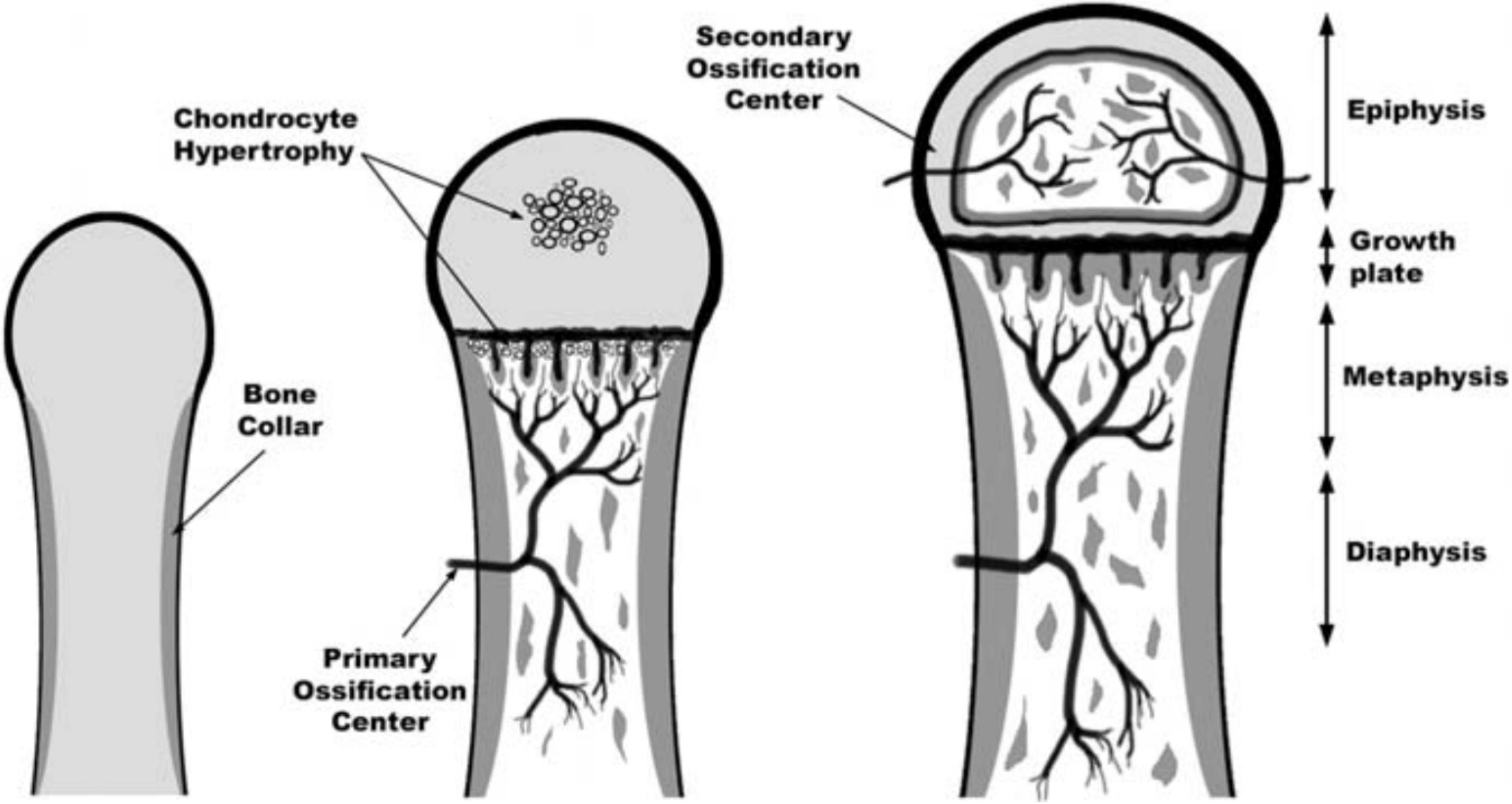

Depiction of the order of appearance of the individual carpal bones

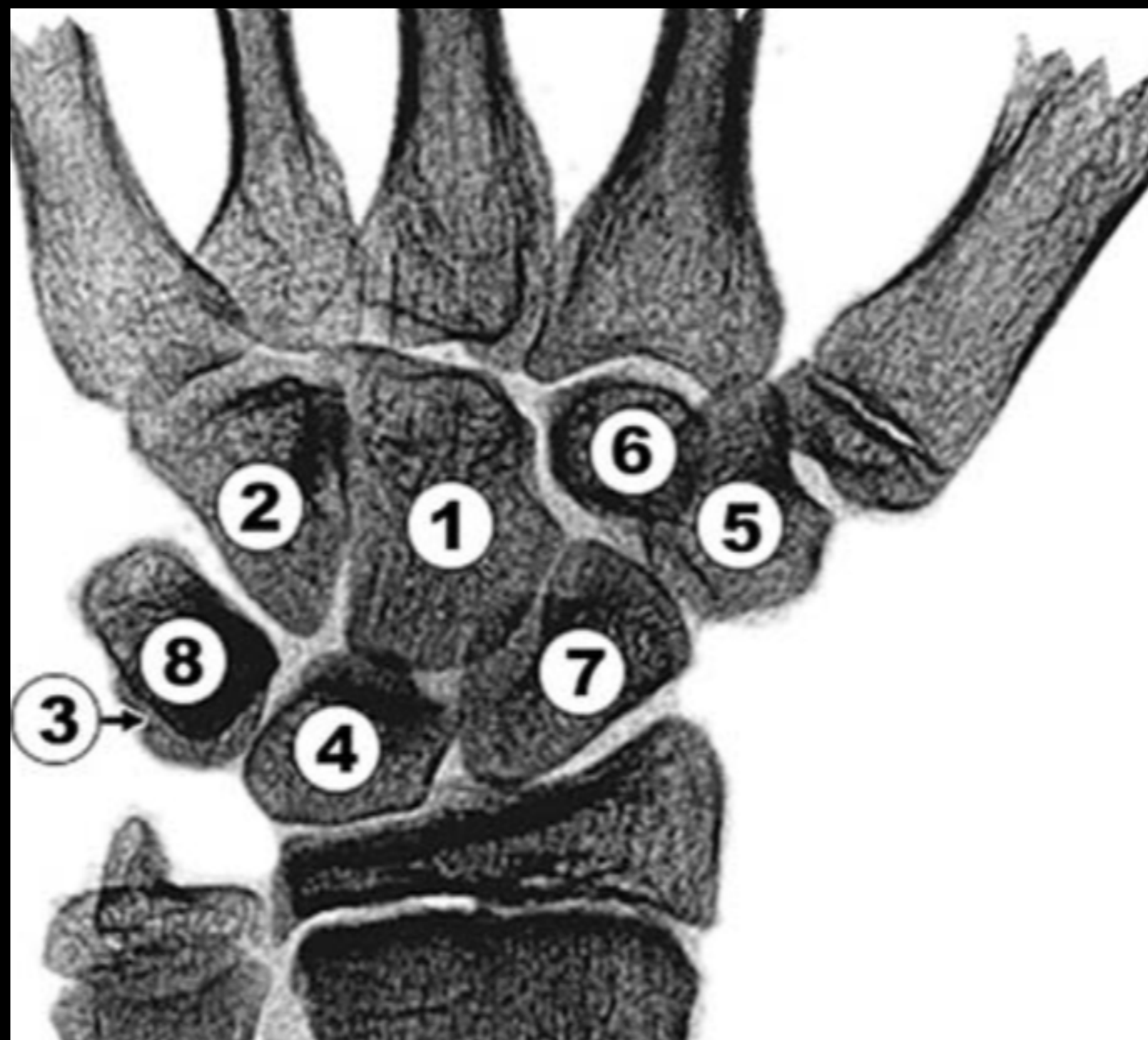

The usual sequence is: capitate (1), hamate (2), triquetral (3), lunate (4), trapezium (5), trapezoid (6), navicular or scaphoid (7) and pisiform (8). The distal epiphysis of the radius ossifies before the triquetrum and that of the ulna before the pisiform

Vicente Gilsanz, Osman Ratib. Hand Bone Age. Springer. Germany: Springer-Verlag Berlin Heidelberg New York; 2005

Bone age
for legal
purposes

CA = 8 years, M

HISTORY

1898	John Poland	Skiagraphic atlas showing developpement of bones of the wrist
1937	T. Wingate Todd	Atlas of the skeletal maturation of the hand
1939	Sontag	Rate of appearance of ossification centers from birth to the age of five years
1946	Elgenmark	Normal development of the ossification centers during infancy and childhood: clinical, roentgenologic and statistical study
1957	Levèbvre-Koifman	Ossification centers
1959	Tanner-Whitehouse	Hand and wrist method
1959	Greulich-Pyle	Radiographic atlas of skeletal development of the hand and wrist
1962	Pyle-Hoerr	Radiographic atlas of skeletal development of the foot and ankle: a standard of reference
1962	Sauvegrain Nahum	Maturation study of the elbow
1969	Hoerr, Pyle, Francis	A radiographic standard of reference for the growing knee
1972	Lamparski	Skeletal assessment using cervical vertebrae

1898

John Poland

Skiagraphic atlas showing developpement of bones of the wrist

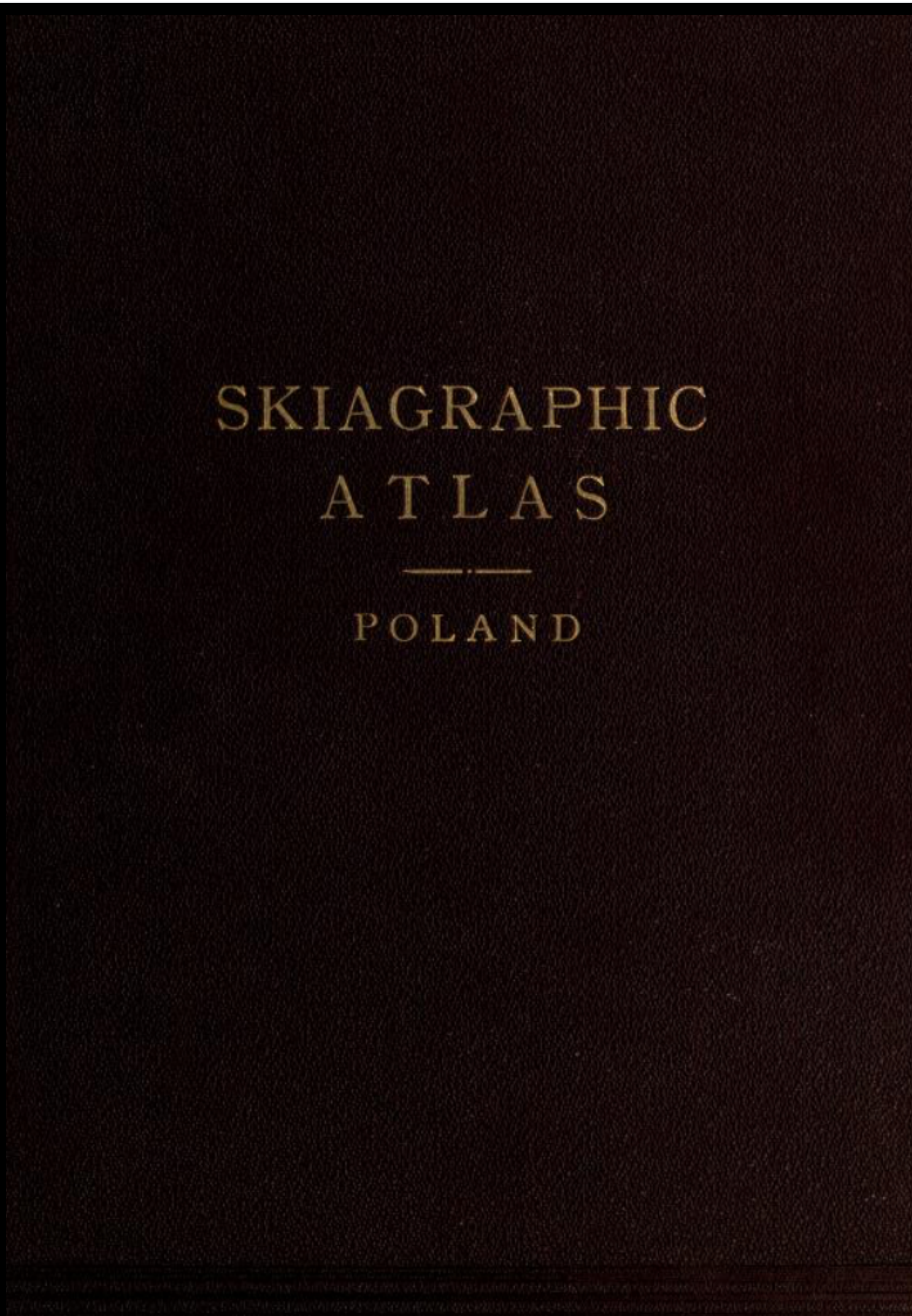

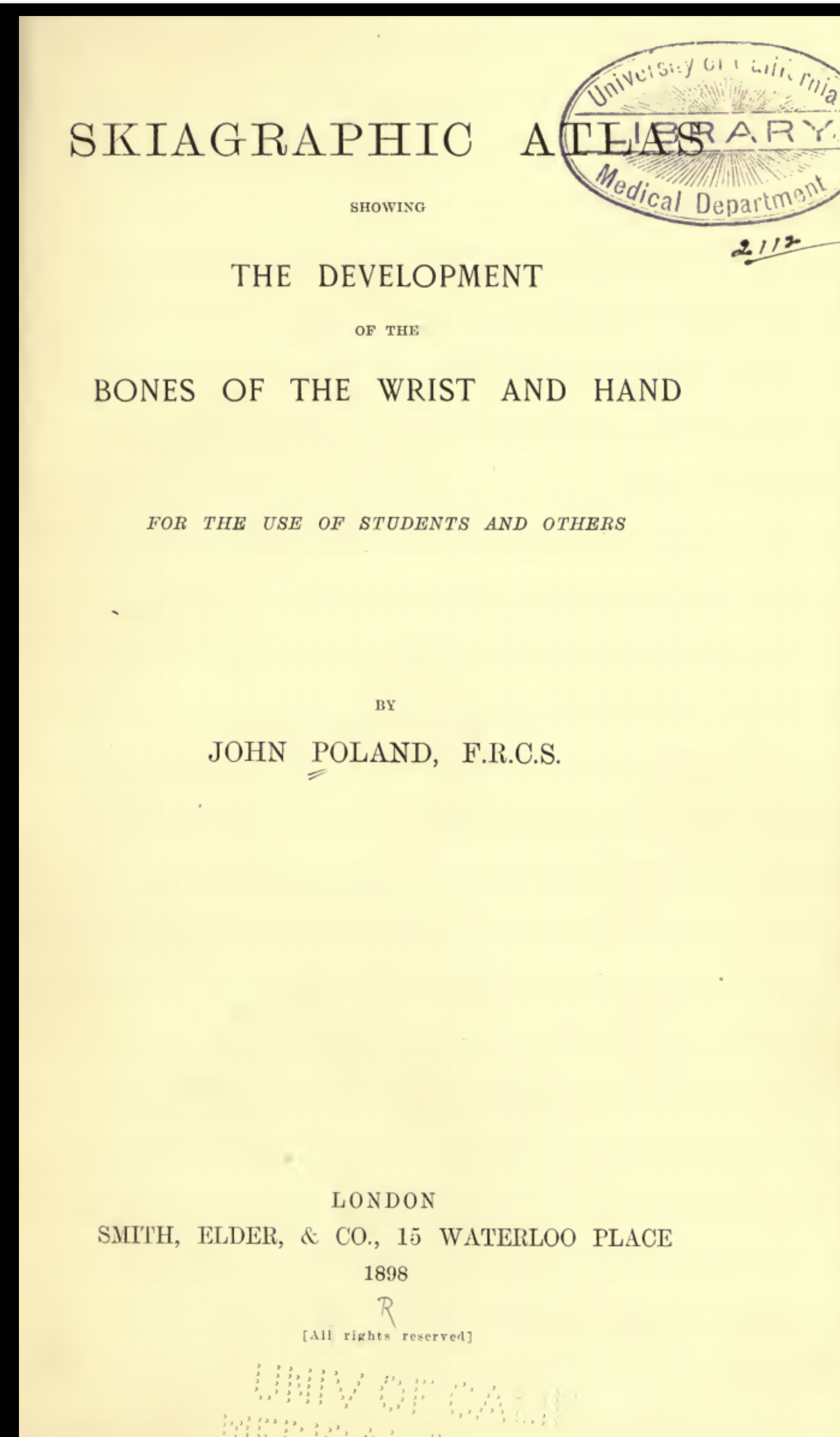

SKIAGRAPHIC ATLAS

SHOWING

THE DEVELOPMENT

OF THE

BONES OF THE WRIST AND HAND

FOR THE USE OF STUDENTS AND OTHERS

BY

JOHN POLAND, F.R.C.S.

LONDON
SMITH, ELDER, & CO., 15 WATERLOO PLACE
1898

PREFACE

It has been suggested that I should publish, in the form of an Atlas, the series of Skiagrams showing the ossification of the bones of the hand and wrist contained in my work on traumatic separation of the epiphyses.

The kindness of my friend, Mr. William Webster, to whom I am indebted for the whole series, with one exception, has enabled me to do this.

To the practical worker in the Röntgen ray process, as well as to anatomists and students, the advantages of such an Atlas are obvious, and it is hoped that in the near future all the bones of the body may be thus portrayed.

It will at once be noticed that the evolution of ossification differs very considerably from that hitherto described. I have, therefore, thought it advisable to reprint the anatomical description of the bones from my work.

JOHN POLAND.

EIGHTH YEAR, AND EIGHT YEARS AND FIVE MONTHS

Note the difference in relation of cuneiform to the epiphyses of the radius and ulna during adduction of the hand in the child of eight years.

Phalanges.—Nucleus of epiphyses of the three rows assuming shape of mature discs.

Nucleus of first phalanx of index finger measures six millimetres transversely

MALE CHILD AGED EIGHT YEARS.

1 second exposure. Taken by Mr. Wm. Webster.

1898	John Poland	Skiagraphic atlas showing developpement of bones of the wrist
1937	T. Wingate Todd	Atlas of the skeletal maturation of the hand

ATLAS OF SKELETAL MATURATION

BY

T. WINGATE TODD
M.B., Ch.B., Manc.; F.R.C.S., Eng.
Henry Willson Payne Professor of Anatomy
Western Reserve University;
Chairman, Brush Foundation;
Director, Hamann Museum;
Director, Developmental Health Inquiry of the Associated Foundations

WITH THE COLLABORATION OF COLLEAGUES AND ASSISTANTS

1926-1936

ST. LOUIS
THE C. V. MOSBY COMPANY
1937

Book Reviews

Atlas of Skeletal Maturation (Hand). T. WINGATE TODD. St. Louis, 1937, The C. V. Mosby Company, pp. 203, price $7.50.

After a brief introduction to the study of the skeletal maturation, which has been the interest and work of Dr. Todd and his associates for a number of years, seventy-five large plates showing the maturation of the bones of the hand from infancy through adolescence are presented. Forty of these are male white hand standards and thirty-five, female. As skeletal maturation is perhaps the best criterion of "growth" which we possess, the importance of the Atlas is obvious. It will be found invaluable for furnishing standards for comparison for workers in the field of child development and pediatricians. It is well printed, and the individual plates have been carefully selected from the many thousands in Dr. Todd's laboratory.

The Compleat Pediatrician. W. C. DAVISON, Ed. 2, Durham, N. C., 1938, Duke University Press, price $3.75.

It is only occasionally that revised editions of an old book are given review space in the JOURNAL. This second edition of Dr. Davison's unusual manual published a few years ago is so completely revised, so bears out the statement "completely rewritten," that it is in reality a new book. The new arrangement of material, the reduction in the numbering of paragraphs which made the first edition rather irritating to use, the inclusion of new material, as for example, the excellent chapter on Growth, Development and Guidance of Children have so improved the book that it is infinitely superior to the first edition, which it has in fact, rendered obsolete. It contains a veritable mine of information, and we know of no other single volume more useful for the pediatrician's desk. We prophesy an even more popular reception than that accorded to the first edition. It is easier in many ways to write a new book than completely to revise and rewrite an old one, and the author is to be congratulated on the unusual success of his efforts.

1898	John Poland	Skiagraphic atlas showing developpement of bones of the wrist
1937	T. Wingate Todd	Atlas of the skeletal maturation of the hand

Male White Hand Standard 20 B. I. male 8 yrs. 9 mo. SS 640

Maturity determinators

1. Metacarpals
   - c. distal ends:
     - no significant changes in contour (female 20)
   - d. epiphyses:
     - I. dense outline of dimple on proximal contour (female 18)
     - II, III. sharpened ulnar basal margin in preparation for further ulnar expansion (female 19)
2. Phalanges
   - A. proximal
   - d. epiphyses:
     - II, III, IV, V. well-rounded peripheral margins and relatively thick bony disc (female 19)
   - B. middle
   - c. distal ends:
     - II, III, IV. dome-shaped contours become flattened (female 17)
   - C. terminal
     - no significant changes in contour (female 15)
3. Radius
   - b. epiphysis:
     - ossification sharpens styloid process, fills in proximal (basal) lateral area, extends ulnar tongue almost to limit of shaft outline and produces a reciprocal parallelism of proximal epiphysial outline with distal contour of shaft (female 18)
4. Carpals
   - capitate: dense outline of articular surface for metacarpal III (female 17)
   - hamate: dense outline of articular surface for metacarpal IV (female 17)
   - triquetrum: no significant change in contour (female 17)
   - lunate: no significant change in contour (female 18)
   - navicular: distal extension preparatory to formation of beak (female 18)
   - multangulum majus: no significant change in contour (female 19)
   - multangulum minus: no significant change in contour (female 18)

Textures of this example
- spongiosa: close
- compacta: dense
- mineralization: lightish
- scorings: none

Growing ends of this example
- radius, ulna: faintly billowed contour

Comparison with female standards:
- approximately at level of female 18-

Male White Hand Standard 20

Hemiskeleton method

- 1940: Pyle and Sontag
- 1946: Elgenmark, hemiskeleton method
  → radiographs of half the child's body (more accurate in young children)
  - radiation exposure
  - review of multiple images
  - less used from 5 and 12 years old

1898	John Poland	Skiagraphic atlas showing developpement of bones of the wrist
1937	T. Wingate Todd	Atlas of the skeletal maturation of the hand
1957	Levèbvre-Koifman	Ossification centers

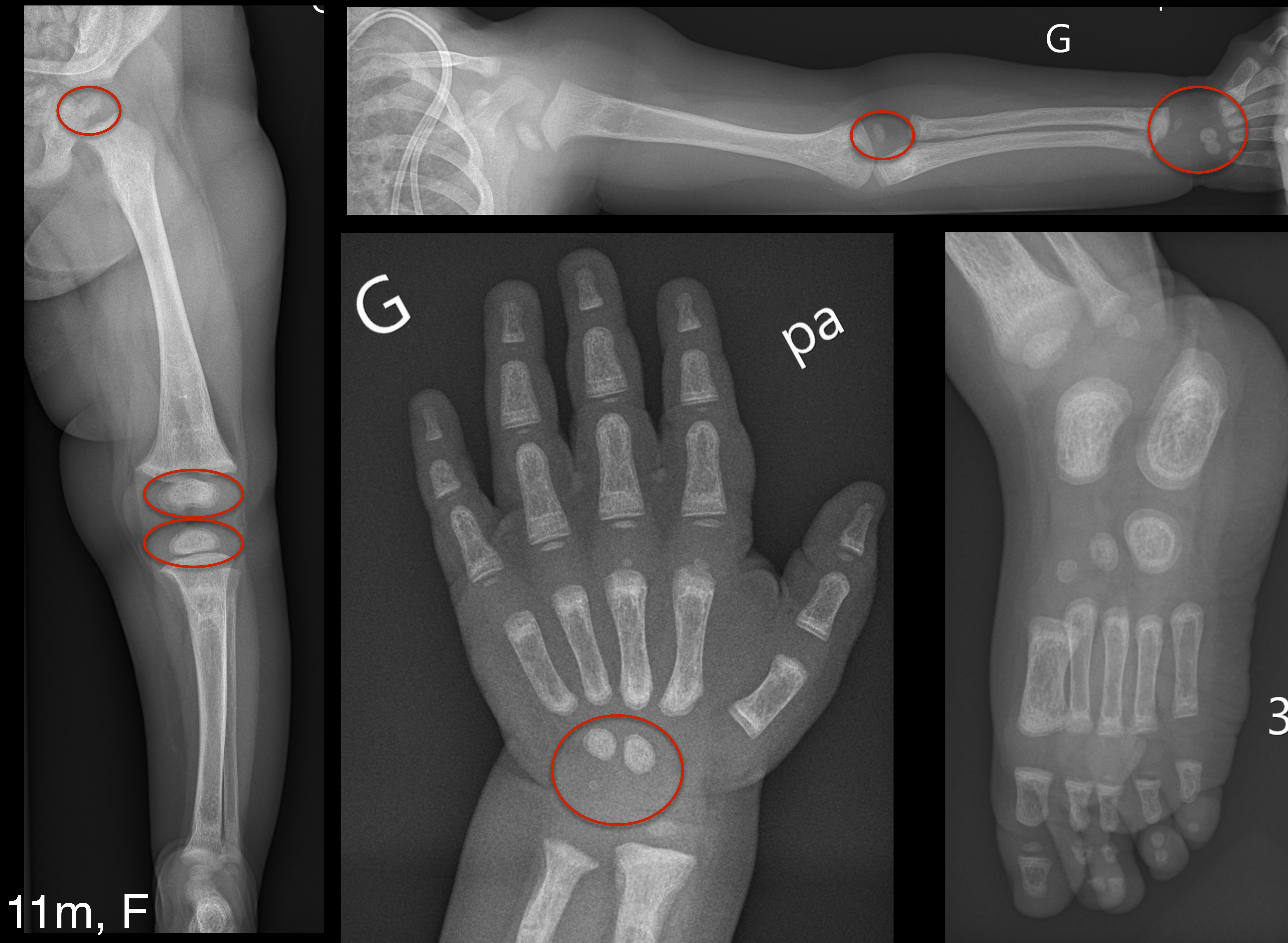
G
G
pa
11m, F

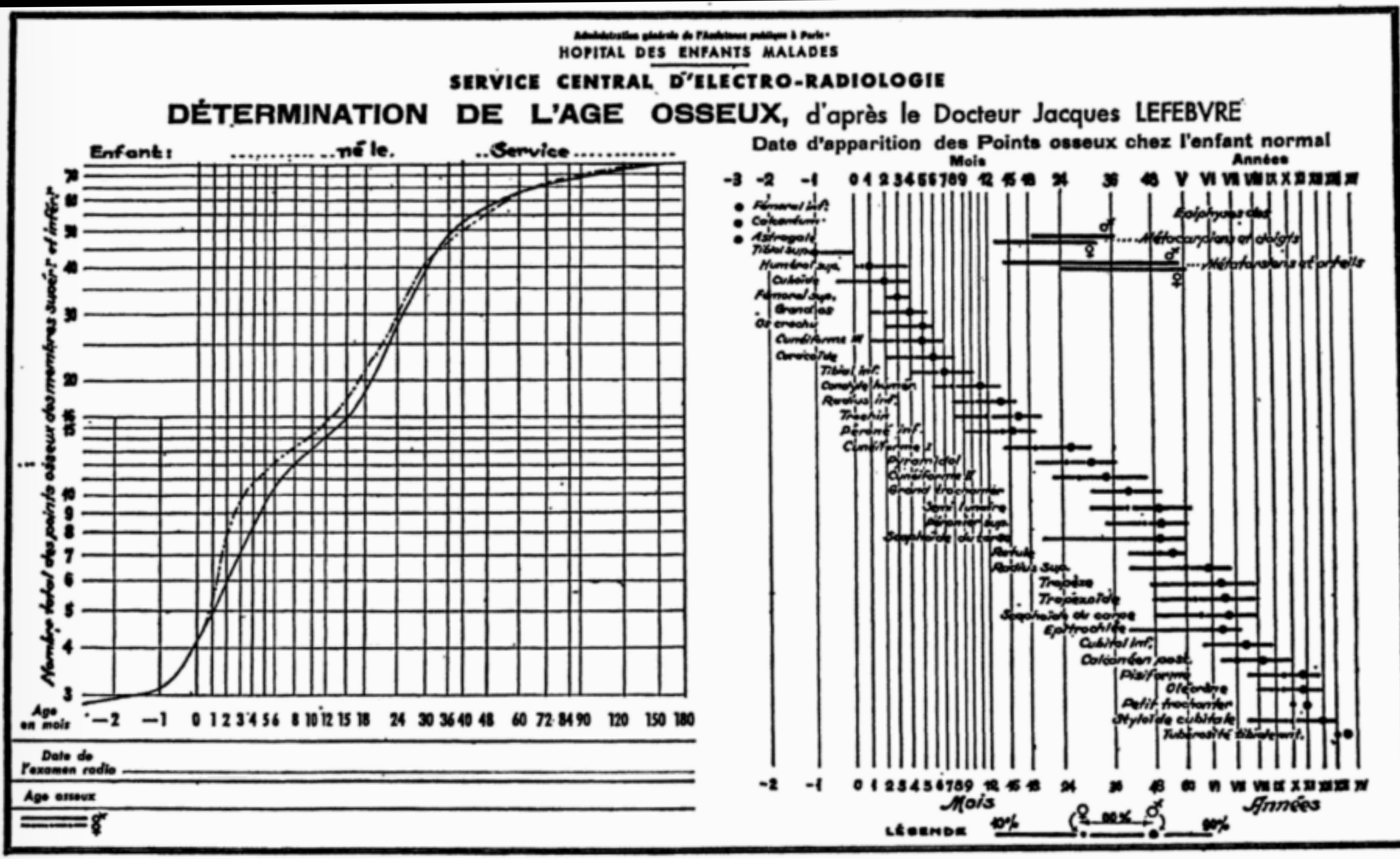

36 bones from 6 joints; wrist, elbow, shoulder, hip, knee, feet (until 2 years old)

Abaque de Lefebvre et Koifman

Figure n° 1

- Encouraged approaches of choice in children:
  - 1955 and 1969: Knee method of Pyle and Hoerr[1]
  - 1962: Foot/ankle method of Hoerr, Pyle and Francis[2]
    - Rough ages approximation (discretized bone age estimates and accuracies largely unknown)

1. Pyle SI, Hoerr NL (1969). Charles C. Thomas, Springfield

2. Hoerr NL, Pyle SI, Francis CC (1962). Charles C. Thomas, Springfield

1898	John Poland	Skiagraphic atlas showing developpement of bones of the wrist
1937	T. Wingate Todd	Atlas of the skeletal maturation of the hand
1939	Sontag	Rate of appearance of ossification centers from birth to the age of five years
1946	Elgenmark	Normal development of the ossific centers during infancy and childhood: clinical, roentgenologic and statistical study
1957	Levèbvre-Koifman	Ossification centers
1959	Tanner-Whitehouse	Hand and wrist method

Tanner-Whitehouse

- 20 bones analysis:
  - Radius, ulna and short bones (metacarpal and phalanges) compared to standards and scored
- Maturity score 0-1000 (each individual score added)
- Maturity score converted to bone age
  - 1959: Tanner
  - reviewed in 1972 and 1975

1898	John Poland	Skiagraphic atlas showing developpement of bones of the wrist
1937	T. Wingate Todd	Atlas of the skeletal maturation of the hand
1957	Levèbvre-Koifman	Ossification centers
1959	Greulich-Pyle	Radiographic atlas of skeletal development of the hand and wrist

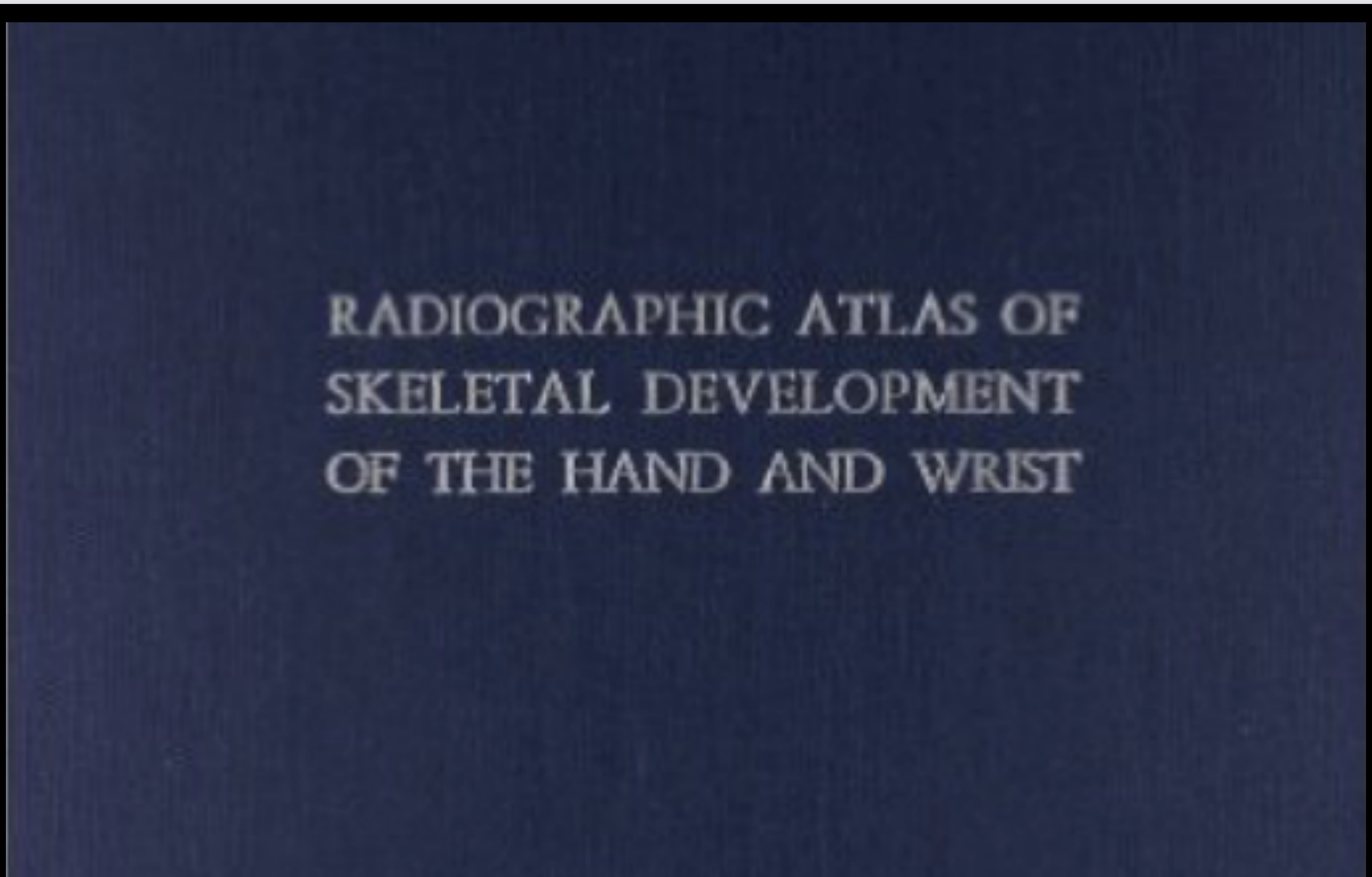

Skeletal Age of Individual Bones

Distal End of Radius	8 yr. 2 mo.	Proximal Phalanx I	8 yr. 0 mo.
Distal End of Ulna	8 yr. 6 mo.	Proximal Phalanx II	8 yr. 0 mo.
		Proximal Phalanx III	8 yr. 0 mo.
Capitate	8 yr. 0 mo.	Proximal Phalanx IV	8 yr. 0 mo.
Hamate	8 yr. 0 mo.	Proximal Phalanx V	8 yr. 0 mo.
Triquetral	8 yr. 0 mo.		
Lunate	8 yr. 8 mo.	Middle Phalanx II	7 yr. 10 mo.
Scaphoid	8 yr. 2 mo.	Middle Phalanx III	7 yr. 10 mo.
Trapezium	8 yr. 2 mo.	Middle Phalanx IV	7 yr. 10 mo.
Trapezoid	8 yr. 2 mo.	Middle Phalanx V	7 yr. 8 mo.
Metacarpal I	8 yr. 0 mo.	Distal Phalanx I	8 yr. 0 mo.
Metacarpal II	8 yr. 0 mo.	Distal Phalanx II	8 yr. 0 mo.
Metacarpal III	8 yr. 0 mo.	Distal Phalanx III	8 yr. 0 mo.
Metacarpal IV	8 yr. 0 mo.	Distal Phalanx IV	8 yr. 0 mo.
Metacarpal V	8 yr. 0 mo.	Distal Phalanx V	8 yr. 0 mo.
Pisiform	*		
Adductor Sesamoid of Thumb	*		
Flexor Sesamoid of Thumb	*		

* These centers are still cartilaginous at this stage of development.

The white lines adjacent to the metacarpal surface of the hamate, capitate, and trapezoid mark a part of their respective volar margins. These markings become more distinct and complete in subsequent standards. As the scaphoid has elongated, its capitate surface has become somewhat less convex.

The concavity in the base of the second metacarpal adjacent to the trapezoid has become more pronounced. The ulnar portion of the base has begun to extend toward the capitate, with which it will later articulate. The oblique view of the first metacarpal, which the ordinary hand-film provides, permits the observation that the epiphysis of this bone reaches the palmar or volar margin of the shaft before it grows far enough dorsally to be aligned with the dorsal margin of the shaft. The proximal epiphysis of the thumb also appears in the oblique view to be the same width as its shaft.

The epiphyses of the distal phalanges of the second, third, fourth, and fifth fingers are now as wide as their shafts. All middle phalangeal epiphyses and the epiphyses of the distal phalanges of the second and third fingers have shaped further to the contours of the trochlear surfaces of the phalanges with which they articulate.

Greulich and Pyle

- Most used method since 1959
- Applying Todd's methodology
- High quality of the second edition
- Each chronological age: 1 image selected
- Two series of standard plates
  - one for ♀
  - one for ♂

Todd TW. Atlas of Skeletal Maturity. Vol Part I. Hand. Kimpton. London; 1937

Greulich and Pyle

- Left hand and wrist radiographs
  - ✦ 90% of the population right-sided
- « Better than average constitution »
  - ✦ White, upper middle-class boys and girls
  - ✦ Enrolled in the Brush Foundation Growth Study from 1931 to 1942

Bone age

- TW2 increases the reproducibility than compared to the GP method
- Intra-observer variation is higher in the GP method than the TW2*
- Time in GP (1,4’) >< TW2 (7,9’)

** Bull RK, et al. Arch Dis Child. 1999;81(2):172-173*

1898	John Poland	Skiagraphic atlas showing developpement of bones of the wrist
1937	T. Wingate Todd	Atlas of the skeletal maturation of the hand
1957	Levèbvre-Koifman	Ossification centers
1959	Greulich-Pyle	Radiographic atlas of skeletal development of the hand and wrist
1962	Pyle-Hoerr	Radiographic atlas of skeletal development of the foot and ankle: a standard of reference

Radiographic Atlas of Skeletal Development of the Foot and Ankle

A STANDARD OF REFERENCE

By

NORMAND L. HOERR, Ph.D., M.D., S. IDELL PYLE, Ph.D.,
and CARL C FRANCIS, M.D.

From the Department of Anatomy
Western Reserve University, School of Medicine
Cleveland, Ohio

CHARLES C THOMAS • PUBLISHER
Springfield • Illinois • U.S.A.

INDIVIDUAL BONE AGES

The skeletal age assigned to each bone in this plate is 8 years 0 months for boys and 6 years 3 months for girls.

SELECTED MATURITY INDICATORS

Hindfoot

Differential markings within the talus, lateral view: The medial and lateral margins of the crest of the trochlea have become thickened. Accordingly, the concavity of the trochlea can be traced backward and downward from the neck of the talus for more than half its extent.

Calcaneus, lateral view: The epiphyseal bone growth center now contains several osseous particles. The largest ossicle is positioned on the longest axis of the epiphysis, and its shape indicates the direction of the axis.

The small indentation on the plantar surface near the anterior tubercle mentioned with the preceding plate is now distinct. It marks the entrance of the groove for the long plantar ligament.

Midfoot

Cuboid, both views: A triangular outline projects backward from the cuboid toward the calcaneus. This is the outline of the medial surface of the bone.

The squarish osseous corner at the junction of its posterior, lateral, and plantar surfaces is distinctly outlined.

Navicular, both views: Its distal margin and its concave talar margin are shaping to the curvature of the distal surface of the talus which remains convex. Thus parallelism of outlines has been established dorsally in the latest of the tarsals to begin its ossification.

Inter-tarsal joints, both views: The free dorsal surfaces of the navicular and three cuneiform bones have become flattened. Blunted osseous corners are forming between the free surfaces and the inter-tarsal articular surfaces on the individual bones.

The facets which face the forefoot tend to be convex; those which face the hindfoot tend to be concave. The facets which face medially tend to be flat or beveled. These differences are becoming apparent throughout the midfoot.

Forefoot

Metatarsals, dorsoplantar view: Osseous beaks and sharp buttresses are forming at the junction of each metaphysis and its diaphysis. The metaphyses present thick white outlines along strips of lesser density. The terminal plates of the epiphyses and the etched outlines of the metaphyses are parallel throughout their extent.

Phalanges, dorsoplantar view: The epiphysis of the distal phalanx of the great toe is beginning to curve distally, that is, to cap the shaft on its medial side.

1898	John Poland	Skiagraphic atlas showing developpement of bones of the wrist
1937	T. Wingate Todd	Atlas of the skeletal maturation of the hand
1957	Levèbvre-Koifman	Ossification centers
1959	Greulich-Pyle	Radiographic atlas of skeletal development of the hand and wrist
1962	Pyle-Hoerr	Radiographic atlas of skeletal development of the foot and ankle: a standard of reference
1962	Sauvegrain Nahum	Maturation study of the elbow

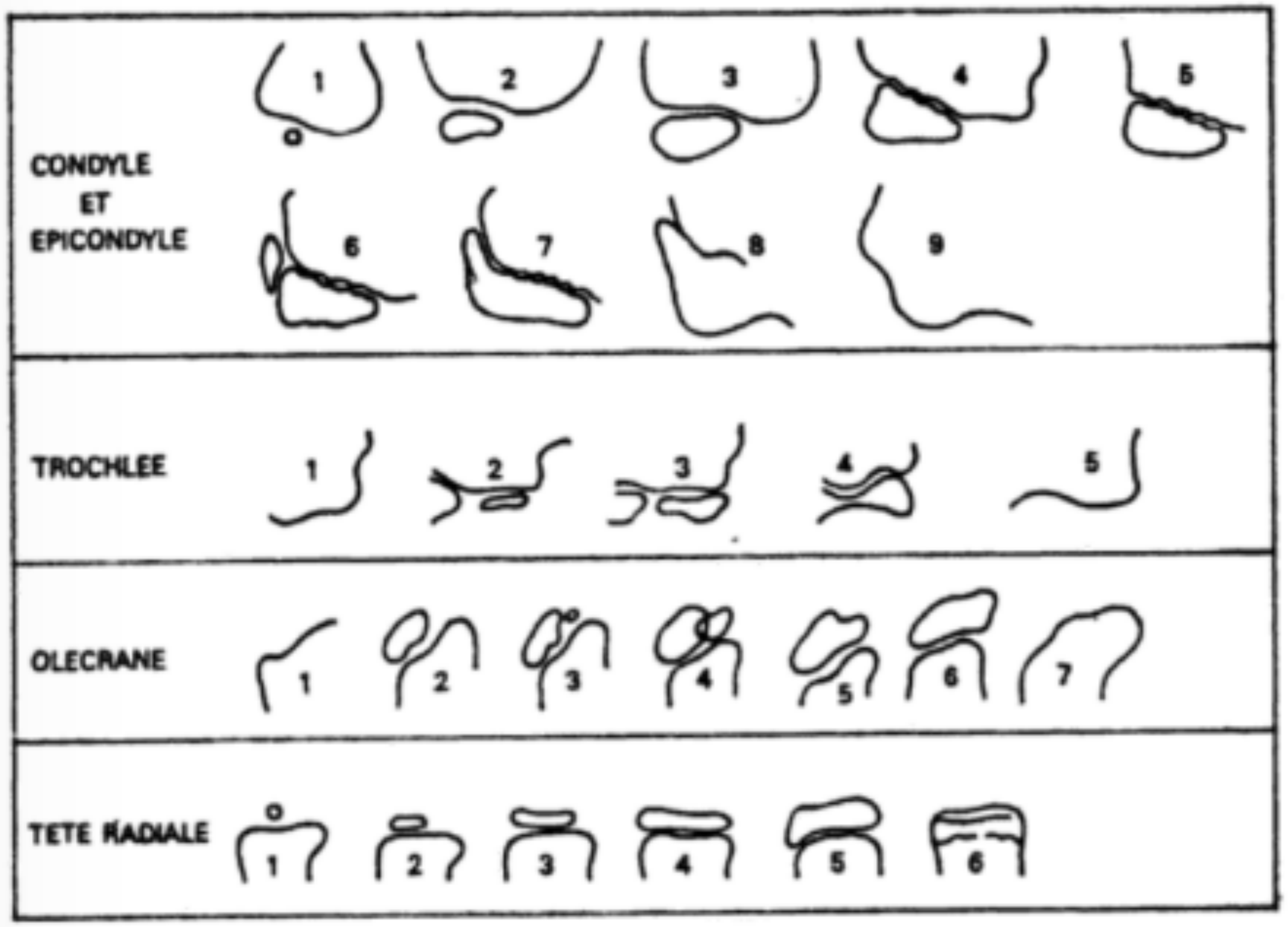

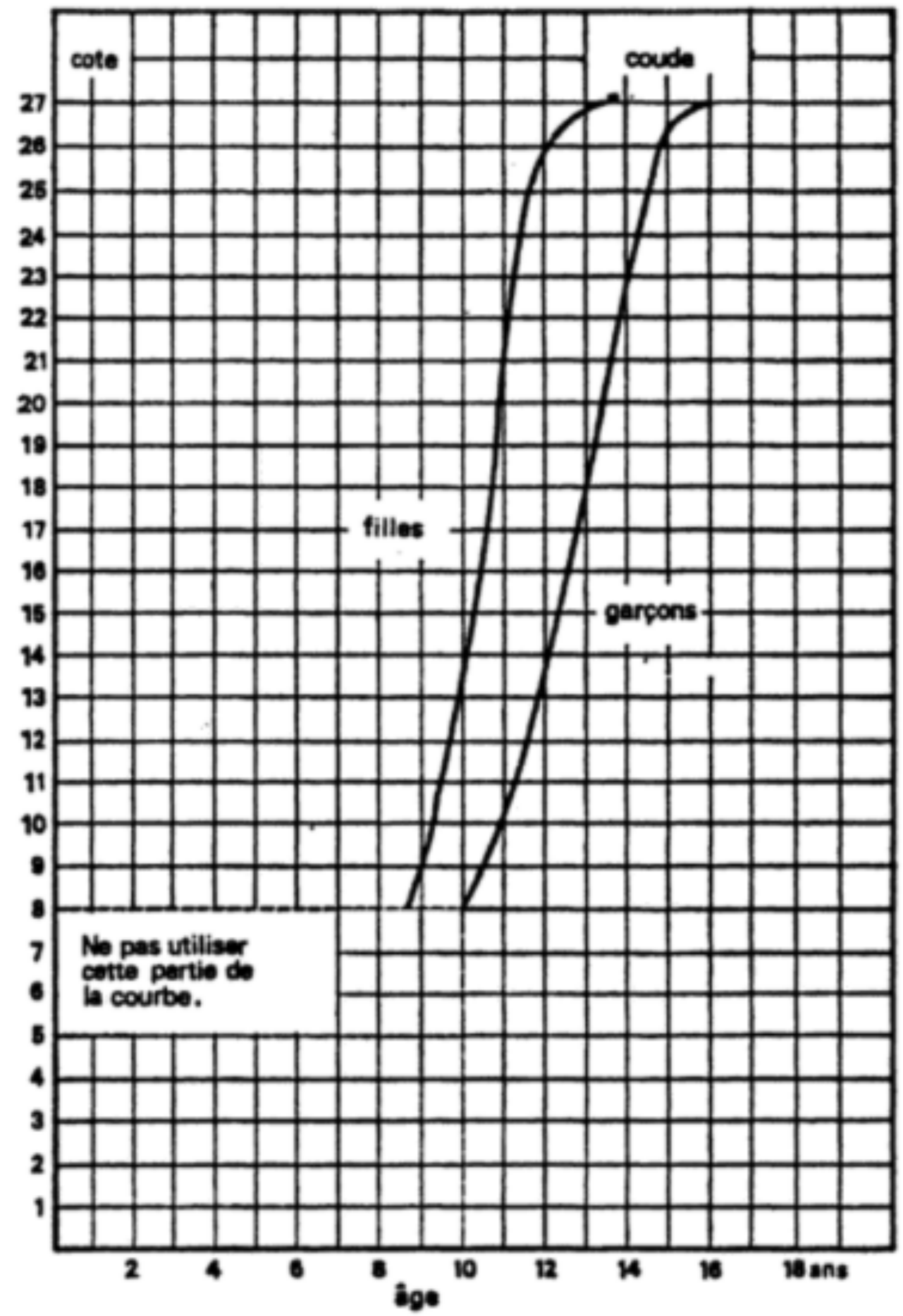

Méthode de Sauvegrain, Nahum et Bronstein
Figure n° 2
Étude de la maturation osseuse du coude

(Chaumoitre K, et al. J Radiol 87:1679–1682)

1898	John Poland	Skiagraphic atlas showing developpement of bones of the wrist
1937	T. Wingate Todd	Atlas of the skeletal maturation of the hand
1957	Levèbvre-Koifman	Ossification centers
1959	Greulich-Pyle	Radiographic atlas of skeletal development of the hand and wrist
1962	Pyle-Hoerr	Radiographic atlas of skeletal development of the foot and ankle: a standard of reference
1962	Sauvegrain Nahum	Maturation study of the elbow
1972	Lamparski	Skeletal assessment using cervical vertebrae

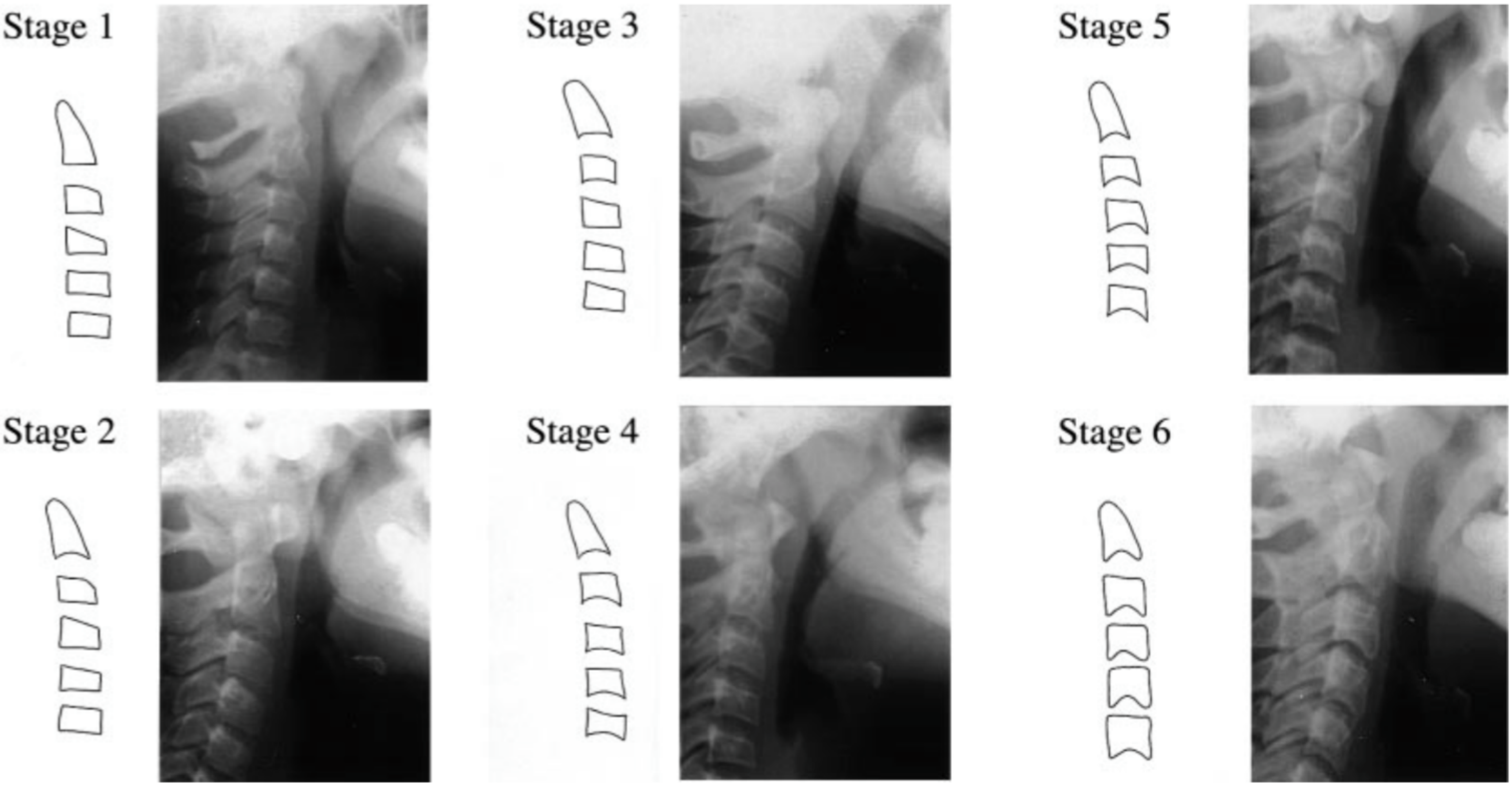

Figure 2 Cervical vertebrae maturation stages according to the concavity of the lower border of the vertebral body. (1) All vertebrae have a flat lower border; (2) a concavity is present in the C_2 lower border; (3) a concavity is present in C_3 lower border; (4) C_2 and C_3 concavity increases and a concavity is present in C_4, C_5, and C_6; (5) concavity increases in all vertebrae; (6) a deep concavity is present in all vertebrae and the inferior angles are rounded.

San Román P, et al. Eur J Orthod. 2002;24(3):303-311.

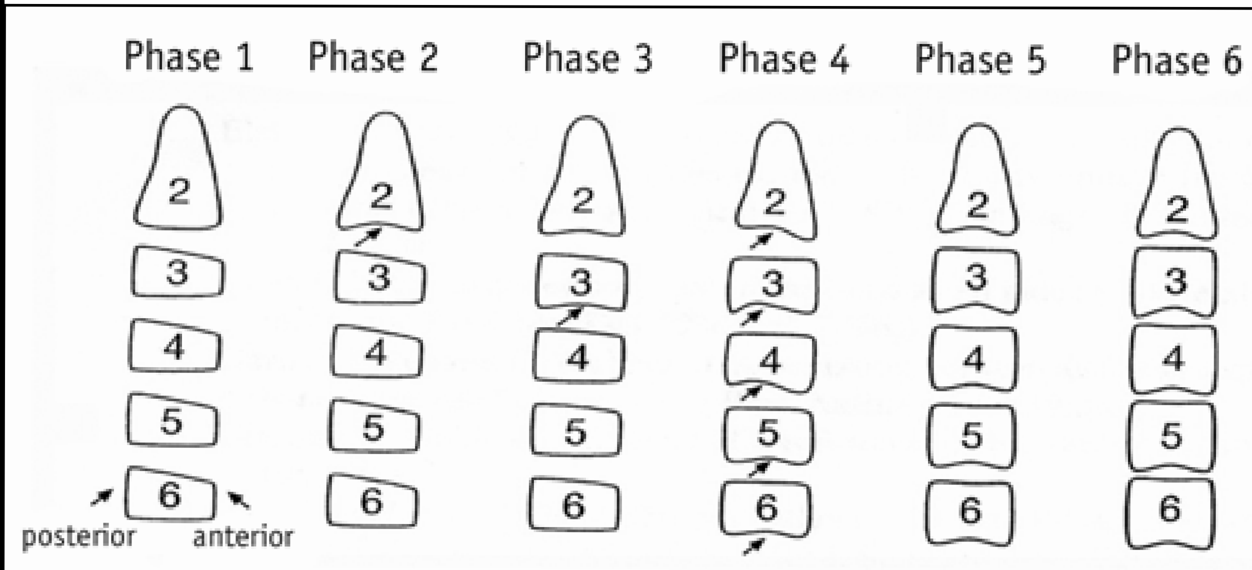

Figure 1. Standards for female vertebral skeletal maturity according to Lamparski & Nanda [14].

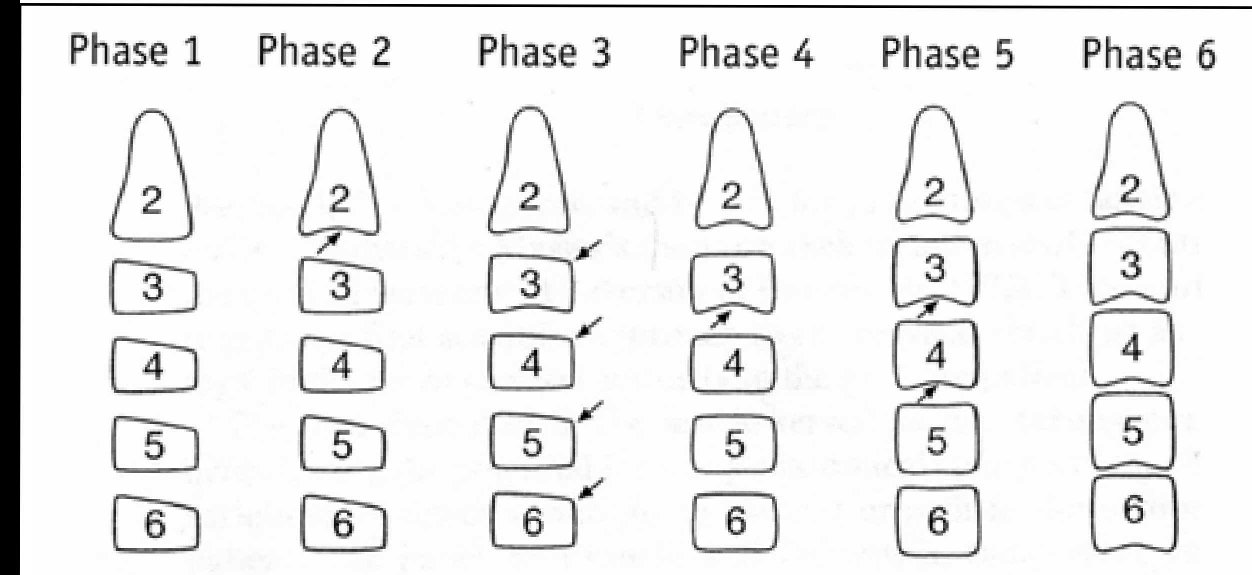

Figure 2. Standards for male vertebral skeletal maturity according to the Lamparski & Nanda [14] method.

San Román P, et al. Skeletal Eur J Orthod. 2002;24(3):303-311.

TODAY

2009

Thodbergh *et al.*

Automated hand and wrist skeletal maturation program

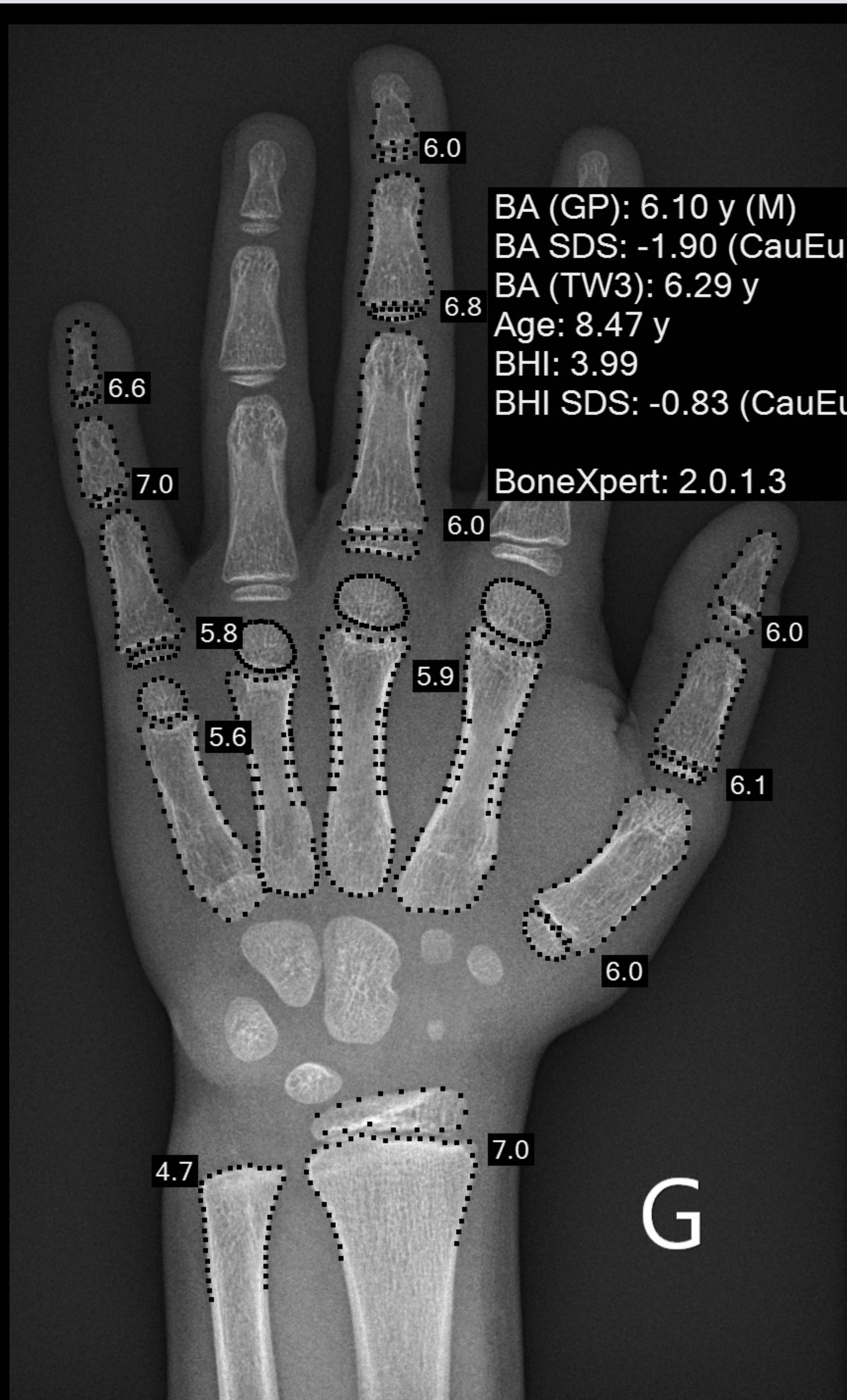

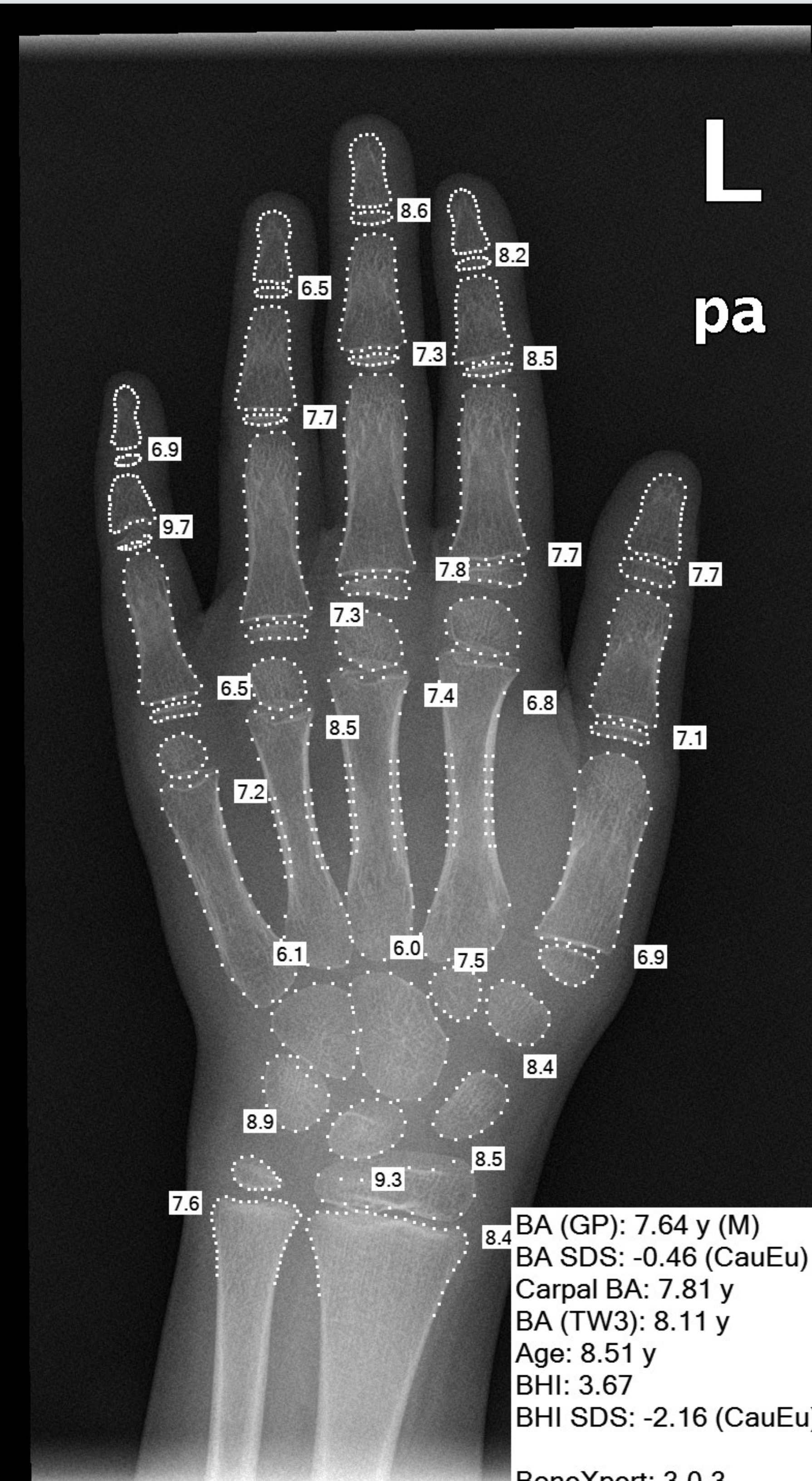

Automated method

- BoneXpert locates 15 bones in the hand (RUS)
- Determines the length of 10 short bones (5 metacarpal, PP1, PP3 and PP5), calculates an average length of these 10 bones
- Advantages:
  - Processes both left and right hand
    - SD moyenne entre la gauche et la droite : 0.25 ans
  - Bone anomalies are accepted
  - Measurement of the size of the bone with 0.7% precision
  - Processes 99% of images automatically without error (reliable for short children - Martin *et al.* Pediatric Radiol 2009)
- Average bone length of the right hand is only a little greater on average
  - 0.2% in boys
  - 0.5% in girls

Martin DD, Neuhof J, Jenni OG, Ranke MB, Thodberg HH.. Horm Res Paediatr. 2010;74(1):50–5.

Automated method

- BoneXpert's Greulich and Pyle bone age
  - non linear function of bone morphology
- More precise during phases of rapid morphological changes

1. Bull RK, et al. Arch Dis Child. 1999;81(2):172-173
2. Roche AF, et al. Am J Roentgenol Radium Ther Nucl Med. 1970;108(3):511-515

Automated method

- Validated
  - Caucasian and Japanese children
  - In short stature children and precocious puberty
- Manual BA rating:
  - 0.25 - 0.82 years [1-2]

1. Bull RK, et al. Arch Dis Child. 1999;81(2):172-173
2. Roche AF, et al. Am J Roentgenol Radium Ther Nucl Med. 1970;108(3):511-515

Automated method

- Shape score, bone density scores, features describing texture of the fusion in the growth plate[1]
- Most accurate:
  - 2.5 - 17 years in ♂
  - 2 - 15 years in ♀

1. *Martin DD, et al. Horm Res Paediatr. 2010;73(5):398-404*

Methodology

- Three layers:
  - A: bone morphology assessment (reconstructs the bone borders)
  - B: if intrinsic BA value for each bone
    - rejection:
      - BA values deviates more than 2.4 years from the average of the hand
      - < 8 bones have been accepted
  - C: transforms the intrinsic BA to either the TW BA or the GP BA (< post processing)

BoneXpert

- Rejection:
  - Bad exposure
  - Bad pose of the hand
  - Abnormal bone shapes

Pediatr Radiol
DOI 10.1007/s00247-016-3618-7

ORIGINAL ARTICLE

Bone age assessment practices in infants and older children among Society for Pediatric Radiology members

Micheál A. Breen[1] · Andy Tsai[1] · Aymeric Stamm[1] · Paul K. Kleinman[1]

Breen MA, et al. Pediatr Radiol. 2016;46(9):1269-1274.

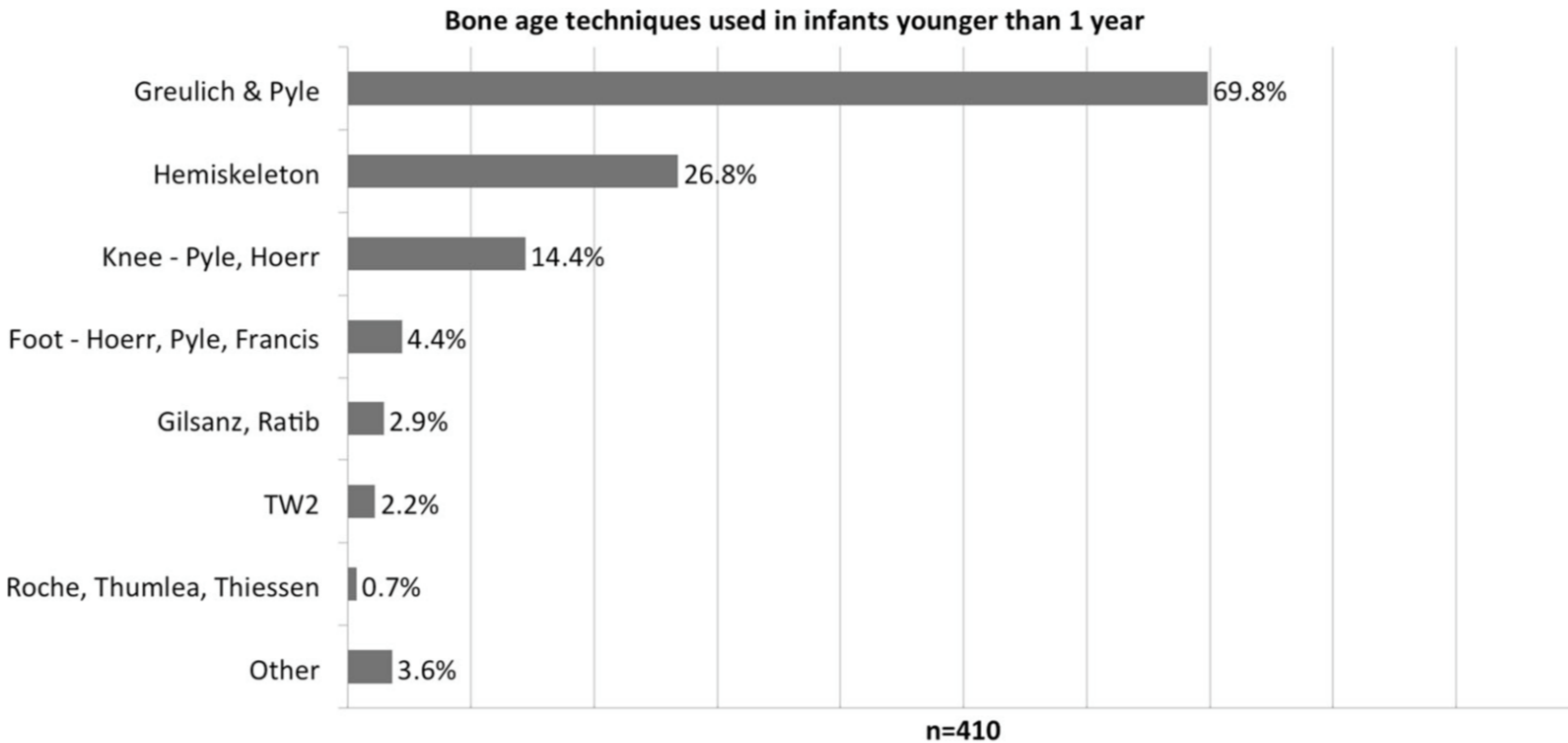

Breen MA, et al. Pediatr Radiol. 2016;46(9):1269-1274.

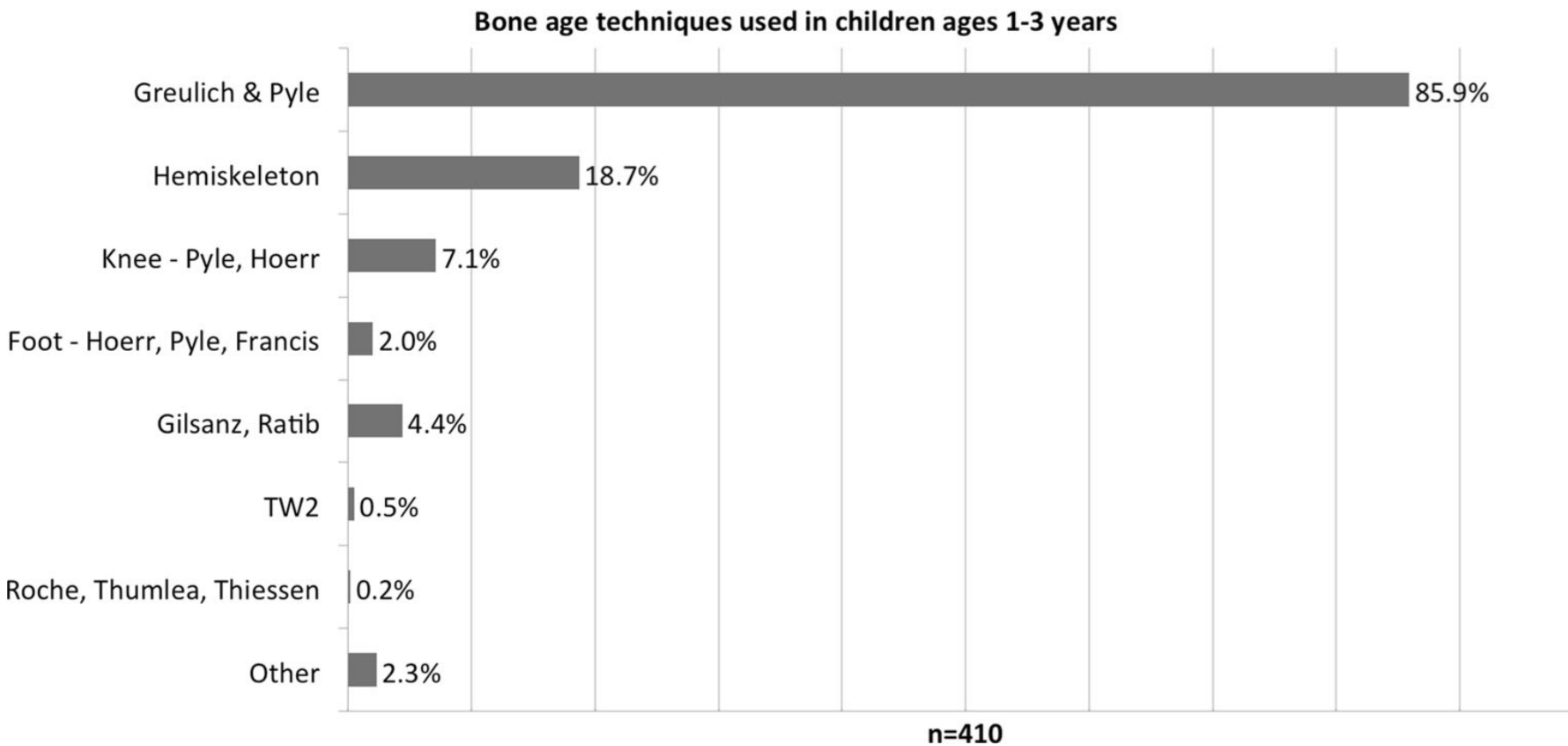

Breen MA, et al. Pediatr Radiol. 2016;46(9):1269-1274.

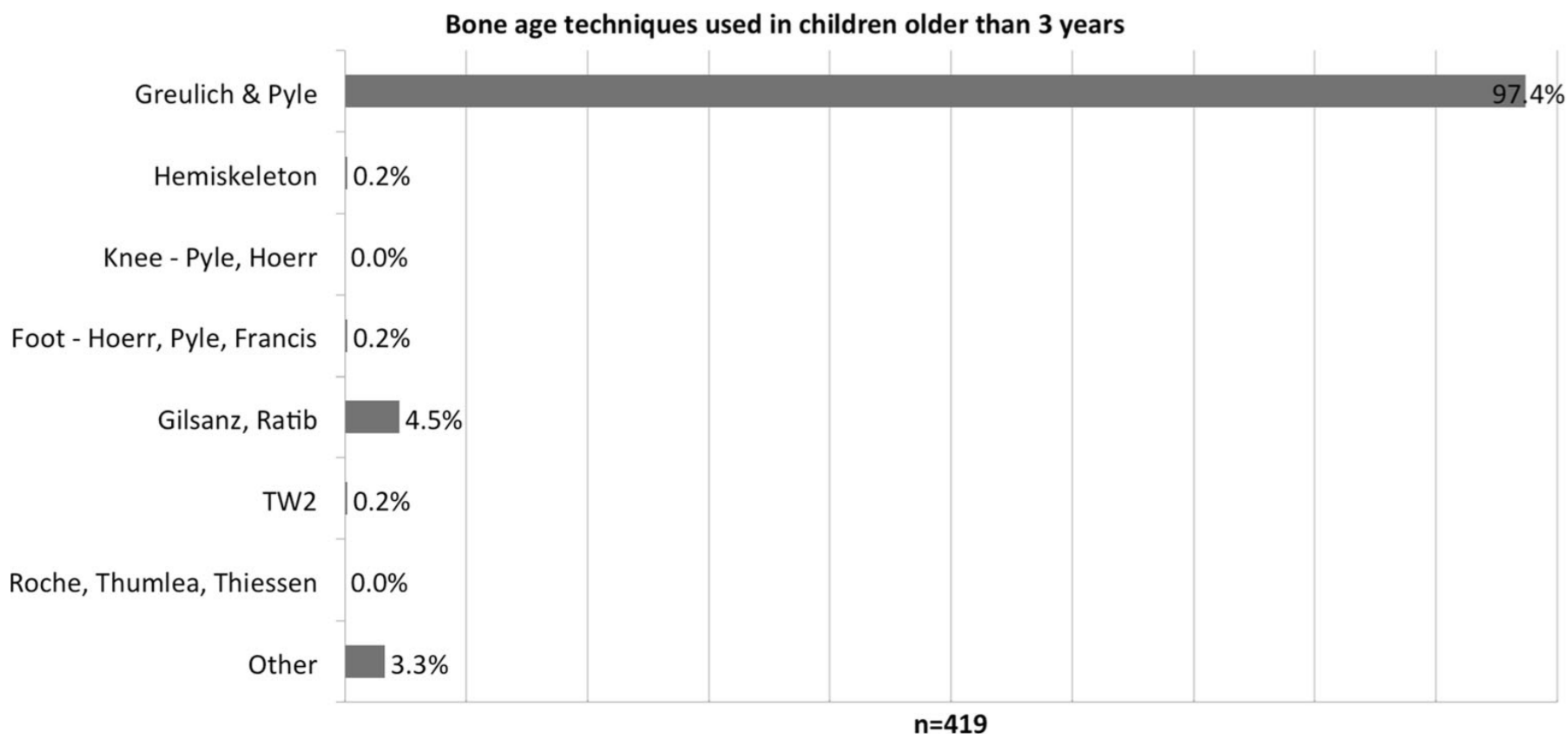

Breen MA, et al. Pediatr Radiol. 2016;46(9):1269-1274.

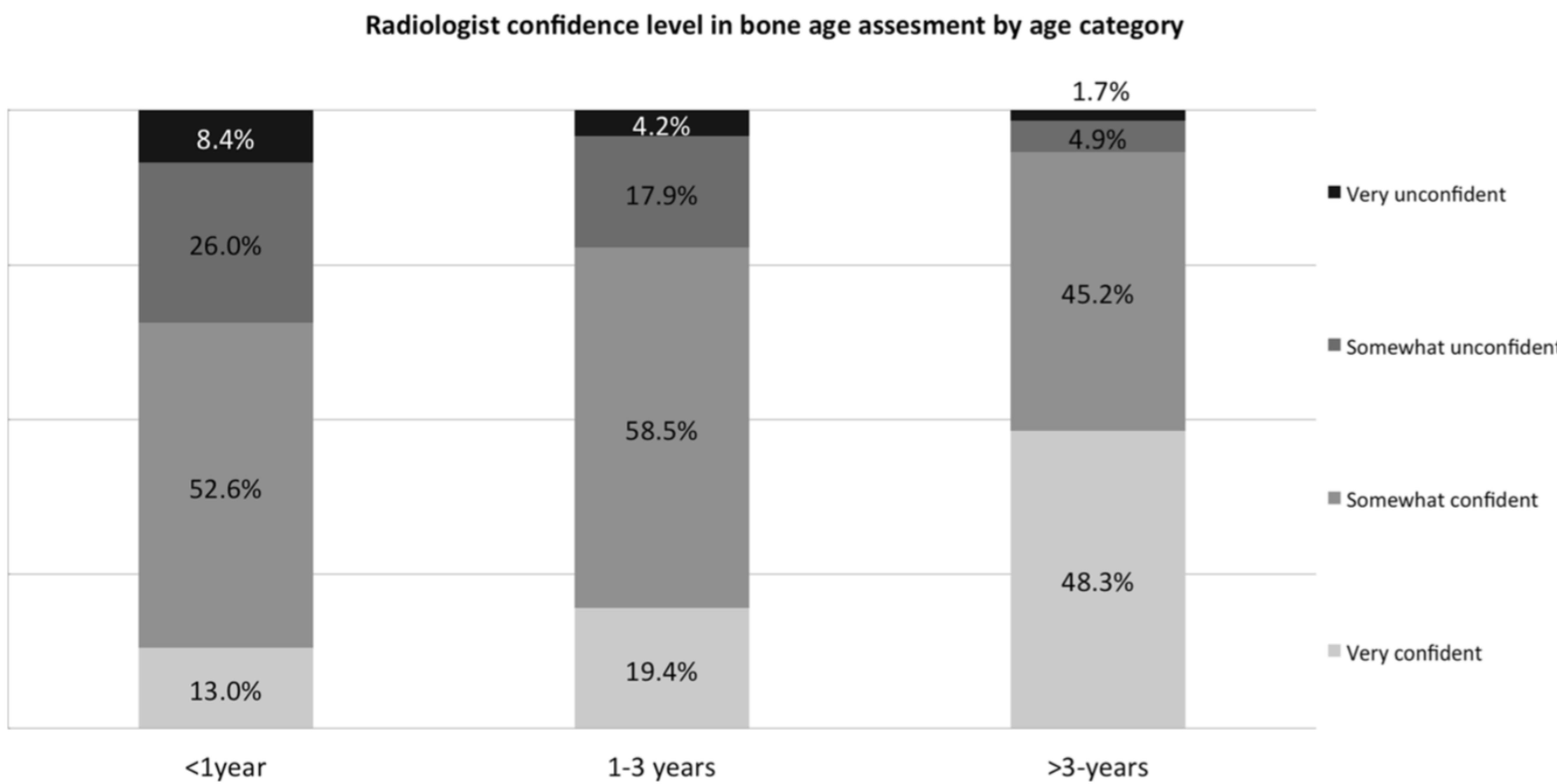

Breen MA, et al. Pediatr Radiol. 2016;46(9):1269-1274.

- 34% of respondents lack confidence when estimating bone age in infants

- Preferred technique of pediatric radiologists: Greulich and Pyle

    - limitations described: little changes in the radiographic appearance of the ossification centers of the hand/wrist in the first months of life

Hemiskeleton techniques	Greulich-Pyle
difficult to justify the acquisition/ interpretation and radiation dose associated with this technique	sub-optimal (< ossification centers of the hand and wrist change little during infancy)

ALTERNATIVE

- Alternative:
    - ✦ Sonographic appearance of the ossification centers of the carpus[1]
    - ✦ Fibula length on a AP radiograph (using standardized reference tables)[2]

1. Tsai A, et al. Pediatr Radiol. 2016;46(3):342-356
2. Daneff M, C et al. Pediatr Radiol. 2015;45(7):1007-1015

Bone age assessment methods

		Structures	Methodology	Date
RX	Greulich-Pyle	Hand and wrist bones	Atlas method	Todd 1931-1942 Edition 1959
	Tanner-Whitehouse	RUS, carpal and 20 bones	Scoring method	1962 Revision 1990
	CASAS	RUS, carpal and 20 bones	Computer-assisted scoring method	1992
	CASMAS	Third phalanges (4 bones)	Automated computerized calculation	1997
	BoneXpert®	RUS (13 bones)	Automated computerized calculation	2009
US	Sunlight BonAge®	Radius and ulnar epiphysis	Sound velocity measurement	2005
MR	Open compact MR imager	RUS	Scoring method	2013

RUS, radius, ulna and short bones; MR, magnetic resonance. CASAS, computerized-assisted skeletal age score; CASMAS, computer-aided skeletal maturity system.

US automated method

- Studies are contradictory (Sunlight BonAge®):
  - Mentzel *et al*. and Shimura *et al*.
    - high correlations between the bone age evaluated by BonAge® and the GP or TW2 methods
  - Khan *et al*.
    - over-read delayed bone age and under-read advanced bone age compared with both the GP and TW3 methods

1994	Tanner-Gibbons	CASAS: A computerized image analysis system for estimating TW-2 bone age
1999	Sato et al.	CASMAS: setting up an automated system for evaluation of bone age
2009	Thodberg et al.	Automated hand and wrist skeletal maturation program
2013	Terrada et al.	Open compact MR imager with a permanent magnet

- Open compact MR
  - ✦ Time consuming (2 min and 44 sec)
  - ✦ Expensive
  - ✦ Not easily available
  - ✦ Body mouvements

US assessment of the ossification centers of the wrist

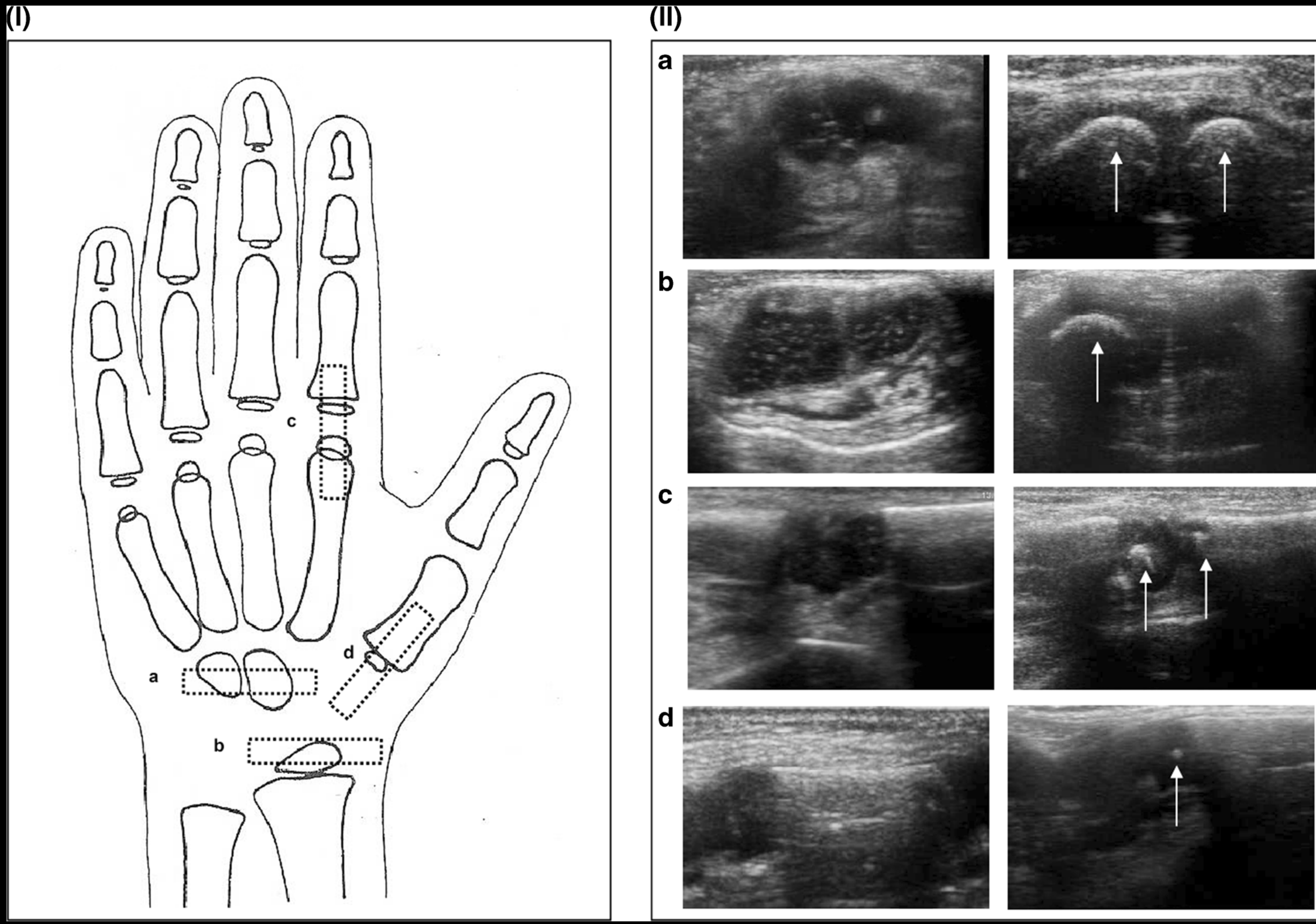

Daneff M, C et al. Pediatr Radiol. 2015;45(7):1007-1015

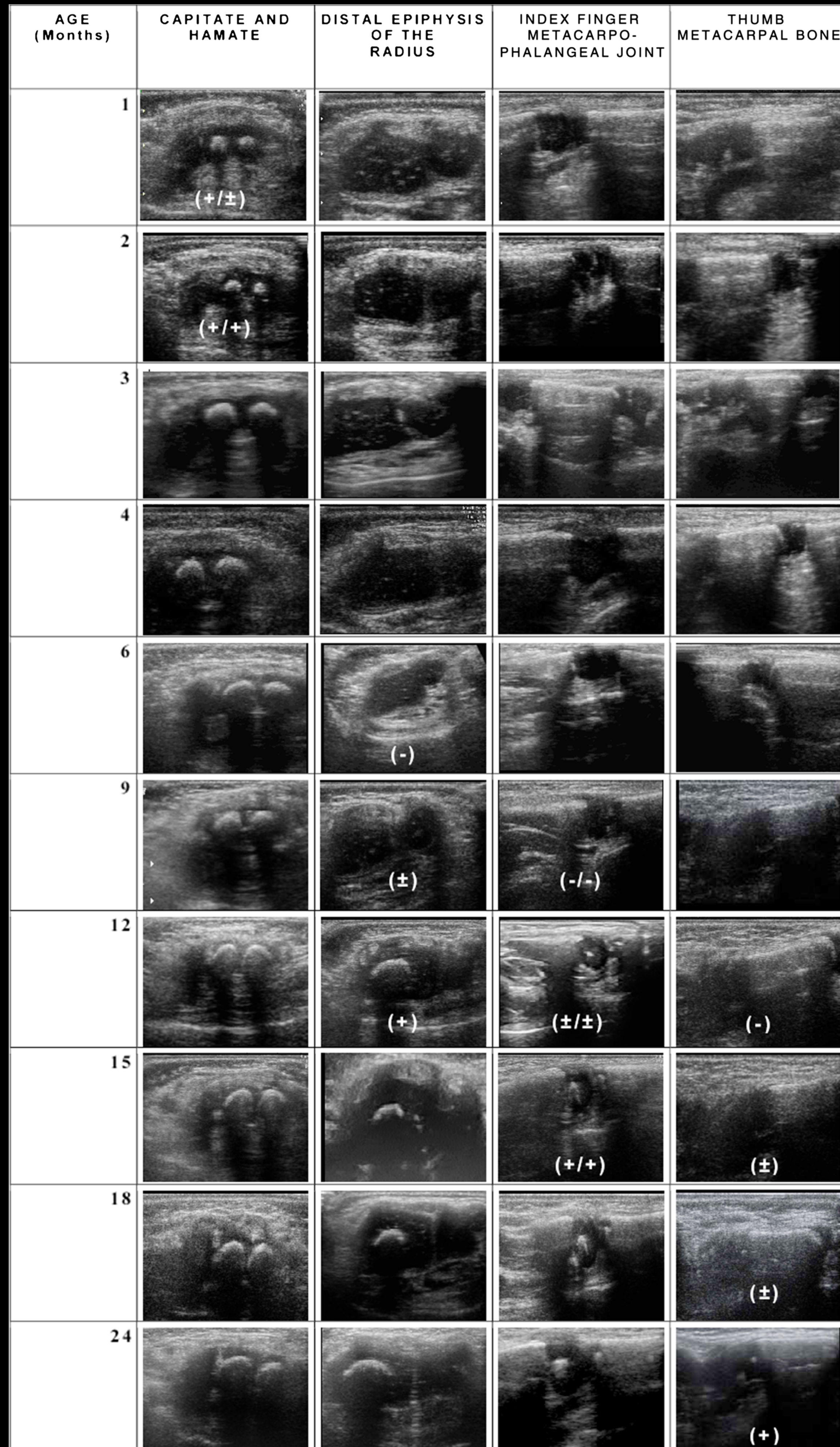

Daneff M, et al. Pediatr Radiol. 2015;45(7):1007-1015.

1994	Tanner-Gibbons	CASAS: A computerized image analysis system for estimating TW-2 bone age
1999	Sato et al.	CASMAS: setting up an automated system for evaluation of bone age
2009	Thodberg et al.	Automated hand and wrist skeletal maturation program
2013	Terrada et al.	Open compact MR imager with a permanent magnet
2016	Tsai et al.	Infant bone age estimation based on fibular shaft length: model development and clinical validation

2016

Tsai et al

Infant bone age estimation based on fibular shaft length: model development and clinical validation

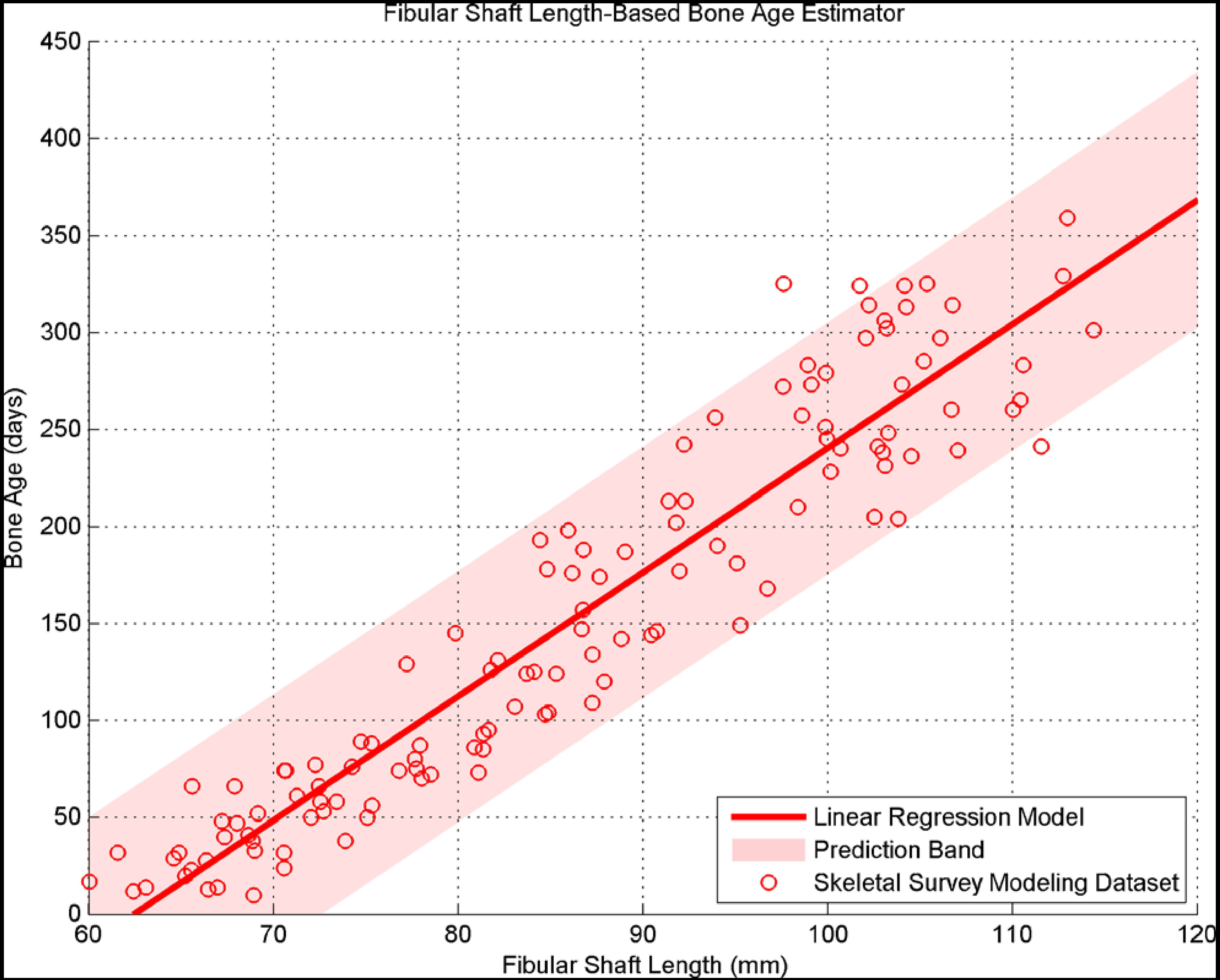

Tsai A, et al. Pediatr Radiol. 2016;46(3):342-356

PERSPECTIVE

Perspectives

- Ideal method for infant bone age assessment:
  - accurate
  - precise
  - reproducible
  - cost
- Non irradiating
- Further studies needed in mixed population

CONCLUSION

Conclusion

- Gold standard for bone age in children: Greulich and Pyle (easy and fast, less accurate)
- Fast evolution of technology, creation of automated methods
- Further studies for a non irradiating, fast and accurate technique

Merci pour votre attention